Development of a Second-Generation, In Vivo Chemical Probe for PIKfyve

Sophia M. Min[1], Frances M. Bashore[1], Jeffery L. Smith[1], Tammy M. Havener[1], Stefanie Howell[1], Haoxi Li[2], Rafael M. Couñago[1,3], Konstantin I. Popov[4], Alison D. Axtman[*,1]

[1] Structural Genomics Consortium, UNC Eshelman School of Pharmacy, University of North Carolina at Chapel Hill, Chapel Hill, NC, 27599, USA

[2] Laboratory for Molecular Modeling, UNC Eshelman School of Pharmacy, University of North Carolina at Chapel Hill, Chapel Hill, NC, 27599, USA

[3] Center of Medicinal Chemistry (CQMED), Center for Molecular Biology and Genetic Engineering (CBMEG), University of Campinas, UNICAMP, 13083-886-Campinas, SP, Brazil

[4] Center for Integrative Chemical Biology and Drug Discovery, UNC Eshelman School of Pharmacy, University of North Carolina at Chapel Hill, Chapel Hill, NC, 27599, USA

Abstract

We optimized our highly potent and cell-active chemical probe for phosphatidylinositol-3-phosphate 5-kinase (PIKfyve), SGC-PIKFYVE-1, resulting in compounds with improved potency and demonstrated *in vivo* stability. Use of an in-cell, kinome-wide selectivity panel allowed for confirmation of excellent in-cell selectivity of our lead compound, **40**, and another promising analogue, **46**. Evaluation of the pharmacokinetic (PK) profiles of these two compounds revealed that both are well tolerated systemically and orally bioavailable. Coupled with its sub-nanomolar cellular potency and impressive selectivity in cells, the long half-life of **40** makes it an ideal candidate for the evaluation of the consequences of PIKfyve inhibition *in vivo*. PIKfyve inhibition has been investigated clinically for indications including rheumatoid arthritis, Crohn's disease, COVID-19, and ALS using a single compound (apilimod), supporting the development of orthogonal PIKfyve inhibitors with *in vivo* stability.
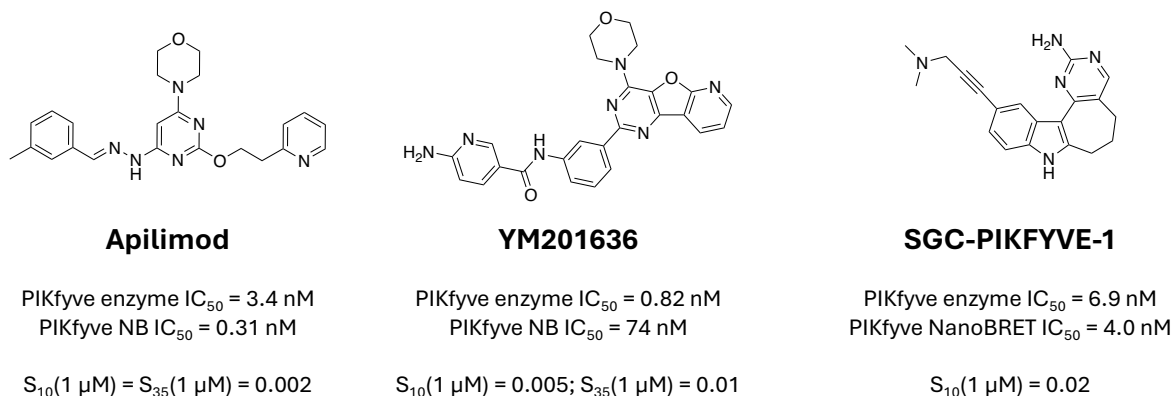
Introduction

Interest in inhibition of phosphatidylinositol-3-phosphate 5-kinase (PIKfyve) as a therapeutic strategy has remained high since the seminal publication on apilimod, which touted it as a treatment for B-cell non-Hodgkin lymphoma.[1] Apilimod (Figure 1) has since been used as an exquisitely selective tool to interrogate PIKfyve biology *in vitro* and *in vivo*. We and other groups have used apilimod to uncover roles of PIKfyve in diseases beyond cancer, including inflammatory and autoimmune diseases,[2-10] ALS and motor neuron diseases,[11-13] anti-viral infections,[14-26] myocardial interstitial fibrosis,[27] and skin disorders.[28, 29] Apilimod, however, may not be the best compound to be used clinically. Reports of unexpectedly low plasma levels, inactivation in cell culture, and failure to show efficacy in clinical trials for multiple indications further impress a need for a structurally unique PIKfyve inhibitor.[7, 8, 25, 30]

Other advanced PIKfyve inhibitors have been evaluated *in vivo* for various therapeutic endpoints. YM201636 (Figure 1) is another potent and selective chemical tool that has been used

to study PIKfyve-mediated pathways in cell- and animal-based systems. YM201636 reduces the proliferation of liver cancer cells and slows tumor growth in a murine hepatic cancer model through a proposed promotion of EGFR expression and resultant induction of autophagy.[31] This inhibitor also suppresses neointima hyperplasia after vascular injury *in vivo*, suggesting it could be a treatment for vascular restenosis.[32] YM201636 lacks the hydrazone functionality found in apilimod that has been suggested as responsible for its inactivation in cell culture. YM201636 does not demonstrate the same loss in efficacy when used for a prolonged period.[30]

Additional PIKfyve inhibitors that have been evaluated *in vivo*, including PIK-001,[33] vacuolin-1,[34, 35] HZX-02-059,[36, 37] WX8,[15] VRG50635, APY0201,[38] and ESK981,[39] have less associated public data that supports their potency and kinome-wide selectivity. While structures for some of these molecules remain unpublished, vacuolin-1, WX8, and APY0201 share the hydrazone liability that is also present in apilimod. Results obtained using antisense oligonucleotides (ASO) targeting PIKfyve, including AS-202 from AcuraStem, have also demonstrated *in vivo* efficacy, but, versus small molecules, suffer with challenges associated with delivery.[40]

Here we present our efforts to optimize our potent and selective PIKfyve chemical probe, SGC-PIKFYVE-1 (Figure 1), to improve its cellular potency and deliver a molecule appropriate for *in vivo* studies. Medicinal chemistry optimization of PIKfyve potency was enabled using a PIKfyve NanoBRET cellular target engagement assay. A panel of 240 NanoBRET cellular target engagement assays was used to confirm the cellular selectivity of lead compounds prior to assessment of PK properties. Our best compound, **40**, demonstrates improved potency and a non-overlapping off-target kinase profile when compared to the parent, SGC-PIKFYVE-1, and robust *in vivo* stability in mice. Therefore, this compound can be used to interrogate the biological consequences of PIKfyve inhibition *in vivo*.

Apilimod	YM201636	SGC-PIKFYVE-1
PIKfyve enzyme IC_{50} = 3.4 nM	PIKfyve enzyme IC_{50} = 0.82 nM	PIKfyve enzyme IC_{50} = 6.9 nM
PIKfyve NB IC_{50} = 0.31 nM	PIKfyve NB IC_{50} = 74 nM	PIKfyve NanoBRET IC_{50} = 4.0 nM
$S_{10}(1 \mu M) = S_{35}(1 \mu M) = 0.002$	$S_{10}(1 \mu M) = 0.005$; $S_{35}(1 \mu M) = 0.01$	$S_{10}(1 \mu M) = 0.02$

**Figure 1.** Structures, potency, and selectivity values for published PIKfyve inhibitors.

Results and Discussion

We previously reported a PIKfyve chemical probe, SGC-PIKFYVE-1, which has IC_{50} values of 6.9 nM and 4.0 nM as determined by PIKfyve enzymatic and NanoBRET assays, respectively (Table 1).[41] Intrigued by the perturbation of the endosomal and lysosomal systems and the lifecycle of β-coronaviruses elicited by SGC-PIKFYVE-1,[41] we designed and synthesized a series of analogues to improve PIKfyve potency while also considering additional properties, including metabolic stability, toxicity, and kinetic solubility. Only through optimization of each of these properties in tandem would we deliver a molecule appropriate for *in vivo* use.
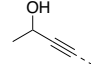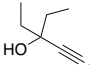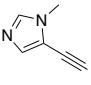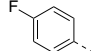
Analogues with Enhanced Rotational Freedom

Our initial efforts focused on exploring the importance of the seven-membered ring in SGC-PIKFYVE-1. To simplify synthesis and probe whether this ring system could be removed without major losses in potency or introducing other liabilities, ring-opened analogues were prepared that varied the group attached at the location of the pendant alkyne in SGC-PIKFYVE-1. A single example, **2**, had been previously exemplified[41] and its evaluation supported that a ring-opened analogue retains PIKfyve potency. This compound was resynthesized and evaluated once again, yielding similar results to what was previously observed. Next, the ring-opened analogue of SGC-PIKFYVE-1, **1** (Table 1), was synthesized and found to retain high cellular affinity for PIKfyve (IC_{50} = 3.7 nM in the PIKfyve NanoBRET assay). These examples encouraged us to make additional analogues and confirm whether the trend was observed for other matched pairs. Other alkynes that had been previously appended to ring-closed analogues were included in compound design. The propargylic alcohol analogues (**3** and **4**) and the biaryl analogue **6** maintained comparable, low nanomolar potency in the PIKfyve enzymatic and NanoBRET assays. The corresponding ring-closed analogues of **3**, **4**, and **6** had PIKfyve NanoBRET IC_{50} values of 4.05, 12.7, and 11.4 nM,[41] respectively. Although **5**, which contains a 1-methylimidazole, displayed improved activity versus its six-membered congener that was inactive in the PIKfyve NanoBRET assay (IC_{50} >10000), its activity was still modest. These analogues demonstrated that PIKfyve is more tolerant of smaller groups at the alkyne terminus and that removal of the locking ring system generally results in analogues with comparable or improved PIKfyve affinity. To further profile the developability of these analogues, we determined their stability when incubated with mouse liver microsomes for 30 mins as well as their impact on the viability of cells in culture and kinetic solubility in aqueous buffer. Like SGC-PIKFYVE-1, **1** and **6** showed rapid metabolism when exposed to mouse liver microsomes (MLM) and did not impact the viability of treated cells.[41] The propargyl alcohol analogues (**2** and **3**) demonstrated improved MLM stability and aqueous solubility, but resulted in diminished cellular viability. These initial results support that structural modification of the ring-opened series of analogues can improve metabolic stability while maintaining PIKfyve potency, but these changes can impact cellular viability.

Table 1. PIKfyve enzymatic and in-cell binding, *in vitro* stability and viability, and kinetic solubility data for analogues with modified alkynes
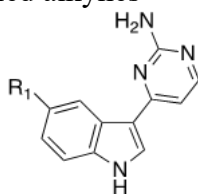
Compd	R₁	PIKfyve enzymatic IC_{50} (nM)	PIKfyve NB IC_{50} (nM)	MLM stability @ 30 min[a]	% Viability at 1 uM[b]	Kinetic Solubility (µM)[c]
SGC-PIKFYVE-1		6.9	4.0	13	91	110
1		21	3.7	8.8	96	120
2		3.3	11	82	51	150

3		6.7	8.0	70	47	160
4		5.1	12	45	90	140
5		NT[d]	220	86	88	86
6		24	11	36	100	4.0

[a]% remaining after 30 min. [b]Mean of quadruplicate experiments. [c]Kinetic solubility of a 10 mM DMSO stock solution in PBS at pH 7.4. [d]NT: not tested.

Indole Core Modification to Address Metabolic Instability

Due to the rapid *in vitro* metabolism observed for SGC-PIKFYVE-1 and **1**, we next focused on enhancing the MLM stability. We first introduced different substituents at the 2-position of the indole ring, which is one of the metabolic sites predicted by the SMARTCyp *in silico* method (Table 2).[42] The 2-methyl analogues **7** and **8** exhibited slightly decreased PIKfyve affinity and poor metabolic stability. Introduction of the *t*-butyl substituent improved metabolic stability and reduced adverse effects on viability but resulted in a complete loss of PIKfyve engagement in cells. We propose based on docking studies that the *t*-butyl group may prevent the coplanarity of the pyrimidine and indole rings, resulting in a clash with the hinge loop and inactivity. The amide substituent, which is more linear and flexible than a *t*-butyl group and bulkier than a methyl group, in **13** and **14** did not alter the coplanarity between the two aromatic rings. While **13** had slightly improved metabolic stability and similar PIKfyve potency when compared to SGC-PIKFYVE-1, **14** demonstrated reduced PIKfyve cellular affinity and metabolic stability compared to the corresponding propargyl alcohol analogue **2**. Furthermore, we prepared an indazole series of analogues as a strategy to reduce metabolism at the 2- and 3-positions of the indole ring. Evaluation of these analogues revealed that this modification did not significantly improve metabolic stability. Analogues with propargylic alcohol groups on the alkyne terminus and a 2-position carbon/nitrogen on the indole/indazole core (**2**, **3**, **16**, **17**, **18**) were observed to consistently elicit cellular toxicity when dosed at 1 μM. However, the potent inhibitory activity of these analogues coupled with the mitigation of toxicity when the 2-position was elaborated (**14**) suggested that further modification could result in both improved potency and metabolic stability without introducing toxicity.

Table 2. PIKfyve enzymatic and in-cell binding, *in vitro* stability and viability, and kinetic solubility data for 2-position indole analogues

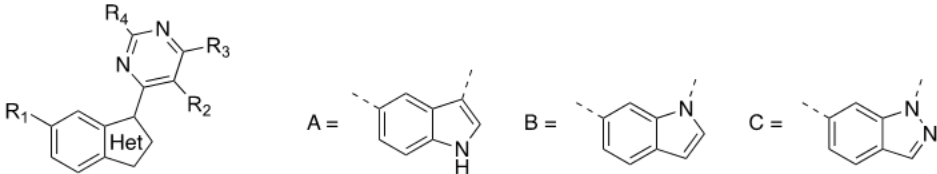| Compd	X	R$_1$	R$_2$	PIKfyve enzymatic IC$_{50}$ (nM)	PIKfyve NB IC$_{50}$ (nM)	MLM stability @ 30 min[a]	% Viability at 1 uM[b]	Kinetic Solubility (μM)[c]
7	C	(dimethylamino propargyl)	Me	52	5.4	4.5	96	100
8	C	(4-fluorophenyl)	Me	51	43	36	92	12
9	C	(dimethylamino propargyl)	t-Bu	NT[d]	>10000	46	95	130
10	C	(hydroxy propargyl)	t-Bu	NT	>10000	76	100	110
11	C	(hydroxy butynyl)	t-Bu	NT	2500	69	100	90
12	C	(hydroxy methylbutynyl)	t-Bu	NT	3500	45	100	140
13	C	(dimethylamino propargyl)	amide-CH$_2$CH$_2$OMe	110	6.2	26	100	130
14	C	(hydroxy methylbutynyl)	amide-CH$_2$CH$_2$OMe	11	41	61	79	31
15	N	(dimethylamino propargyl)	-	5.3	7.4	29	88	67
16	N	(hydroxy methylbutynyl)	-	2.2	53	72	41	65
17	N	(hydroxy butynyl)	-	2.0	44	53	41	65
18	N	(hydroxy methylbutynyl)	-	3.4	15	57	30	78

[a]% remaining after 30 min. [b]Mean of quadruplicate experiments. [c]Kinetic solubility of a 10 mM DMSO stock solution in PBS at pH 7.4. [d]NT: not tested.

Aminopyrimidine Ring Modification

Next, we explored the impact of modifying the proposed hinge binding aminopyrimidine ring within the indole and the indazole series (Table 3). While there are no co-crystal structures of inhibitors bound to PIKfyve, the co-crystal structure of structurally related compounds bound to TTBK1 support our proposed binding mode with the aminopyrimidine interacting with the hinge residues in the ATP site.[43] The introduction of methoxy ethyl ether at the R$_2$ position of the aminopyrimidine (Table 3) yielded analogues 19 and 20, which demonstrated high PIKfyve affinity but poor metabolic stability. Compound 20 once again elicited cellular toxicity, supporting our previous statement about propargyl alcohol analogues. Removal of the amino group (R$_4$ position) from the aminopyrimidine ring (21) led to a significant drop in PIKfyve potency, indicating that the amino group is important for PIKfyve binding. Regioisomeric N-linked indole and indazole analogues bearing a dimethyl amino group on the alkyne terminus (22 and 24) maintained the potency of SGC-PIKFYVE-1 but were rapidly metabolized when exposed to MLM. The regioisomeric N-linked indole and indazole pair bearing a propargyl alcohol on the

alkyne terminus (**23** and **25**) bound to PIKfyve with modest affinity but suffered from cellular toxicity, as was observed for structurally related analogues. Further modification of the aminopyrimidine ring to include a methoxy or methyl group (**26–28**) did not improve the potency or metabolic stability. In summary, our efforts to modify the aminopyrimidine ring did not result in analogues with increased PIKfyve affinity and metabolic stability.

Table 3. PIKfyve enzymatic and in-cell binding, *in vitro* stability and viability, and kinetic solubility data for aminopyrimidine analogues

Compd	Het Core	R₁	R₂	R₃	R₄	PIKfyve enzymatic IC_{50} (nM)	PIKfyve NB IC_{50} (nM)	MLM stability @ 30 min[a]	% Viability at 1 µM[b]	Kinetic Solubility (µM)[c]
19	A	(alkyne)	O—CH₂CH₂—OMe	H	NH_2	46	11	33	99	88
20	A	HO-(alkyne)	O—CH₂CH₂—OMe	H	NH_2	4.1	13	50	41	110
21	A	(alkyne)	H	H	H	NT[d]	150	2.3	100	120
22	B	(alkyne)	H	H	NH_2	40	6.3	0	78	36
23	B	HO-(alkyne)	H	H	NH_2	10	76	53	31	110
24	C	(alkyne)	H	H	NH_2	12	3.4	0	74	14
25	C	HO-(alkyne)	H	H	NH_2	2.1	18	78	31	8.8
26	C	(alkyne)	OMe	H	NH_2	180	78	4.9	100	110
27	C	(alkyne)	Me	H	NH_2	68	8.9	0	100	14
28	C	(alkyne)	H	Me	NH_2	150	46	1.3	100	99

[a]% remaining after 30 min. [b]Mean of quadruplicate experiments. [c]Kinetic solubility of a 10 mM DMSO stock solution in PBS at pH 7.4. [d]NT: not tested.

Probing Alkyne Modification and Replacement

To further refine structure–activity relationships for our chemical series of PIKfyve inhibitors, we investigated an additional series of analogues where we varied the alkyne (R₁ in Table 4). That ring-opened analogues with an indole core bearing varied alkynes demonstrated the

most consistently potent PIKfyve affinity (Table 1) motivated synthesis of another series. We aimed to identify structural changes that do not elicit cytotoxicity and improve metabolic stability by designing and synthesizing further analogues. We first prepared and evaluated analogues with a nitrogen-containing substituent, including an amine, amide, pyrrolidine, or morpholine, at the alkyne terminus (29–36) in the PIKfyve NanoBRET target engagement assay. The dimethyl amine at the terminus of the alkyne on SGC-PIKFYVE-1 was a predicted site of metabolism by the SMARTCyp *in silico* method and thus we attempted to modify it and produce more stable analogues. While these analogues had improved metabolic stability, only the pyrrolidine analogue, 35, demonstrated modest inhibition of and affinity for PIKfyve. While these structural changes were quite minimal when compared to SGC-PIKFYVE-1 and its ring-opened congener, 1, dramatic changes in PIKfyve binding were observed. These results support that the part of the ATP site where the dimethyl amine on SGC-PIKFYVE-1 and 1 projects is quite restricted, such that sterically bulky groups and extended linear groups are not tolerated. The significant loss in affinity of 30 when compared to 1, which differs only by a methyl group on the terminal amine, supports that a hydrogen bond donor is not as tolerated in the site that binds the pendant amine.
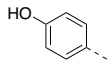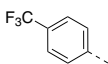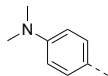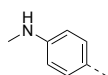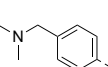
Next, we evaluated whether nitrogen-containing heterocycles on the alkyne terminus were tolerated by PIKfyve. These analogues demonstrated a complete loss of PIKfyve affinity (37–39). Less bulky, linear hydrophobic groups were then appended at the alkyne terminus. Introduction of either a thioether or an aliphatic propyl group resulted in analogues with remarkable PIKfyve potency (40 and 41) but decreased metabolic stability. Notably, 40 exhibited sub-nanomolar activity in both PIKfyve enzymatic and NanoBRET assays with $IC_{50} = 0.6$ nM and 0.35 nM in each assay, respectively, and was not toxic when cells were treated at 1 μM. Finally, based on the potency of biaryl analogue 6 (Table 1, PIKfyve NanoBRET $IC_{50} = 110$ nM), we explored replacement of the alkyne with different phenyl rings. We found the *ortho*- and *meta*-fluorine substituted analogues (42 and 43) exhibited comparable PIKfyve affinity to 6 but with reduced metabolic stability and solubility. Although the introduction of the *para*-hydroxyl group (44) improved the stability and solubility while maintaining PIKfyve affinity, substitution with the *para*-trifluoromethyl ring (45) resulted in an analogue with reduced PIKfyve affinity. Next, a dimethyl amino group was introduced at the *para*-position of the pendant aryl ring, akin to the group that is found at the alkyne terminus of SGC-PIKFYVE-1. The resultant analogue (46) demonstrated significantly increased metabolic stability and maintained modest PIKfyve affinity (PIKfyve NanoBRET $IC_{50} = 24.7$ nM). Removal of a single methyl group from the amino group of 46 yielded mono-methylated analogue 47, which was more active than 46 and 6 but suffered from poor metabolic stability. Finally, insertion of a methylene group between the dimethyl amino group and phenyl ring of 46 yielded 48, which lacked PIKfyve affinity. Overall, modifications to the R_1 group resulted in dramatic changes in PIKfyve affinity. Biological evaluation of this series of analogues led us to conclude that smaller and more hydrophobic R_1 groups result in more high affinity binding within a tight back pocket of PIKfyve. Taken together, 40 and 46 were selected as potent and non-toxic PIKfyve inhibitor leads with orthogonal structures that warranted additional investigation.

Table 4. PIKfyve enzymatic and in-cell binding, *in vitro* stability and viability, and kinetic solubility data for second generation analogues with modified alkynes
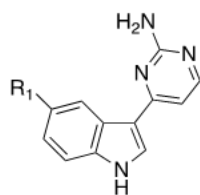
Compd	R₁	PIKfyve enzymatic IC$_{50}$ (nM)	PIKfyve NB IC$_{50}$ (nM)	MLM stability @ 30 min[a]	% Viability at 1 uM[b]	Kinetic Solubility (μM)[c]
29		NT[d]	2000	NT	100	NT
30		NT	600	NT	91	NT
31		NT	640	39	79	130
32		NT	4400	39	98	110
33		NT	>10000	48	99	110
34		NT	2000	78	100	110
35		190	38	17	98	140
36		NT	1200	29	100	130
37		NT	5200	NT	100	NT
38		NT	510	NT	100	NT
39		NT	>10000	NT	100	NT
40		0.60	0.35	<1	83	73
41		16	1.8	2.1	96	1.9
42		13	14	16	100	5.1
43		14	33	<1	97	6.5

44	![structure: HO-phenyl]	47	22	44	97	130
45	![structure: F₃C-phenyl]	NT	290	NT	100	NT
46	![structure: dimethylamino-phenyl]	20	25	74	94	13
47	![structure: methylamino-phenyl]	26	8.4	4.6	83	68
48	![structure: dimethylaminomethyl-phenyl]	NT	9500	32	100	130

[a]% remaining after 30 min. [b]Mean of quadruplicate experiments. [c]Kinetic solubility of a 10 mM DMSO stock solution in PBS at pH 7.4. [d]NT: not tested.

## Molecular Docking and Structural Alignment Studies
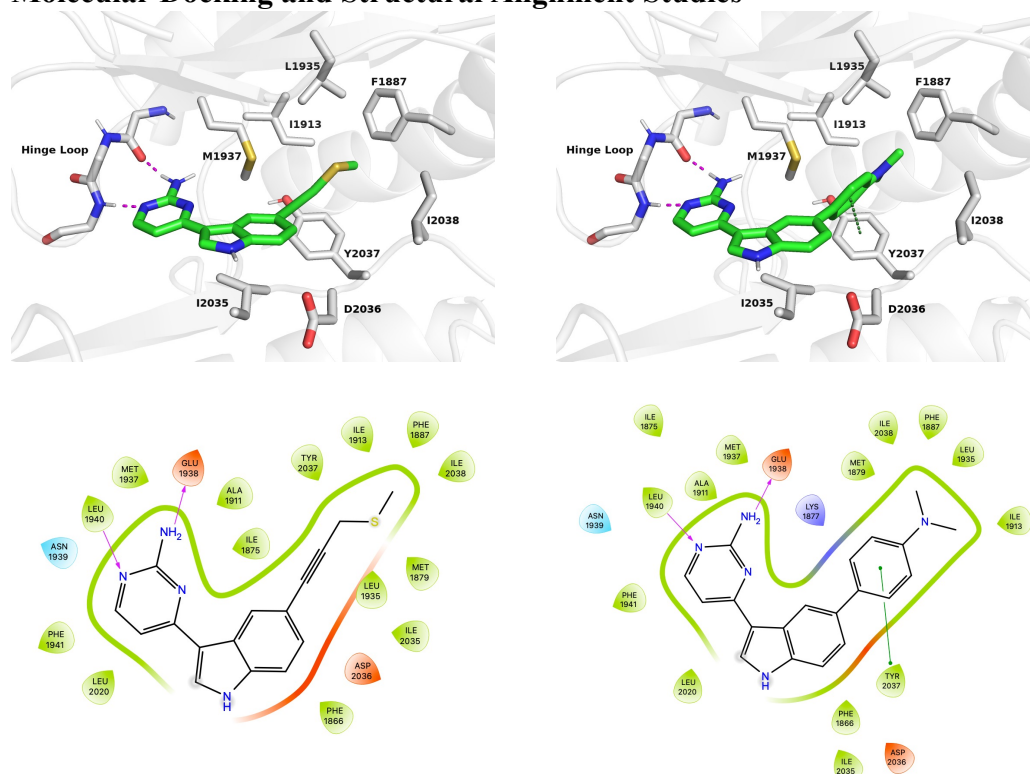
Figure 2. Docking models of **40** (left) and **46** (right) into active site of PIKfyve. The residue numbers from the PDB structure (7K2V, chain P) have been converted to the residue numbers corresponding with the full length PIKfyve protein. The ligand molecules are displayed in green. The main hydrogen bond and π–π stacking interactions are represented by magenta and green dotted lines, respectively.

To better understand the binding mode of compounds **40** and **46** to PIKfyve in the absence of co-crystal structures, we conducted a molecular docking study utilizing the reported cryo-EM structure of PIKfyve in complex with proteins Fig4 and Vac14 (PDB code: 7K2V, chain: P). As shown in Figure 2, both compounds exhibited a similar binding mode in top-ranked docking poses and displayed some coplanarity between the pyrimidine and indole rings. The aminopyrimidine

rings present in both compounds were found to form two hydrogen bonds with backbone residues Glu1938 and Leu1940 in the hinge region of PIKfyve, while the indole amines were positioned in a solvent-exposed region of the binding site. Docking models also indicated that the thioether group on the alkyne terminus of **40** inserts into a hydrophobic region of the binding pocket, and the benzene ring of **46** engages in a π−π stacking interaction with Tyr2037.

To gain insight into the protein–ligand interaction patterns and their relationship to measured binding affinities, we performed a comparative analysis of the docking poses for the alkyne, indole, and aminopyrimidine analogues (Figure S1). SGC-PIKFYVE-1 and **1** were found to adopt very similar conformations with coplanarity of the aminopyrimidine and indole rings, supporting their nearly identical binding affinities for PIKfyve. Additionally, the docking model for our inactive compound **39** supports our hypothesis that a bulky group on the alkyne terminus is not tolerated by the back, buried portion of the PIKfyve pocket. Interestingly, our modeling suggests that the flexibility of the amide on the indole analogue bearing a 2-position alkyl amide, **13,** allows it to shift into the solvent while maintaining the coplanarity between the pyrimidine and indole rings. This finding explains its nearly equivalent PIKfyve binding affinity compared to that of compound **1**. Finally, examination of the docking pose of aminopyrimidine analogue **26** revealed that the methoxy group on the aminopyrimidine ring creates steric clash with hinge residues that is proposed to weaken the key hinge binding interaction.
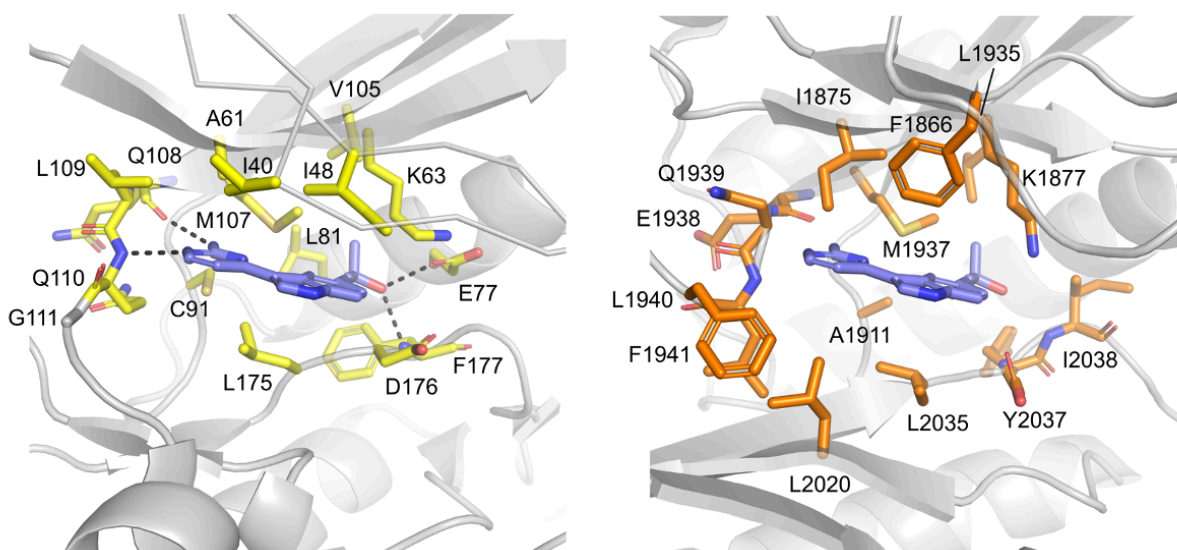
Figure 3. Structural comparison of TTBK1 bound to **2** (left, PDB ID: 7ZHO) and docked into PIKfyve (right, PDB ID: 7K2V) ATP-binding sites.

To gain a better understanding of the docking models and their correlation with the measured binding data for the indolyl pyrimidinamine series and TTBK1, we conducted additional *in silico* studies. We performed a structural alignment of the kinase domains of PIKfyve (PDB code: 7K2V and AlphaFold DB: AF-Q9Y2I7-F1; residues 1822-2085) and the kinase domain of TTBK1 bound to **2** (PDB code: 7ZHO; residues 21-317) (Figure 3). This structural alignment allowed us to identify co-located residues in the binding sites of PIKfyve and TTBK1, despite the low amino acid sequence conservation between PIKfyve and other proteins, including TTBK1. Examination of the crystal structure of TTBK1 bound to **2** shows that Gln108 and Gln110 make key backbone hinge hydrogen bonds with the aminopyrimidine core.[43] Our analyses suggested that

in PIKfyve, main chain atoms from residues Glu1938 and Leu1940 could support similar interactions to **2**, indicating that ligands within this chemical series may have equivalent binding modes to these two non-homologous kinases. Furthermore, the deep, buried portion of the pocket in TTBK1, which accommodates binding of groups on the alkyne terminus, includes the residues Lys63, Glu77, Val105, Met107, and Phe177. Within this pocket, **2** engages TTBK1 via hydrogen bonds to the side chain of Glu77 and the main chain of Phe177. A structurally equivalent back pocket is found in PIKfyve, composed of Lys1877, Ile2038, Leu1935, Met1937, and Tyr2037. Our *in silico* analyses suggested that the main chain of Tyr 2037 in PIKfyve may engage **2** via hydrogen bonds, akin to the interaction facilitated by Phe177 in TTBK1. Nevertheless, the second hydrogen bond facilitated by the side chain of TTBK1 back pocket residue Glu77 would not be supported by the structurally equivalent residue in PIKfyve, Ile2038. The insertion of hydrophobic groups into the back pocket of TTBK1[43] resulted in enhanced binding, suggesting that the placement of the thioether in this pocket may help explain the high PIKfyve affinity of **40**.
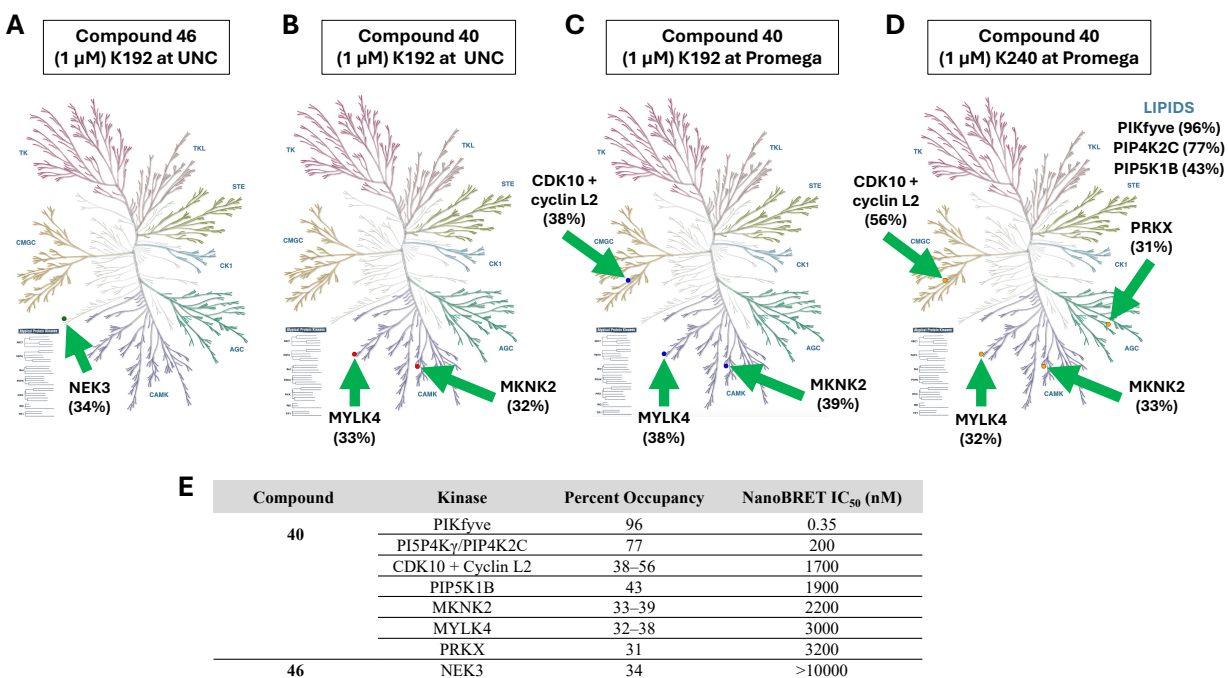
Figure 4. In-cell selectivity profiles of **40** and **46**. (A) In-cell selectivity profiling of **46** in K192, run at UNC; (B) In-cell selectivity profiling of **40** in K192, run at UNC; (C) In-cell selectivity profiling of **40** in K192, run at Promega; (D) In-cell selectivity profiling of **40** in K240, run at Promega; and (E) Summary table showing all kinases engaged with >30% occupancy in one or more selectivity panel runs and IC$_{50}$ value generated when the NanoBRET assay was run in dose–response format.

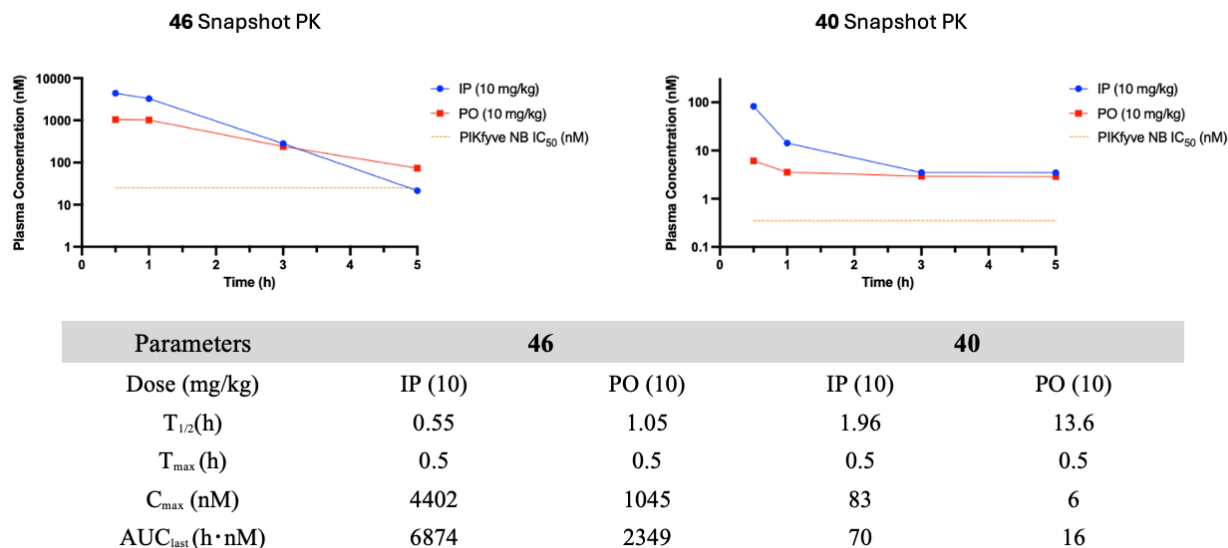## Kinome-Wide Selectivity Evaluation

Inspired by their potency and overall physicochemical properties, we chose to next evaluate the in-cell selectivity of **40** and **46** using panels of 192–240 kinase NanoBRET assays[44] at a concentration of 1 µM. This concentration is well above the PIKfyve NanoBRET IC$_{50}$ of these compounds and was selected to identify kinases that bind with weaker affinity, allowing us to define the selectivity window and appropriate *in vitro* dosing range for each compound. The results, which are expressed as percent occupancy of a kinase by the test compound at 1 µM, are summarized in Figure 4. Compound **40** bound to MYLK4, MKNK2, and CDK10 and compound

46 bound NEK3 when these compounds were profiled in the K192 NanoBRET assay panel (Figures 4A–C). There was excellent agreement amongst the two runs of the K192 NanoBRET assay panel when executed for compound **40** at UNC and at Promega (Figures 4B and 4C). These compounds did not bind to any other kinases in the 192-member panel with >30% occupancy at 1 μM. Compound **40** was further profiled in a panel of 240 kinase NanoBRET assays, which generated similar percent occupancy for the kinases also in the K192 NanoBRET assay panel but also uncovered binding affinity for PIKfyve, PIP4K2C, PIP5K1B, and PRKX. While PRKX was present in the K192 NanoBRET assay panel, it fell below the 30% occupancy cutoff in these runs. Lipid kinases PIKfyve, PIP4K2C, PIP5K1B, on the other hand, were present only in the K240 NanoBRET assay panel. Consequently, the respective NanoBRET assays were executed in dose–response format to generate IC_{50} values for the binding of **40** and **46** to those kinases where >30% occupancy was observed in at least one in-cell selectivity screen. For **40**, there is excellent correlation between the percent occupancy and NanoBRET IC_{50} values. The compound demonstrated weak binding (IC_{50} > 1700 nM) to all kinases except for PIP4K2C. Still, when considering the PIP4K2C IC_{50} = 200 nM, **40** has a >500-fold in-cell selectivity for PIKfyve versus the remainder of kinases in the 240-member NanoBRET panel. Similarly, **46** showed no binding to NEK3 (IC_{50} > 10000 nM) and thus has excellent in-cell selectivity versus the 192 kinases in the K192 NanoBRET assay panel. These IC_{50} values align with what we would expect given the low occupancy values at 1 μM and support that, in cells, both **40** and **46** bind with high affinity to PIKfyve and do not bind the other 192–240 kinases profiled.

To supplement this data, we also sent **40** and **46** to be profiled in enzymatic assays for TTBK1 and TTBK2. These kinases were not included in the 192-member panel, and we have demonstrated binding of related indolyl pyrimidinamine analogues to TTBK1 and TTBK2.[43] When evaluated at 1 μM, both **40** and **46** demonstrated ≤8% inhibition of TTBK1 and TTBK2 and were thus considered to be inactive versus these two kinases.

Preliminary pharmacokinetic profiling of lead compounds.

Based on their *in vitro* potency and selectivity, **46** and **40** were selected for preliminary evaluation of pharmacokinetic (PK) properties in CD-1 mice over the course of five hours. Two routes of administration, intraperitoneal (IP) and oral (PO), were explored for a single dose (10 mg/kg). Importantly, no treatment-related adverse effects were observed in the animals during the exposure period. As shown in Figure 5, **46** demonstrated decent exposure as reflected by the AUC values (6874 and 2349 h·nM for IP and PO) but was mostly consumed over the 5-hour exposure period and had similarly short half-lives (0.55 and 1.05 h for IP and PO). Plasma concentrations of **46** remained above its cellular target engagement IC_{50} value for PIKfyve when dosed orally. In comparison, **40** showed low exposure after IP and PO administrations (AUC values <75 h·nM) but remained at concentrations well above its PIKfyve cellular affinity, as assessed using the PIKfyve NanoBRET assay. The extrapolated half-life ($T_{1/2}$ = 13.6 h) after oral administration suggests that increasing the dose of **40** should result in high plasma concentrations of this compound over an extended dosing period.

| Parameters	46		40	
Dose (mg/kg)	IP (10)	PO (10)	IP (10)	PO (10)
$T_{1/2}$ (h)	0.55	1.05	1.96	13.6
T_{max} (h)	0.5	0.5	0.5	0.5
C_{max} (nM)	4402	1045	83	6
AUC_{last} (h·nM)	6874	2349	70	16

Figure 5. Preliminary pharmacokinetic profiles of **40** and **46** in CD-1 mice.

Chemistry

SGC-PIKFYVE-1 consists of three functional groups: alkyne, indole, and aminopyrimidine. We opened the cycloheptadiene ring of SGC-PIKFYVE-1 to enable more facile synthesis and optimization. Structure–activity relationships were established for this ring-opened series of analogues by introducing various functional groups at the alkyne, indole, and aminopyrimidine regions.

The chemical syntheses of final compounds **1**–**48** are outlined in Schemes 1–3. As shown in Scheme 1, the alkyne region analogues were synthesized from commercially available indole **49** using Sonogashira or Suzuki coupling conditions.
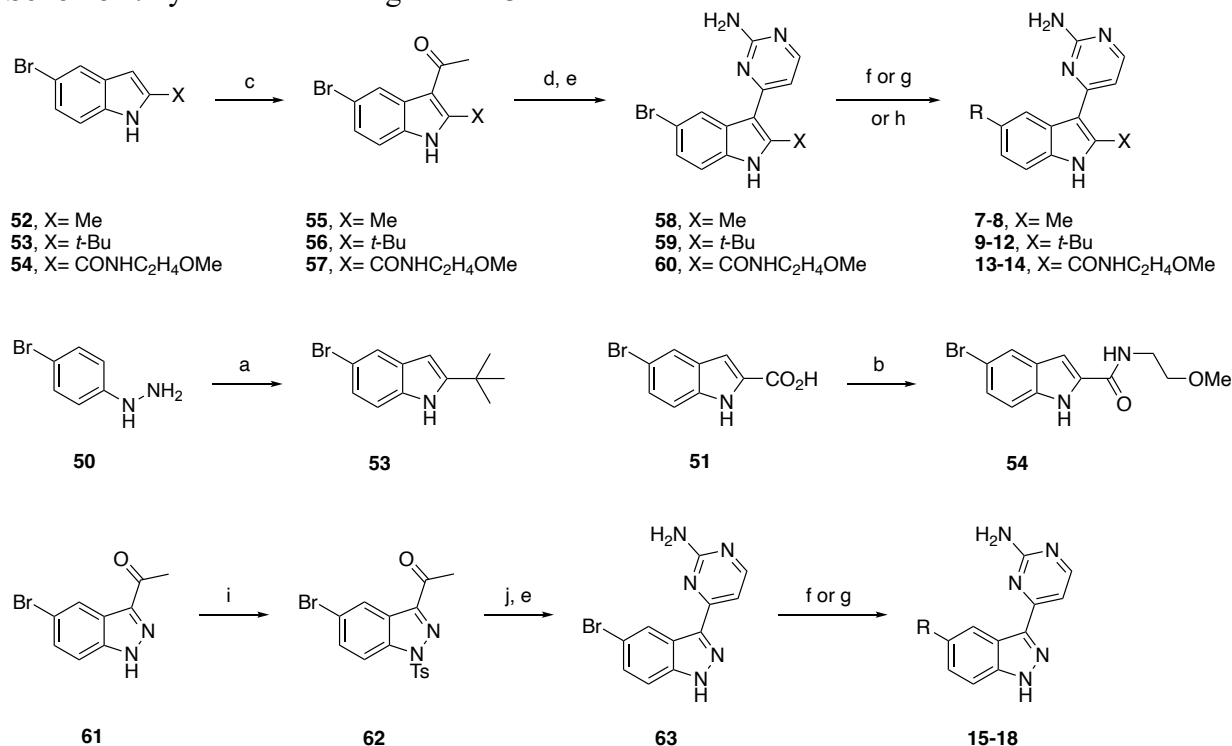
Scheme 1. Synthesis of analogues **1−6, 29–48**[a]
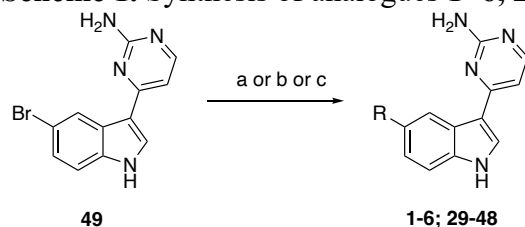
[a]Reagents and conditions: (a) alkyne R, Et$_3$N, Pd(PPh$_3$)$_4$, CuI, *N,N*-dimethylformamide (DMF), 85 °C, 18–22 h; (b) alkyne R, *N,N*-diisopropylamine (DIPA), PdCl$_2$(PPh$_3$)$_2$, CuI, 1-propanol, 85 °C, 16–23 h; (c) boronic acid R or boronic ester R, Pd(PPh$_3$)$_4$, K$_2$CO$_3$, dioxane/water, 85 °C, 16–22 h

Indole region analogues **7**–**18** were synthesized as shown in Scheme 2. Preparation of **55** began from commercially available bromoindole **52**, which was refluxed with Bredereck's reagent and then cyclized to the corresponding aminopyrimidine **58**. Similar routes were used to prepare intermediates **59** and **60** from indole **53** and carboxamide **54**, respectively. As shown in the middle of Scheme 2, both **53** and **54** required a Fischer indole synthesis for their preparation. Final Sonogashira and Suzuki cross coupling reactions were conducted to obtain compounds **7**–**14**.

Indazole analogues **15**–**18** were prepared following the procedure shown in the bottom of Scheme 2. Intermediate **62** was obtained from tosylation of 3-acetyl-5-bromo-1*H*-indazole **61**. Treatment of **62** with DMF-DMA followed by cyclization afforded intermediate **63**, which was converted to final analogues **15**–**18** via Sonogashira coupling conditions.

Scheme 2. Synthesis of analogues **7**−**18**[a]

52, X= Me
53, X= *t*-Bu
54, X= CONHC₂H₄OMe

55, X= Me
56, X= *t*-Bu
57, X= CONHC₂H₄OMe

58, X= Me
59, X= *t*-Bu
60, X= CONHC₂H₄OMe

7-8, X= Me
9-12, X= *t*-Bu
13-14, X= CONHC₂H₄OMe

50   **53**   **51**   **54**

61   **62**   **63**   **15-18**

[a]Reagents and conditions: (a) pinacolone, ZnCl₂, 190 °C, 1 h; (b) 2-methoxyethylamine, EDC, DMAP, DCM, 25 °C,18 h; (c) AlCl₃, Ac₂O, DCM, 0 to 25 °C, 15 h; (d) Bredereck's reagent, 105 °C, 17 h; (e) guanidine HCl, K₂CO₃, 2-methoxyethanol, 125 °C, 15–72 h; (f) alkyne R, Et₃N, Pd(PPh₃)₄, CuI, DMF, 85 °C, 16–22 h; (g) alkyne R, DIPA, PdCl₂(PPh₃)₂, CuI, 1-propanol, 85 °C, 16–21 h; (h) Boronic acid R or boronic ester R, Pd(PPh₃)₄, K₂CO₃, dioxane/water, 85 °C, 17–22 h; (i) TsCl, Et₃N, DMAP, DCM, 0 to 25 °C, 2 h; (j) DMF-DMA, 80 °C, 16 h

Next, we synthesized aminopyrimidine region analogues as shown in Scheme 3. Starting from 5-bromoindole **64**, a Friedel–Crafts acylation reaction was employed to generate **65**. A base-mediated nucleophilic substitution reaction with 2-methoxyethanol provided **66**, which was refluxed with Bredereck's reagent and then cyclized to aminopyrimidine **67**. Finally, Sonogashira coupling conditions were used to convert **67** to analogues **19**–**20**.

To prepare **21**, a different route was employed, which is included in the middle of Scheme 3. A dimethylamino alkyne group was installed on the indole using a Sonogashira coupling reaction to obtain **68**. Bromination was accomplished using NBS, and the indole nitrogen was protected to yield intermediate **70**. This intermediate was subsequently used in a Stille reaction with 4-(tributylstannyl)pyrimidine to provide **21**.

As shown in the bottom of Scheme 3, analogues **22**−**28** were synthesized from commercially available 6-bromo-1*H*-indole **71** or 6-bromo-1*H*-indazole **72**. These starting materials were reacted with chloropyrimidineamines (**73**−**76**) in the presence of Cs₂CO₃ to provide

intermediates **77−81**. Next, Sonogashira reaction conditions were employed to combine intermediates **77−81** with corresponding alkynes and afford the desired analogues.

Scheme 3. Synthetic route for analogues **19−28**[a]
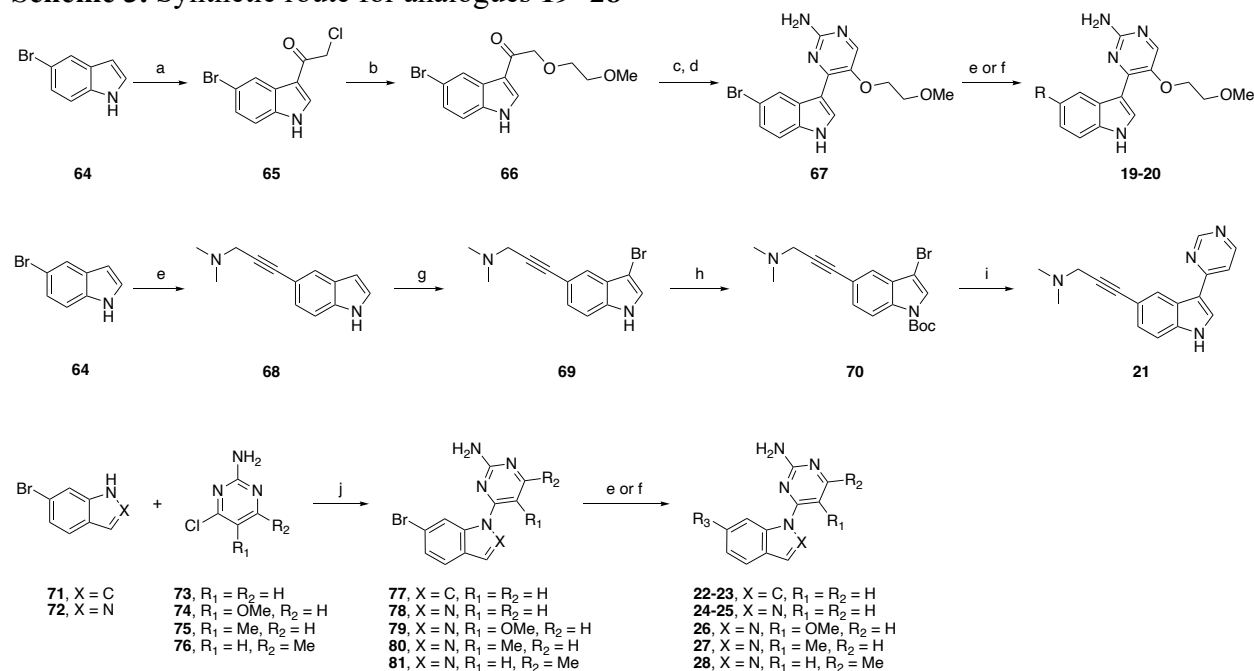
[a]Reagents and conditions: (a) chloroacetyl chloride, AlCl$_3$, DCM, 0 to 25 °C, 4 h; (b) 2-methoxyethanol, NaH, DMF, 0 to 25 °C, 6 h; (c) Bredereck's reagent, 105 °C, 17 h; (d) guanidine HCl, NaOMe/MeOH, 1-propanol, 95 °C, 42 h; (e) alkyne R, Et$_3$N, Pd(PPh$_3$)$_4$, CuI, DMF, 85 °C, 16–21 h; (f) alkyne R, DIPA, PdCl$_2$(PPh$_3$)$_2$, CuI, 1-propanol, 85 °C, 18–23 h; (g) NBS, DCM, 25 °C, 16 h; (h) Boc$_2$O, Et$_3$N, DMAP, DCM, 25 °C, 16 h; (i) 4-(tributylstannyl)pyrimidine, Pd(PPh$_3$)$_2$Cl$_2$, dioxane, 85 °C, 17 h; (j) Cs$_2$CO$_3$, DMF, 80 °C, 17–23 h

Conclusions

Based on our results, **40** represents a potent and selective PIKfyve inhibitor with sufficient *in vivo* stability and oral bioavailability to be used in animal studies and which does not elicit adverse side effects when mice are treated. Our previously disclosed negative control compound[16] can be utilized alongside this second-generation PIKfyve chemical probe, **40**, in efficacy studies. In summary, we provide an orthogonal scaffold to those that have been used to interrogate PIKfyve inhibition *in vivo* and which lacks a structural liability of the most advanced PIKfyve inhibitor, apilimod. The half-life of **40** (>5 hours) suggests that it may have optimal pharmacokinetic properties compared to apilimod, but more extensive studies are required to confirm this hypothesis. As a promising second-generation PIKfyve probe, compound **40** can be used to interrogate the effect of PIKfyve inhibition *in vivo* with the goal of identifying diseases that are responsive to this therapeutic approach.

Experimental Section
Chemistry. General Information.
All reagents and solvents were purchased from verified commercial suppliers and used without further purification. No unexpected safety hazards were faced during chemical synthesis.

Temperatures are reported in degrees Celsius (°C), and reactions were run at room temperature (25 °C) where no temperature is listed. Reactions were carried out under a nitrogen atmosphere unless otherwise noted. Once reactions were complete and worked up, where necessary, solvent was removed via a rotary evaporator under reduced pressure. Purification via column chromatography was performed using pre-loaded silica gel cartridges on a Biotage automated purification system. The following abbreviations are used in schemes and/or experimental procedures: equiv (equivalent(s)), h (hours), mmol (millimoles), mg (milligrams), min (minutes), μmol (micromoles), and r.t. (room temperature). ^{1}H NMR and additional microanalytical data was collected for intermediates and all final compounds to confirm their identity and assess their purity. ^{1}H and ^{13}C NMR spectra were obtained in DMSO-d_6, CD$_3$OD, CDCl$_3$, or CD$_3$CN and recorded using Bruker instruments. The strength of the magnet on the spectrometer used is included in each line listing. Chemical shifts are reported in parts per million (ppm) and calibrated versus the shift of the deuterated solvent used. Coupling constants (*J* values) are reported in hertz (Hz) and spin multiplicities are listed as follows: singlet (s), doublet (d), doublet of doublets/triplets/quartets (dd/dt/dq), doublet of doublet of doublets (ddd), triplet (t), triplet of doublets/triplets (td/tt), quartet (q), quartet of doublets (qd), pentent (p), and multiplet (m). HRMS samples were analyzed at the UNC Department of Chemistry Mass Spectrometry Core Laboratory using a Q Exactive HF-X mass spectrometer. Preparative HPLC was performed using an Agilent 1260 Infinity II LC System equipped with a Phenomenex C18 Phenyl-Hexyl column (30 °C, 5 μm particle size, 75 x 30 mm) or an Agilent 1100 Series System equipped with a Phenomenex Luna Phenyl-Hexyl column (5 μm particle size, 100 Å pore size, 75 × 30 mm). LCMS analyses were executed using an Agilent 1290 Infinity II LC System equipped with an Agilent Infinity Lab PoroShell 120 EC-C18 column (30 °C, 2.7 μm particle size, 2.1 × 50 mm), eluent 5−95% CH$_3$CN in water with 0.2% formic acid (v/v), and flow rate of 1 mL/min. All final compounds were determined to be >95% pure by HPLC analysis.

General Procedure A
A mixture of bromide (1 equiv), alkyne (1.5−5 equiv), and TEA (1−3 equiv) in DMF was degassed, followed by addition of Pd(PPh$_3$)$_4$ (0.1−0.2 equiv) and CuI (0.1−0.2 equiv). The reaction mixture was heated to 85 °C and stirred overnight. After completion of the reaction, the mixture was cooled to r.t., diluted with EtOAc, and passed through a thin pad of celite. The filtrate was concentrated *in vacuo* and the crude residue was purified by preparative HPLC (10−100% MeOH in H$_2$O + 0.05% TFA) to give the title compounds.

General Procedure B
A mixture of bromide (1 equiv), alkyne (1.5−5 equiv), and DIPA (1−3 equiv) in 1-propanol was degassed, followed by addition of PdCl$_2$(PPh$_3$)$_2$ (0.1−0.2 equiv) and CuI (0.1−0.2 equiv). The reaction mixture was heated to 85 °C and stirred overnight. After completion of the reaction, the mixture was cooled to r.t., diluted with EtOAc, and passed through a thin pad of celite. The filtrate was concentrated *in vacuo* and the crude residue was purified by preparative HPLC (10−100% MeOH in H$_2$O + 0.05% TFA) to give the title compounds.

General Procedure C
A mixture of bromide (1 equiv), boronic acid or boronic ester (1.2−2 equiv), and K$_2$CO$_3$ (2 equiv) in a mixture of dioxane and water (1.0−2.0 M) was degassed, followed by addition of Pd(PPh$_3$)$_4$ (0.05−0.1 equiv). The reaction mixture was heated to 85 °C and stirred overnight. After completion

of the reaction, the mixture was cooled to r.t., diluted with EtOAc and water. The organic layer was washed with brine and concentrated *in vacuo*. The crude residue was purified by preparative HPLC (10−100% MeOH in H_2O + 0.05% TFA) to give the title compounds.

4-(5-(3-(Dimethylamino)prop-1-yn-1-yl)-1H-indol-3-yl)pyrimidin-2-amine (1).

The reaction was carried out according to general procedure A starting from 4-(5-bromo-1*H*-indol-3-yl)pyrimidin-2-amine (40 mg, 0.14 mmol), *N,N*-dimethylprop-2-yn-1-amine (46 mg, 0.55 mmol), TEA (28 mg, 0.28 mmol), Pd(PPh$_3$)$_4$ (16 mg, 14 μmol), and CuI (2.6 mg, 14 μmol) in DMF (1.5 mL) at 85 °C overnight to afford the title compound (13 mg, 23% yield) as a TFA salt. ^{1}H NMR (400 MHz, CD$_3$OD) δ 8.88 (dd, J = 1.6, 0.8 Hz, 1H), 8.53 (s, 1H), 7.98 (d, J = 7.2 Hz, 1H), 7.54 (dd, J = 8.4, 0.8 Hz, 1H), 7.46 (dd, J = 8.4, 1.6 Hz, 1H), 7.35 (d, J = 7.2 Hz, 1H), 4.34 (s, 2H), 3.05 (s, 6H). ^{13}C NMR (101 MHz, CD$_3$OD) δ 170.53, 157.41, 143.79, 139.58, 136.42, 128.51, 128.38, 126.66, 116.00, 114.66, 113.83, 106.71, 92.67, 76.51, 49.29, 42.79 (2C). HPLC purity: 100%. HRMS (ESI): *m/z* calculated for C$_{17}$H$_{18}$N$_5$ [M + H]$^+$: 292.1562. Found: 292.1555.

4-(3-(2-Aminopyrimidin-4-yl)-1H-indol-5-yl)-2-methylbut-3-yn-2-ol (2).

The reaction was carried out according to general procedure B starting from 4-(5-bromo-1*H*-indol-3-yl)pyrimidin-2-amine (30 mg, 0.10 mmol), 2-methylbut-3-yn-2-ol (35 mg, 0.42 mmol), DIPA (21 mg, 0.21 mmol), PdCl$_2$(PPh$_3$)$_2$ (7.3 mg, 10 μmol), and CuI (2.0 mg, 10 μmol) in 1-propanol (1 mL) at 85 °C overnight to afford the title compound (5.0 mg, 16% yield). ^{1}H NMR (400 MHz, CD$_3$OD) δ 8.54 (dd, J = 1.6, 0.8 Hz, 1H), 8.10 (d, J = 5.6 Hz, 1H), 8.06 (s, 1H), 7.39 (dd, J = 8.4, 0.8 Hz, 1H), 7.24 (dd, J = 8.4, 1.6 Hz, 1H), 7.04 (d, J = 5.6 Hz, 1H), 1.60 (s, 6H). ^{13}C NMR (214 MHz, CD$_3$OD) δ 165.30, 164.65, 157.47, 138.40, 130.09, 127.03, 126.62, 126.52, 116.66, 115.49, 112.86, 107.46, 92.75, 84.27, 66.06, 31.95 (2C). HPLC purity: 100%. HRMS (ESI): *m/z* calculated for C$_{17}$H$_{17}$N$_4$O [M + H]$^+$: 293.1402. Found: 293.1394.

4-(3-(2-Aminopyrimidin-4-yl)-1H-indol-5-yl)but-3-yn-2-ol (3).

The reaction was carried out according to general procedure B starting from 4-(5-bromo-1*H*-indol-3-yl)pyrimidin-2-amine (30 mg, 0.10 mmol), but-3-yn-2-ol (22 mg, 0.31 mmol), DIPA (21 mg, 0.21 mmol), PdCl$_2$(PPh$_3$)$_2$ (7.3 mg, 10 μmol), and CuI (2.0 mg, 10 μmol) in 1-propanol (1 mL) at 85 °C overnight to afford the title compound (4.5 mg, 16% yield). ^{1}H NMR (400 MHz, CD$_3$OD) δ 8.76 (dd, J = 1.6, 0.8 Hz, 1H), 8.47 (s, 1H), 7.95 (d, J = 6.8 Hz, 1H), 7.46 (dd, J = 8.4, 0.8 Hz, 1H), 7.36–7.32 (m, 2H), 4.73 (q, J = 6.4 Hz, 1H), 1.53 (d, J = 6.4 Hz, 3H). ^{13}C NMR (126 MHz, CD$_3$OD) δ 170.63, 157.32, 143.45, 138.85, 136.09, 128.39, 127.44, 126.63, 118.45, 114.56, 113.45, 106.68, 90.85, 85.37, 59.23, 24.94. HPLC purity: 100%. HRMS (ESI): *m/z* calculated for C$_{16}$H$_{15}$N$_4$O [M + H]$^+$: 279.1246. Found: 279.1238.

1-(3-(2-Aminopyrimidin-4-yl)-1H-indol-5-yl)-3-ethylpent-1-yn-3-ol (4).

The reaction was carried out according to general procedure B starting from 4-(5-bromo-1*H*-indol-3-yl)pyrimidin-2-amine (30 mg, 0.10 mmol), 3-ethylpent-1-yn-3-ol (35 mg, 0.31 mmol), DIPA (21 mg, 0.21 mmol), PdCl$_2$(PPh$_3$)$_2$ (7.3 mg, 10 μmol), and CuI (2.0 mg, 10 μmol) in 1-propanol (1 mL) at 85 °C overnight to afford the title compound (7.5 mg, 23% yield). ^{1}H NMR (400 MHz, CD$_3$OD) δ 8.52 (dd, J = 1.6, 0.8 Hz, 1H), 8.11 (d, J = 5.6 Hz, 1H), 8.05 (s, 1H), 7.39 (dd, J = 8.4, 0.8 Hz, 1H), 7.26 (dd, J = 8.4, 1.6 Hz, 1H), 7.04 (d, J = 5.2 Hz, 1H), 1.85 – 1.70 (m, 4H), 1.13 (t, J = 7.2 Hz, 6H). ^{13}C NMR (101 MHz, CD$_3$OD) δ 165.24, 164.63, 157.51, 138.38, 130.08, 127.13,

126.58, 126.36, 116.76, 115.50, 112.89, 107.56, 90.62, 86.74, 73.29, 35.56 (2C), 9.16 (2C). HPLC purity: >98%. HRMS (ESI): *m/z* calculated for $C_{19}H_{21}N_4O$ [M + H]$^+$: 321.1715. Found: 321.1712.

4-(5-((1-Methyl-1H-imidazol-5-yl)ethynyl)-1H-indol-3-yl)pyrimidin-2-amine (5).

The reaction was carried out according to general procedure A starting from 4-(5-bromo-1*H*-indol-3-yl)pyrimidin-2-amine (30 mg, 0.10 mmol), 5-ethynyl-1-methyl-1*H*-imidazole (44 mg, 0.42 mmol), TEA (21 mg, 0.21 mmol), Pd(PPh$_3$)$_4$ (12 mg, 10 μmol), and CuI (2.0 mg, 10 μmol) in DMF (1 mL) at 85 °C overnight to afford the title compound (16 mg, 37% yield) as a TFA salt. ^{1}H NMR (400 MHz, CD$_3$OD) δ 8.96 (m, 1H), 8.95 (dd, *J* = 1.2, 0.8 Hz, 1H), 8.53 (s, 1H), 7.97 (d, *J* = 7.2 Hz, 1H), 7.83 (d, *J* = 1.6 Hz, 1H), 7.58 (dd, *J* = 8.4, 0.8 Hz, 1H), 7.53 (dd, *J* = 8.4, 1.6 Hz, 1H), 7.33 (d, *J* = 7.2 Hz, 1H), 4.03 (d, *J* = 0.4 Hz, 3H). ^{13}C NMR (126 MHz, CD$_3$OD) δ 170.60, 157.37, 143.73, 139.77, 137.85, 136.60, 128.34, 128.28, 126.76, 125.20, 120.25, 115.91, 114.74, 114.02, 106.73, 101.27, 72.83, 34.44. HPLC purity: 100%. HRMS (ESI): *m/z* calculated $C_{18}H_{15}N_6$ for [M + H]$^+$: 315.1358. Found: 315.1350.

4-(5-(4-Fluorophenyl)-1H-indol-3-yl)pyrimidin-2-amine (6).

The reaction was carried out according to general procedure C starting from 4-(5-bromo-1*H*-indol-3-yl)pyrimidin-2-amine (20 mg, 69 μmol), (4-fluorophenyl)boronic acid (15 mg, 0.10 mmol), K$_2$CO$_3$ (19 mg, 0.14 mmol), and Pd(PPh$_3$)$_4$ (4.0 mg, 3.5 μmol) in a mixture of 1,4-dioxane (0.7 mL) and water (0.1 mL) at 85 °C overnight to afford the title compound (9.3 mg, 44% yield). ^{1}H NMR (400 MHz, CD$_3$OD) δ 8.81 (dd, *J* = 1.6, 0.8 Hz, 1H), 8.46 (s, 1H), 7.93 (d, *J* = 6.8 Hz, 1H), 7.76–7.71 (m, 2H), 7.58–7.52 (m, 2H), 7.33 (d, *J* = 6.8 Hz, 1H), 7.21–7.15 (m, 2H). ^{13}C NMR (101 MHz, DMSO-*d*$_6$) δ 167.80, 162.72, 160.30, 156.11, 137.71, 136.99, 135.08, 133.63, 129.08, 129.00, 125.72, 122.61, 120.41, 115.56, 115.35, 112.99, 112.95, 105.19. HPLC purity: 100%. HRMS (ESI): *m/z* calculated for $C_{18}H_{14}N_4F$ [M + H]$^+$: 305.1202. Found: 305.1196.

5-Bromo-2-(tert-butyl)-1H-indole (53).

The mixture of (4-bromophenyl)hydrazine (155 mg, 829 μmol), 3,3-dimethylbutan-2-one (664 mg, 6.63 mmol), and zinc (II) chloride (452 mg, 3.31 mmol) was heated at 190 °C for 1 h. After the completion of the reaction as indicated by TLC, the reaction mixture was cooled to r.t., diluted with water, extracted with EtOAc. The combined organic phases were washed with brine and dried over Na$_2$SO$_4$. The residue was purified with column chromatography (SiO$_2$, 0−5% EtOAc in hexane) to yield the title compound (84 mg, 40% yield). ^{1}H NMR (400 MHz, CDCl$_3$) δ 7.97 (s, 1H), 7.65 (dt, *J* = 1.6, 0.8 Hz, 1H), 7.21–7.16 (m, 2H), 6.20 (dd, *J* = 2.0, 0.8 Hz, 1H), 1.39 (s, 9H). ^{13}C NMR (101 MHz, CDCl$_3$) δ 150.30, 134.51, 130.49, 123.95, 122.59, 112.86, 111.88, 96.87, 32.02, 30.36 (3C). HRMS (ESI): *m/z* calculated $C_{12}H_{15}BrN$ for [M + H]$^+$: 252.0388. Found: 252.0382.

5-Bromo-N-(2-methoxyethyl)-1H-indole-2-carboxamide (54).

A mixture of 5-bromo-1*H*-indole-2-carboxylic acid (700 mg, 2.92 mmol), 2-methoxyethan-1-amine (263 mg, 3.50 mmol), EDC (671 mg, 3.50 mmol), and DMAP (570 mg, 4.67 mmol) in DCM (15 mL) was stirred at r.t. for 18 h. The mixture was concentrated under reduced pressure and the residue was dissolved in EtOAc. The organic phase was washed with 2N HCl, water, and saturated aq. NaHCO$_3$, dried over Na$_2$SO$_4$, and concentrated in vacuo. The residue was purified with flash column chromatography (SiO$_2$, 0−3% MeOH in DCM) to obtain the title compound (477.2 mg, 55% yield). ^{1}H NMR (400 MHz, DMSO-*d*$_6$) δ 11.77 (s, 1H), 8.60 (t, *J* = 5.6 Hz, 1H),

7.83 (d, J = 2.0 Hz, 1H), 7.38 (d, J = 8.4 Hz, 1H), 7.28 (dd, J = 8.4, 2.0 Hz, 1H), 7.11 (d, J = 2.0 Hz, 1H), 3.49–3.42 (m, 4H), 3.28 (s, 3H). ^{13}C NMR (126 MHz, DMSO-d_6) δ 160.76, 134.97, 133.01, 128.88, 125.80, 123.64, 114.29, 112.11, 101.96, 70.52, 57.93, 38.64. HRMS (ESI): m/z calculated $C_{12}H_{14}BrN_2O_2$ for [M + H]$^+$: 297.0239. Found: 297.0231.

General Procedure D
To a cooled (0 °C) solution of aluminum chloride (3 equiv) in DCM was added dropwise acetic anhydride (3 equiv) for 30 min. To the cooled mixture was added a suspension of the corresponding bromo indole (1 equiv) in DCM at 0 °C and the mixture was stirred at r.t. overnight. The reaction mixture was poured into ice saturated NH$_4$Cl, and the aqueous layer was extracted with DCM. The organic extracts were washed with brine and dried over Na$_2$SO$_4$, and the residue was purified with flash column chromatography (SiO$_2$, 0−20% EtOAc in hexane or 0−10% MeOH in DCM) to obtain the title compounds.

1-(5-Bromo-2-methyl-1H-indol-3-yl)ethan-1-one (55).
The reaction was carried out according to general procedure D starting from 5-bromo-2-methyl-1H-indole (1 g, 4.760 mmol), aluminum chloride (1.904 g, 14.28 mmol), and acetic anhydride (1.458 g, 14.28 mmol) in DCM (20 mL) at r.t. overnight to afford the title compound (780 mg, 65% yield). ^{1}H NMR (400 MHz, DMSO-d_6) δ 12.14 (s, 1H), 8.19 (d, J = 2.0 Hz, 1H), 7.34 (d, J = 8.4 Hz, 1H), 7.26 (dd, J = 8.8, 2.0 Hz, 1H), 2.69 (s, 3H), 2.49 (s, 3H). ^{13}C NMR (101 MHz, DMSO-d_6) δ 192.94, 145.47, 133.43, 128.82, 124.30, 122.85, 114.12, 113.17, 113.11, 30.69, 15.03. HRMS (ESI): m/z calculated $C_{11}H_{11}BrNO$ for [M + H]$^+$: 252.0024. Found: 252.0018.

1-(5-Bromo-2-(tert-butyl)-1H-indol-3-yl)ethan-1-one (56).
The reaction was carried out according to general procedure D starting from 5-bromo-2-(tert-butyl)-1H-indole (288 mg, 1.14 mmol), aluminum chloride (457 mg, 3.43 mmol), and acetic anhydride (350 mg, 3.43 mmol) in DCM (11 mL) at r.t. overnight to afford the title compound (119 mg, 35% yield). ^{1}H NMR (400 MHz, CDCl$_3$) δ 8.77 (s, 1H), 7.96 (d, J = 1.6 Hz, 1H), 7.32–7.25 (m, 2H), 2.70 (s, 3H), 1.54 (s, 9H). ^{13}C NMR (101 MHz, CDCl$_3$) δ 195.06, 154.57, 131.98, 129.85, 125.09, 123.30, 115.49, 113.90, 112.82, 34.29, 32.79, 28.49 (3C). HRMS (ESI): m/z calculated $C_{14}H_{17}BrNO$ for [M + H]$^+$: 294.0494. Found: 294.0486.

3-Acetyl-5-bromo-N-(2-methoxyethyl)-1H-indole-2-carboxamide (57).
The reaction was carried out according to general procedure D starting from 5-bromo-N-(2-methoxyethyl)-1H-indole-2-carboxamide (393 mg, 1.32 mmol), aluminum chloride (529 mg, 3.97 mmol), and acetic anhydride (405 mg, 3.97 mmol) in DCM (13 mL) at r.t. overnight to afford the title compound (421.7 mg, 94% yield). ^{1}H NMR (400 MHz, DMSO-d_6) δ 12.76 (s, 1H), 10.29 (s, 1H), 8.23 (d, J = 2.0 Hz, 1H), 7.52 (dd, J = 8.4, 0.8 Hz, 1H), 7.45 (dd, J = 8.4, 2.0 Hz, 1H), 3.54–3.52 (m, 4H), 3.30 (s, 3H), 2.65 (s, 3H). ^{13}C NMR (126 MHz, DMSO-d_6) δ 195.18, 160.32, 138.13, 133.39, 127.85, 126.74, 124.23, 115.37, 114.97, 113.61, 70.16, 57.98, 39.13, 30.64. HRMS (ESI): m/z calculated $C_{14}H_{16}BrN_2O_3$ for [M + H]$^+$: 339.0344. Found: 339.0339.

General Procedure E
Indole or indazole intermediates were treated neat with Bredereck's reagent (2−3.5 equiv) at 105 °C under N$_2$ overnight. After cooling, to this mixture was added 2-methoxyethanol or 1-propanol, anhydrous potassium carbonate (3.5 equiv) or sodium methoxide (3 equiv), and guanidine

hydrochloride (2.5−5 equiv). The reaction mixture was refluxed for 15−72 h. The solution was poured into water and then extracted with EtOAc. The organic layer was washed with brine and dried over Na_2SO_4, and the residue was purified with flash column chromatography (SiO_2, 0−5% MeOH in DCM) to obtain the title compounds.

4-(5-Bromo-2-methyl-1H-indol-3-yl)pyrimidin-2-amine (58).

The reaction was carried out according to general procedure E starting from 1-(5-bromo-2-methyl-1*H*-indol-3-yl)ethan-1-one (**55**) (227 mg, 0.9 mmol) and Bredereck's reagent (314 mg, 1.8 mmol) at 105 °C overnight, and then anhydrous potassium carbonate (436 mg, 3.16 mmol) and guanidine hydrochloride (215 mg, 2.25 mmol) in 2-methoxyethanol (9 mL) at reflux to afford the title compound (213.2 mg, 78% yield). ^{1}H NMR (400 MHz, CD_3OD) δ 8.23 (dd, J = 1.6, 0.8 Hz, 1H), 8.18 (d, J = 5.6 Hz, 1H), 7.25–7.20 (m, 2H), 6.87 (d, J = 5.2 Hz, 1H), 2.68 (s, 3H). ^{13}C NMR (101 MHz, CD_3OD) δ 165.37, 164.44, 157.85, 141.19, 135.74, 130.05, 125.39, 123.65, 114.76, 113.35, 111.26, 109.79, 14.23. HRMS (ESI): m/z calculated $C_{13}H_{12}BrN_4$ for [M + H]$^+$: 303.0245. Found: 303.0239.

4-(5-Bromo-2-(tert-butyl)-1H-indol-3-yl)pyrimidin-2-amine (59).

The reaction was carried out according to general procedure E starting from 1-(5-bromo-2-(*tert*-butyl)-1*H*-indol-3-yl)ethan-1-one (**56**) (167 mg, 568 µmol) and Bredereck's reagent (198 mg, 1.14 mmol) at 105 °C overnight, and then anhydrous potassium carbonate (274 mg, 1.98 mmol) and guanidine hydrochloride (135 mg, 1.42 mmol) in 2-methoxyethanol (5 mL) at reflux to afford the title compound (118 mg, 60% yield). ^{1}H NMR (400 MHz, DMSO-d_6) δ 11.15 (s, 1H), 8.24 (d, J = 4.8 Hz, 1H), 7.38 (d, J = 2.0 Hz, 1H), 7.35 (d, J = 8.4 Hz, 1H), 7.18 (dd, J = 8.4, 2.0 Hz, 1H), 6.64 (d, J = 4.8 Hz, 1H), 6.51 (s, 2H), 1.39 (s, 9H). ^{13}C NMR (101 MHz, DMSO-d_6) δ 163.86, 163.48, 157.54, 146.85, 132.98, 129.82, 123.35, 120.00, 113.10, 111.82, 111.76, 110.32, 33.45, 30.45 (3C). HRMS (ESI): m/z calculated $C_{16}H_{18}BrN_4$ for [M + H]$^+$: 345.0715. Found: 345.0707.

3-(2-Aminopyrimidin-4-yl)-5-bromo-N-(2-methoxyethyl)-1H-indole-2-carboxamide (60).

The reaction was carried out according to general procedure E starting from 3-acetyl-5-bromo-*N*-(2-methoxyethyl)-1*H*-indole-2-carboxamide (**57**) (150 mg, 442 µmol) and Bredereck's reagent (270 mg, 1.55 mmol) at 105 °C overnight, and then sodium methoxide (2.65 mL, 0.5 M in methanol, 1.32 mmol) and guanidine hydrochloride (211 mg, 2.21 mmol) in 1-propanol (2 mL) at reflux to afford the title compound (140 mg, 81% yield). ^{1}H NMR (400 MHz, DMSO-d_6) δ 12.33 (s, 1H), 11.14 (s, 1H), 8.39 (d, J = 5.2 Hz, 1H), 8.04 (d, J = 1.6 Hz, 1H), 7.51 (d, J = 8.8 Hz, 1H), 7.41 (dd, J = 8.8, 2.0 Hz, 1H), 7.00 (d, J = 5.2 Hz, 1H), 6.84 (s, 2H), 3.58–3.54 (m, 4H), 3.28 (s, 3H). ^{13}C NMR (126 MHz, DMSO-d_6) δ 163.14, 160.85, 160.18, 160.02, 134.25, 133.03, 128.22, 127.15, 123.38, 115.41, 114.33, 112.28, 110.24, 71.03, 58.26, 39.20. HRMS (ESI): m/z calculated $C_{16}H_{17}BrN_5O_2$ for [M + H]$^+$: 390.0566. Found: 390.0558.

4-(5-(3-(Dimethylamino)prop-1-yn-1-yl)-2-methyl-1H-indol-3-yl)pyrimidin-2-amine (7).

The reaction was carried out according to general procedure A starting from 4-(5-bromo-2-methyl-1*H*-indol-3-yl)pyrimidin-2-amine (**58**) (40 mg, 0.13 mmol), *N,N*-dimethylprop-2-yn-1-amine (44 mg, 0.53 mmol), TEA (27 mg, 0.26 mmol), Pd(PPh$_3$)$_4$ (15 mg, 13 µmol), and CuI (2.5 mg, 13 µmol) in DMF (1.5 mL) at 85 °C overnight to afford the title compound (5.8 mg, 11% yield) as a TFA salt. ^{1}H NMR (400 MHz, CD_3OD) δ 8.56 (t, J = 1.2 Hz, 1H), 8.05 (d, J = 7.2 Hz, 1H), 7.43–7.37 (m, 2H), 7.23 (d, J = 7.2 Hz, 1H), 4.32 (s, 2H), 3.04 (s, 6H), 2.82 (s, 3H). ^{13}C NMR (126

MHz, CD$_3$OD) δ 170.50, 156.96, 148.35, 144.76, 137.72, 128.20, 127.80, 126.73, 115.55, 112.91, 111.02, 108.12, 92.82, 76.31, 49.11, 42.78 (2C), 15.85. HPLC purity: >98%. HRMS (ESI): *m/z* calculated C$_{18}$H$_{20}$N$_5$ for [M + H]$^+$: 306.1719. Found: 306.1711.

*4-(5-(4-Fluorophenyl)-2-methyl-1H-indol-3-yl)pyrimidin-2-amine (**8**).*
The reaction was carried out according to general procedure C starting from 4-(5-bromo-2-methyl-1*H*-indol-3-yl)pyrimidin-2-amine (**58**) (20 mg, 66 μmol), (4-fluorophenyl)boronic acid (14 mg, 99 μmol), K$_2$CO$_3$ (18 mg, 0.13 mmol), and Pd(PPh$_3$)$_4$ (3.8 mg, 3.3 μmol) in a mixture of 1,4-dioxane (0.7 mL) and water (0.1 mL) at 85 °C overnight to afford the title compound (5.8 mg, 28% yield). ^{1}H NMR (400 MHz, CD$_3$OD) δ 8.45 (t, *J* = 1.2 Hz, 1H), 8.03 (d, *J* = 7.2 Hz, 1H), 7.72–7.67 (m, 2H), 7.47 (d, *J* = 1.2 Hz, 2H), 7.31 (d, *J* = 7.2 Hz, 1H), 7.20–7.14 (m, 2H), 2.85 (s, 3H). ^{13}C NMR (126 MHz, CD$_3$OD) δ 164.58, 162.64, 156.74, 147.92, 144.30, 139.94, 136.85, 136.21, 130.23, 130.17, 128.79, 123.62, 120.47, 116.41, 116.24, 112.87, 111.26, 108.21, 16.05. HPLC purity: >96%. HRMS (ESI): *m/z* calculated for C$_{19}$H$_{16}$N$_4$F [M + H]$^+$: 319.1359. Found: 319.1351.

*4-(2-(tert-Butyl)-5-(3-(dimethylamino)prop-1-yn-1-yl)-1H-indol-3-yl)pyrimidin-2-amine (**9**).*
The reaction was carried out according to general procedure B starting from 4-(5-bromo-2-(*tert*-butyl)-1*H*-indol-3-yl)pyrimidin-2-amine (**59**) (30 mg, 87 μmol), *N*,*N*-dimethylprop-2-yn-1-amine (29 mg, 0.35 mmol), DIPA (18 mg, 0.17 mmol), PdCl$_2$(PPh$_3$)$_2$ (12 mg, 17 μmol), and CuI (3.3 mg, 17 μmol) in 1-propanol (1 mL) at 85 °C overnight to afford the title compound (11.3 mg, 28% yield) as a TFA salt. ^{1}H NMR (400 MHz, CD$_3$OD) δ 8.25 (d, *J* = 6.4 Hz, 1H), 7.82 (s, 1H), 7.50 (dd, *J* = 8.4, 0.4 Hz, 1H), 7.35 (dd, *J* = 8.4, 1.6 Hz, 1H), 7.20 (d, *J* = 6.4 Hz, 1H), 4.30 (s, 2H), 3.02 (s, 6H), 1.56 (s, 9H). ^{13}C NMR (101 MHz, CD$_3$OD) δ 171.53, 157.58, 153.87, 147.97, 136.79, 129.01, 127.12, 123.84, 114.58, 113.21, 112.72, 110.32, 92.73, 76.13, 48.73, 42.72 (2C), 35.38, 30.69 (3C). HPLC purity: 100%. HRMS (ESI): *m/z* calculated for C$_{21}$H$_{26}$N$_5$ [M + H]$^+$: 348.2188. Found: 348.2181.

*4-(3-(2-Aminopyrimidin-4-yl)-2-(tert-butyl)-1H-indol-5-yl)-2-methylbut-3-yn-2-ol (**10**).*
The reaction was carried out according to general procedure B starting from 4-(5-bromo-2-(*tert*-butyl)-1*H*-indol-3-yl)pyrimidin-2-amine (**59**) (25 mg, 72 μmol), 2-methylbut-3-yn-2-ol (24 mg, 0.29 mmol), DIPA (15 mg, 0.14 mmol), PdCl$_2$(PPh$_3$)$_2$ (10 mg, 14 μmol), and CuI (2.8 mg, 14 μmol) in 1-propanol (0.8 mL) at 85 °C overnight to afford the title compound (2.5 mg, 10% yield). ^{1}H NMR (400 MHz, CD$_3$OD) δ 8.25 (d, *J* = 5.6 Hz, 1H), 7.51 (dd, *J* = 1.6, 0.8 Hz, 1H), 7.37 (dd, *J* = 8.4, 0.4 Hz, 1H), 7.18 (dd, *J* = 8.4, 1.6 Hz, 1H), 7.00 (d, *J* = 5.6 Hz, 1H), 1.55 (s, 6H), 1.49 (s, 9H). ^{13}C NMR (214 MHz, CD$_3$OD) δ 167.40, 164.40, 158.46, 147.89, 135.77, 129.67, 125.96, 122.73, 115.40, 114.36, 111.92, 111.56, 92.31, 84.23, 66.00, 34.78, 31.92 (2C), 31.17 (3C). HPLC purity: >95%. HRMS (ESI): *m/z* calculated for C$_{21}$H$_{25}$N$_4$O [M + H]$^+$: 349.2028. Found: 349.2022.

*4-(3-(2-Aminopyrimidin-4-yl)-2-(tert-butyl)-1H-indol-5-yl)but-3-yn-2-ol (**11**).*
The reaction was carried out according to general procedure B starting from 4-(5-bromo-2-(*tert*-butyl)-1*H*-indol-3-yl)pyrimidin-2-amine (**59**) (25 mg, 72 μmol), but-3-yn-2-ol (20 mg, 0.29 mmol), DIPA (15 mg, 0.14 mmol), PdCl$_2$(PPh$_3$)$_2$ (10 mg, 14 μmol), and CuI (2.8 mg, 14 μmol) in 1-propanol (0.8 mL) at 85 °C overnight to afford the title compound (1.7mg, 7% yield). ^{1}H NMR (500 MHz, CD$_3$OD) δ 8.27 (d, *J* = 5.0 Hz, 1H), 7.36 (dd, *J* = 1.5, 0.5 Hz, 1H), 7.32 (dd, *J* = 8.5, 0.5 Hz, 1H), 7.15 (dd, *J* = 8.0, 1.5 Hz, 1H), 6.79 (d, *J* = 5.0 Hz, 1H), 4.66 (q, *J* = 6.5 Hz, 1H), 1.47 (d, *J* = 6.5 Hz, 3H), 1.43 (s, 9H). ^{13}C NMR (214 MHz, CD$_3$OD) δ 167.36, 164.40, 158.46, 147.95,

135.83, 129.66, 125.98, 122.83, 115.29, 114.33, 111.94, 111.57, 89.57, 85.86, 59.19, 34.79, 31.16 (3C), 24.97. HPLC purity: >95%. HRMS (ESI): m/z calculated for $C_{20}H_{23}N_4O$ [M + H]$^+$: 335.1872. Found: 335.1865.

*1-(3-(2-Aminopyrimidin-4-yl)-2-(tert-butyl)-1H-indol-5-yl)-3-methylpent-1-yn-3-ol (**12**).*
The reaction was carried out according to general procedure B starting from 4-(5-bromo-2-(*tert*-butyl)-1*H*-indol-3-yl)pyrimidin-2-amine (**59**) (30 mg, 87 μmol), 3-methylpent-1-yn-3-ol (34 mg, 0.35 mmol), DIPA (18 mg, 0.17 mmol), PdCl$_2$(PPh$_3$)$_2$ (12 mg, 17 μmol), and CuI (3.3 mg, 17 μmol) in 1-propanol (0.9 mL) at 85 °C overnight to afford the title compound (10 mg, 32% yield). ^{1}H NMR (400 MHz, DMSO-d_6) δ 11.11 (s, 1H), 8.25 (s, 1H), 7.35 (dd, J = 8.4, 0.8 Hz, 1H), 7.27 (d, J = 1.6 Hz, 1H), 7.08 (dd, J = 8.4, 1.6 Hz, 1H), 6.64 (d, J = 4.8 Hz, 1H), 6.51 (s, 2H), 5.21 (s, 1H), 1.67–1.57 (m, 2H), 1.39 (s, 12H), 0.98 (t, J = 7.2 Hz, 3H). ^{13}C NMR (101 MHz, CD$_3$CN) δ 165.58, 164.54, 158.62, 147.86, 134.90, 129.33, 125.84, 122.64, 118.30, 115.16, 112.13, 111.95, 91.99, 84.81, 69.15, 37.60, 34.43, 30.76 (3C), 29.91, 9.52. HPLC purity: >95%. HRMS (ESI): m/z calculated for $C_{22}H_{27}N_4O$ [M + H]$^+$: 363.2185. Found: 363.2179.

*3-(2-Aminopyrimidin-4-yl)-5-(3-(dimethylamino)prop-1-yn-1-yl)-N-(2-methoxyethyl)-1H-indole-2-carboxamide (**13**).*
The reaction was carried out according to general procedure A starting from 3-(2-aminopyrimidin-4-yl)-5-bromo-*N*-(2-methoxyethyl)-1*H*-indole-2-carboxamide (**60**) (30 mg, 77 μmol), *N*,*N*-dimethylprop-2-yn-1-amine (26 mg, 0.31 mmol), TEA (16 mg, 0.15 mmol), Pd(PPh$_3$)$_4$ (8.9 mg, 7.7 μmol), and CuI (1.5 mg, 7.7 μmol) in DMF (1 mL) at 85 °C overnight to afford the title compound (5.8 mg, 14% yield) as a TFA salt. ^{1}H NMR (400 MHz, CD$_3$OD) δ 8.34 (m, 1H), 8.30 (d, J = 6.4 Hz, 1H), 7.59 (dd, J = 8.4, 0.8 Hz, 1H), 7.49 (dd, J = 8.4, 1.6 Hz, 1H), 7.26 (d, J = 6.0 Hz, 1H), 4.33 (s, 2H), 3.70–3.64 (m, 4H), 3.42 (s, 3H), 3.04 (s, 6H). ^{13}C NMR (101 MHz, CD$_3$OD) δ 165.51, 162.95, 160.81, 153.93, 137.18, 136.24, 129.16, 127.57, 127.10, 115.77, 114.36, 113.48, 110.94, 92.27, 76.86, 72.06, 58.75, 48.73, 42.82 (2C), 40.47. HPLC purity: >98%. HRMS (ESI): m/z calculated $C_{21}H_{25}N_6O_2$ for [M + H]$^+$: 393.2039. Found: 393.2032.

*3-(2-Aminopyrimidin-4-yl)-5-(3-hydroxy-3-methylbut-1-yn-1-yl)-N-(2-methoxyethyl)-1H-indole-2-carboxamide (**14**).*
The reaction was carried out according to general procedure B starting from 3-(2-aminopyrimidin-4-yl)-5-bromo-*N*-(2-methoxyethyl)-1*H*-indole-2-carboxamide (**60**) (30 mg, 77 μmol), 2-methylbut-3-yn-2-ol (26 mg, 0.31 mmol), DIPA (16 mg, 0.15 mmol), PdCl$_2$(PPh$_3$)$_2$ (5.4 mg, 7.7 μmol), and CuI (1.5 mg, 7.7 μmol) in 1-propanol (1 mL) at 85 °C overnight to afford the title compound (8 mg, 26% yield). ^{1}H NMR (400 MHz, CD$_3$OD) δ 8.24–8.22 (m, 2H), 7.51 (dd, J = 8.8, 0.8 Hz, 1H), 7.38 (dd, J = 8.8, 1.6 Hz, 1H), 7.31 (d, J = 6.4 Hz, 1H), 3.70–3.64 (m, 4H), 3.42 (s, 3H), 1.59 (s, 6H). ^{13}C NMR (214 MHz, CD$_3$OD) δ 167.30, 163.16, 158.90, 150.56, 136.92, 136.51, 129.34, 127.49, 125.94, 118.73, 114.07, 112.74, 110.66, 94.10, 83.36, 71.96, 66.01, 58.75, 40.49, 31.84 (2C). HPLC purity: 100%. HRMS (ESI): m/z calculated for $C_{21}H_{24}N_5O_3$ [M + H]$^+$: 394.1879. Found: 394.1871.

*1-(5-Bromo-1-tosyl-1H-indazol-3-yl)ethan-1-one (**62**).*
To a solution of 1-(5-bromo-1*H*-indazol-3-yl)ethan-1-one (500 mg, 2.09 mmol), DMAP (63.9 mg, 523 μmol), and TEA (783 mg, 7.74 mmol) in DCM (20 mL) was added *p*-toluenesulfonyl chloride (598 mg, 3.14 mmol) at 0 °C and stirred at r.t. for 2 h. The reaction mixture was diluted with DCM,

and washed with saturated NaHCO$_3$, water and brine. The combined organic layers were dried over Na$_2$SO$_4$ and concentrated *in vacuo* to afford the title compound (800 mg, 97% yield), which was used in the next step without further purification.

4-(5-Bromo-1H-indazol-3-yl)pyrimidin-2-amine (63).
A solution of 1-(5-bromo-1-tosyl-1*H*-indazol-3-yl)ethan-1-one (**62**) (800 mg, 2.03 mmol) in DMF-DMA (10 mL) was stirred at 80 °C overnight and concentrated *in vacuo*. To this mixture was added guanidine hydrochloride (486 mg, 5.09 mmol), potassium carbonate (984 mg, 7.12 mmol), and 2-methoxyethanol (20 mL). The reaction mixture was refluxed for 22 h, poured into water, and then extracted with EtOAc. The organic layer was washed with brine and dried over Na$_2$SO$_4$, and the residue was purified with flash column chromatography on SiO$_2$ with 0−5 % MeOH in DCM to obtain the title compound (164 mg, 28% yield). ^{1}H NMR (400 MHz, DMSO-d_6) δ 13.72 (s, 1H), 8.86 (dd, J = 1.6, 0.8 Hz, 1H), 8.29 (d, J = 5.2 Hz, 1H), 7.60 (dd, J = 8.8, 0.8 Hz, 1H), 7.53 (dd, J = 8.8, 1.6 Hz, 1H), 7.25 (d, J = 4.8 Hz, 1H), 6.80 (s, 2H). ^{13}C NMR (101 MHz, DMSO-d_6) δ 163.69, 160.28, 158.39, 140.86, 140.18, 129.32, 125.33, 122.55, 114.39, 112.62, 105.15. HRMS (ESI): *m/z* calculated C$_{11}$H$_9$BrN$_5$ for [M + H]$^+$: 290.0041. Found: 290.0031.

4-(5-(3-(Dimethylamino)prop-1-yn-1-yl)-1H-indazol-3-yl)pyrimidin-2-amine (15).
The reaction was carried out according to general procedure A starting from 4-(5-bromo-1*H*-indazol-3-yl)pyrimidin-2-amine (**63**) (30 mg, 0.10 mmol), *N*,*N*-dimethylprop-2-yn-1-amine (26 mg, 0.31 mmol), TEA (21 mg, 0.21 mmol), Pd(PPh$_3$)$_4$ (12 mg, 10 μmol), and CuI (2.0 mg, 10 μmol) in DMF (1 mL) at 85 °C overnight to afford the title compound (12 mg, 30% yield) as a TFA salt. ^{1}H NMR (400 MHz, CD$_3$OD) δ 8.91 (t, J = 1.2 Hz, 1H), 8.26 (d, J = 6.4 Hz, 1H), 7.73–7.69 (m, 2H), 7.62 (dd, J = 8.4, 1.6 Hz, 1H), 4.36 (s, 2H), 3.06 (s, 6H). ^{13}C NMR (101 MHz, CD$_3$OD) δ 169.21, 158.06, 146.58, 143.27, 141.49, 131.69, 128.82, 123.11, 117.39, 112.62, 107.07, 91.51, 77.66, 49.50, 42.85 (2C). HPLC purity: 100%. HRMS (ESI): *m/z* calculated C$_{16}$H$_{17}$N$_6$ for [M + H]$^+$: 293.1515. Found: 293.1507.

4-(3-(2-Aminopyrimidin-4-yl)-1H-indazol-5-yl)-2-methylbut-3-yn-2-ol (16).
The reaction was carried out according to general procedure B starting from 4-(5-bromo-1*H*-indazol-3-yl)pyrimidin-2-amine (**63**) (25 mg, 86 μmol), 2-methylbut-3-yn-2-ol (29 mg, 0.34 mmol), DIPA (17 mg, 0.17 mmol), PdCl$_2$(PPh$_3$)$_2$ (6.0 mg, 8.6 μmol), and CuI (1.6 mg, 8.6 μmol) in 1-propanol (0.8 mL) at 85 °C overnight to afford the title compound (4.5 mg, 18% yield). ^{1}H NMR (400 MHz, CD$_3$OD) δ 8.75 (dd, J = 1.6, 0.8 Hz, 1H), 8.22 (d, J = 6.8 Hz, 1H), 7.75 (d, J = 6.4 Hz, 1H), 7.63 (dd, J = 8.4, 0.8 Hz, 1H), 7.51 (dd, J = 8.8, 1.6 Hz, 1H), 1.61 (s, 6H). ^{13}C NMR (214 MHz, CD$_3$OD) δ 168.85, 158.69, 147.53, 142.74, 141.42, 131.81, 127.32, 123.18, 119.76, 112.12, 107.17, 94.77, 82.84, 66.01, 31.81 (2C). HRMS (ESI): *m/z* calculated for C$_{16}$H$_{16}$N$_5$O [M + H]$^+$: 294.1355. Found: 294.1348.

4-(3-(2-Aminopyrimidin-4-yl)-1H-indazol-5-yl)but-3-yn-2-ol (17).
The reaction was carried out according to general procedure B starting from 4-(5-bromo-1*H*-indazol-3-yl)pyrimidin-2-amine (**63**) (25 mg, 86 μmol), but-3-yn-2-ol (24 mg, 0.34 mmol), DIPA (17 mg, 0.17 mmol), PdCl$_2$(PPh$_3$)$_2$ (6.0 mg, 8.6 μmol), and CuI (1.6 mg, 8.6 μmol) in 1-propanol (0.8 mL) at 85 °C overnight to afford the title compound (4.0 mg, 17% yield). ^{1}H NMR (400 MHz, CD$_3$OD) δ 8.78 (t, J = 1.2 Hz, 1H), 8.22 (d, J = 6.4 Hz, 1H), 7.72 (d, J = 6.4 Hz, 1H), 7.62 (dd, J

= 8.8, 0.8 Hz, 1H), 7.51 (dd, J = 8.4, 1.6 Hz, 1H), 4.73 (q, J = 6.8 Hz, 1H), 1.53 (d, J = 6.8 Hz, 3H). ^{13}C NMR (214 MHz, CD$_3$OD) δ 168.59, 158.94, 148.03, 142.76, 141.50, 131.70, 127.61, 123.17, 119.58, 112.11, 107.17, 91.98, 84.43, 59.14, 24.84. HPLC purity: >97%. HRMS (ESI): m/z calculated for C$_{15}$H$_{14}$N$_5$O [M + H]$^+$: 280.1198. Found: 280.1193.

1-(3-(2-Aminopyrimidin-4-yl)-1H-indazol-5-yl)-3-methylpent-1-yn-3-ol (18).
The reaction was carried out according to general procedure B starting from 4-(5-bromo-1*H*-indazol-3-yl)pyrimidin-2-amine (**63**) (25 mg, 86 μmol), 3-methylpent-1-yn-3-ol (34 mg, 0.34 mmol), DIPA (17 mg, 0.17 mmol), PdCl$_2$(PPh$_3$)$_2$ (12 mg, 17 μmol), and CuI (3.3 mg, 17 μmol) in 1-propanol (0.9 mL) at 85 °C overnight to afford the title compound (11 mg, 42% yield). ^{1}H NMR (400 MHz, CD$_3$OD) δ 8.71 (dd, J = 1.6, 0.8 Hz, 1H), 8.21 (d, J = 6.8 Hz, 1H), 7.72 (d, J = 6.8 Hz, 1H), 7.62 (dd, J = 8.8, 0.8 Hz, 1H), 7.50 (dd, J = 8.8, 1.6 Hz, 1H), 1.88–1.74 (m, 2H), 1.56 (s, 3H), 1.13 (t, J = 7.2 Hz, 3H). ^{13}C NMR (100 MHz, CD$_3$OD) δ 169.29, 158.14, 146.50, 142.73, 141.24, 131.93, 127.17, 123.18, 119.89, 112.17, 107.10, 93.78, 84.10, 69.68, 37.73, 29.56, 9.52. HPLC purity: 100%. HRMS (ESI): m/z calculated for C$_{17}$H$_{18}$N$_5$O [M + H]$^+$: 308.1511. Found: 308.1505.

1-(5-Bromo-1H-indol-3-yl)-2-chloroethan-1-one (65).
To stirred ice-cooled suspension of aluminum chloride (1.360 g, 10.20 mmol) in DCM (10 mL) was slowly added chloroacetyl chloride (864.1 mg, 7.651 mmol). To this solution was added 5-bromo-1*H*-indole (**64**) (1 g, 5.101 mmol) in DCM (10 mL) and the resulting mixture was stirred at 0 °C for 10 min and at r.t. for 4 h. The mixture was poured into stirred ice water and extracted with EtOAc, and the combined organic layers were washed with brine and dried over Na$_2$SO$_4$. The residue was purified with flash column chromatography (SiO$_2$, 0−40% EtOAc in hexane) to obtain the title compound (823 mg, 59% yield). ^{1}H NMR (400 MHz, DMSO-d_6) δ 12.31 (s, 1H), 8.48 (s, 1H), 8.29 (dd, J = 2.0, 0.4 Hz, 1H), 7.49 (dd, J = 8.4, 0.4 Hz, 1H), 7.38 (dd, J = 8.4, 2.0 Hz, 1H), 4.89 (s, 2H). ^{13}C NMR (126 MHz, DMSO-d_6) δ 186.28, 135.87, 135.35, 127.15, 125.82, 123.24, 114.92, 114.48, 113.05, 46.36. HRMS (ESI): m/z calculated for C$_{10}$H$_8$NOClBr [M + H]$^+$: 271.9478. Found: 271.9471.

1-(5-Bromo-1H-indol-3-yl)-2-(2-methoxyethoxy)ethan-1-one (66).
To a stirred ice-cooled suspension of NaH (242 mg, 6.05 mmol) in DMF (2mL) was added dropwise 2-methoxyethanol (419 mg, 5.50 mmol). The resulting mixture was stirred at 0 °C for 10 min before the ice bath was removed and a solution of 1-(5-bromo-1*H*-indol-3-yl)-2-chloroethan-1-one (**65**) (750 mg, 2.75 mmol) in DMF (1 mL) was added. The resulting mixture was stirred at r.t. for 6 h. The mixture was poured into ice and saturated NH$_4$Cl aqueous solution and extracted with EtOAc, and the combined organic layers were washed with brine and dried over Na$_2$SO$_4$. The residue was purified with flash column chromatography (SiO$_2$, 0−5% MeOH in DCM) to obtain the title compound (420 mg, 49% yield). ^{1}H NMR (400 MHz, DMSO-d_6) δ 8.42 (s, 1H), 8.31 (d, J = 2.0 Hz, 1H), 7.46 (d, J = 8.4 Hz, 1H), 7.35 (dd, J = 8.8, 2.0 Hz, 1H), 4.03 (s, 1H), 3.67–3.65 (m, 2H), 3.53–3.50 (m, 2H), 3.27 (s, 3H). ^{13}C NMR (214 MHz, DMSO-d_6) δ 195.38, 138.26, 138.09, 130.46, 128.62, 126.47, 117.77, 117.39, 116.34, 77.11, 74.34, 73.05, 61.19. HRMS (ESI): m/z calculated for C$_{13}$H$_{15}$BrNO$_3$ [M + H]$^+$: 312.0235. Found: 312.0226.

4-(5-Bromo-1H-indol-3-yl)-5-(2-methoxyethoxy)pyrimidin-2-amine (67).

The reaction was carried out according to general procedure E starting from 1-(5-bromo-1*H*-indol-3-yl)-2-(2-methoxyethoxy)ethan-1-one (**66**) (150 mg, 481 µmol) and Bredereck's reagent (293 mg, 1.68 mmol) at 105 °C overnight, and then sodium methoxide (2.88 mL, 0.5 M in methanol, 1.44 mmol) and guanidine hydrochloride (229 mg, 2.40 mmol) in 1-propanol (2 mL) at reflux to afford the title compound (44 mg, 25% yield).^{1}H NMR (400 MHz, CD$_3$OD) δ 8.92 (dd, *J* = 1.6, 0.4 Hz, 1H), 8.47 (s, 1H), 7.93 (s, 1H), 7.33 (dd, *J* = 8.4, 0.4 Hz, 1H), 7.28 (dd, *J* = 8.4, 2.0 Hz, 1H), 4.16–4.14 (m, 2H), 3.78–3.76 (m, 2H), 3.43 (s, 3H). ^{13}C NMR (101 MHz, CD$_3$OD) δ 159.77, 155.68, 144.24, 143.07, 136.51, 134.43, 129.45, 126.72, 126.22, 115.12, 113.89, 111.47, 72.38, 70.56, 59.09. HRMS (ESI): *m/z* calculated C$_{15}$H$_{16}$BrN$_4$O$_2$ for [M + H]$^+$: 363.0457. Found: 363.0446.

4-(5-(3-(Dimethylamino)prop-1-yn-1-yl)-1H-indol-3-yl)-5-(2-methoxyethoxy)pyrimidin-2-amine (19).

The reaction was carried out according to general procedure A starting from 4-(5-bromo-1*H*-indol-3-yl)-5-(2-methoxyethoxy)pyrimidin-2-amine (**67**) (25 mg, 69 µmol), *N*,*N*-dimethylprop-2-yn-1-amine (23 mg, 0.28 mmol), TEA (14 mg, 0.14 mmol), Pd(PPh$_3$)$_4$ (8.0 mg, 6.9 µmol), and CuI (1.3 mg, 6.9 µmol) in DMF (0.7 mL) at 85 °C overnight to afford the title compound (4 mg, 12% yield) as a TFA salt. ^{1}H NMR (400 MHz, CD$_3$OD) δ 9.04 (dd, *J* = 1.6, 0.8 Hz, 1H), 8.91 (s, 1H), 7.84 (s, 1H), 7.54 (dd, *J* = 8.4, 0.8 Hz, 1H), 7.46 (dd, *J* = 8.4, 1.6 Hz, 1H), 4.33 (s, 2H), 4.30–4.28 (m, 2H), 3.90–3.87 (m, 2H), 3.49 (s, 3H), 3.06 (s, 6H). ^{13}C NMR (214 MHz, CD$_3$OD) δ 161.97, 154.21, 143.40, 139.55, 138.49, 129.06 (2C), 128.47, 127.64, 115.77, 113.51, 111.89, 92.98, 76.35, 71.85, 70.61, 59.15, 48.98, 42.83 (2C). HPLC purity: 100%. HRMS (ESI): *m/z* calculated C$_{20}$H$_{24}$N$_5$O$_2$ for [M + H]$^+$: 366.1930. Found: 366.1922.

4-(3-(2-Amino-5-(2-methoxyethoxy)pyrimidin-4-yl)-1H-indol-5-yl)-2-methylbut-3-yn-2-ol (20).

The reaction was carried out according to general procedure B starting from 4-(5-bromo-1*H*-indol-3-yl)-5-(2-methoxyethoxy)pyrimidin-2-amine (**67**) (17 mg, 47 µmol), 2-methylbut-3-yn-2-ol (16 mg, 0.19 mmol), DIPA (9.5 mg, 94 µmol), PdCl$_2$(PPh$_3$)$_2$ (3.3 mg, 4.7 µmol), and CuI (0.9 mg, 4.7 µmol) in 1-propanol (0.6 mL) at 85 °C overnight to afford the title compound (4 mg, 23% yield). ^{1}H NMR (400 MHz, CD$_3$OD) δ 8.88 (dd, *J* = 1.6, 0.8 Hz, 1H), 8.87 (s, 1H), 7.77 (s, 1H), 7.46 (dd, *J* = 8.4, 0.8 Hz, 1H), 7.35 (dd, *J* = 8.4, 1.6 Hz, 1H), 4.28–4.26 (m, 2H), 3.89–3.86 (m, 2H), 3.49 (s, 3H), 1.61 (s, 6H). ^{13}C NMR (214 MHz, CD$_3$OD) δ 162.60, 153.69, 143.25, 139.60, 137.67, 128.48, 127.91, 127.58, 125.92, 118.49, 113.16, 111.79, 93.51, 84.01, 71.82, 70.55, 66.13, 59.16, 31.90 (2C). HPLC purity: >98%. HRMS (ESI): *m/z* calculated for C$_{20}$H$_{23}$N$_4$O$_3$ [M + H]$^+$: 367.1770. Found: 367.1766.

3-(1H-Indol-5-yl)-N,N-dimethylprop-2-yn-1-amine (68).

The reaction was carried out according to general procedure A starting from 5-bromo-1*H*-indole (500 mg, 2.55 mmol), *N*,*N*-dimethylprop-2-yn-1-amine (636 mg, 7.65 mmol), TEA (516 mg, 5.10 mmol), Pd(PPh$_3$)$_4$ (295 mg, 255 µmol), and CuI (48.6 mg, 255 µmol) in DMF (7 mL) at 85 °C overnight to afford the title compound (102 mg, 20% yield). ^{1}H NMR (400 MHz, CDCl$_3$) δ 8.43 (s, 1H), 7.73 (dt, *J* = 1.6, 0.8 Hz, 1H), 7.29–7.22 (m, 2H), 7.17 (dd, *J* = 3.2, 2.4 Hz, 1H), 6.48 (m, 1H), 3.46 (s, 2H), 2.36 (s, 6H). ^{13}C NMR (126 MHz, CD$_3$OD) δ 138.01, 129.31, 127.30, 126.02, 125.83, 112.59, 112.12, 102.73, 93.58, 75.17, 48.95, 42.74 (2C). HRMS (ESI): *m/z* calculated C$_{13}$H$_{15}$N$_2$ for [M + H]$^+$: 199.1235. Found: 199.1227.

3-(3-Bromo-1H-indol-5-yl)-N,N-dimethylprop-2-yn-1-amine (69).
To a solution of 3-(1*H*-indol-5-yl)-*N,N*-dimethylprop-2-yn-1-amine (**68**) (97 mg, 0.49 mmol) in DCM (3 mL) was added NBS (87 mg, 0.49 mmol). The mixture was stirred at r.t. overnight and the solvent was evaporated. The residue was taken up in EtOAc and washed with water and dried over Na_2SO_4. The residue was purified with flash column chromatography (SiO_2, 0−40% EtOAc in hexane) to obtain the title compound (82 mg, 60% yield). ^1H NMR (850 MHz, CD_3OD) δ 7.67 (dd, *J* = 1.6, 0.7 Hz, 1H), 7.42 (dd, *J* = 8.4, 0.7 Hz, 1H), 7.40 (s, 1H), 7.32 (dd, *J* = 8.4, 1.6 Hz, 1H), 4.32 (s, 2H), 3.04 (s, 6H). ^{13}C NMR (214 MHz, CD_3OD) δ 137.51, 127.98, 127.04, 126.93, 124.13, 113.35, 113.27, 92.74, 91.05, 75.93, 48.99, 42.78 (2C).

tert-Butyl 3-bromo-5-(3-(dimethylamino)prop-1-yn-1-yl)-1H-indole-1-carboxylate (70).
To a solution of 3-(3-bromo-1*H*-indol-5-yl)-*N,N*-dimethylprop-2-yn-1-amine (**69**) (82 mg, 0.30 mmol), TEA (90 mg, 0.89 mmol), and DMAP (3.6 mg, 30 μmol) in DCM (2 mL) was added di-*tert*-butyl dicarbonate (77 mg, 0.36 mmol) at 0 °C and the mixture was stirred at r.t. for 16 h. The reaction mixture was diluted in DCM, washed with water and brine, and dried over Na_2SO_4. The residue was purified with flash column chromatography (SiO_2, 0−40% EtOAc in hexane) to obtain the title compound (95.6 mg, 86% yield). ^1H NMR (400 MHz, CD_3OD) δ 8.12 (d, *J* = 8.4 Hz, 1H), 7.76 (s, 1H), 7.55 (dd, *J* = 1.6, 0.8 Hz, 1H), 7.45 (dd, *J* = 8.8, 1.6 Hz, 1H), 3.52 (s, 2H), 2.41 (s, 6H), 1.68 (s, 9H). ^{13}C NMR (214 MHz, CD_3OD) δ 149.92, 135.53, 130.65, 129.92, 127.21, 123.62, 119.39, 116.39, 98.17, 86.52, 86.19, 84.13, 49.02, 44.31 (2C), 28.25 (3C). HRMS (ESI): *m/z* calculated $C_{18}H_{22}BrN_2O_2$ for $[M + H]^+$: 377.0865. Found: 377.0853.

N,N-dimethyl-3-(3-(pyrimidin-4-yl)-1H-indol-5-yl)prop-2-yn-1-amine (21).
A mixture of *tert*-butyl 3-bromo-5-(3-(dimethylamino)prop-1-yn-1-yl)-1*H*-indole-1-carboxylate (**70**) (30 mg, 80 μmol), 4-(tributylstannyl)pyrimidine (44 mg, 0.12 mmol), and $PdCl_2(PPh_3)_2$ (5.6 mg, 8.0 μmol) in 1,4-dioxane (0.8 mL) was degassed and then stirred at 85 °C for 17 h. After completion of the reaction, the mixture was cooled to r.t., diluted with EtOAc, and passed through a thin pad of celite. The filtrate was concentrated *in vacuo* and the crude residue was purified by preparative HPLC (10−100% MeOH in H_2O + 0.05% TFA) to give the title compound (6.2 mg, 20% yield) as a TFA salt. ^1H NMR (400 MHz, CD_3OD) δ 9.18 (s, 1H), 8.79 (dd, *J* = 1.6, 0.8 Hz, 1H), 8.62 (s, 1H), 8.52 (s, 1H), 8.06 (d, *J* = 6.0 Hz, 1H), 7.54 (dd, *J* = 8.4, 0.8 Hz, 1H), 7.44 (dd, *J* = 8.4, 1.6 Hz, 1H), 4.35 (s, 2H), 3.05 (s, 6H). ^{13}C NMR (101 MHz, CD_3OD) δ 166.47, 156.26, 151.66, 139.56, 134.39, 128.04, 127.95, 126.65, 117.40, 115.51, 114.86, 113.84, 92.69, 76.44, 49.29, 42.79 (2C). HRMS (ESI): *m/z* calculated for $C_{17}H_{17}N_4$ $[M + H]^+$: 277.1453. Found: 277.1448.

General Procedure F
To a solution of 6-bromo-1*H*-indole (1 equiv) or 6-bromo-1*H*-indazole (1 equiv) in DMF was added cesium carbonate (3 equiv) and chloropyrimidineamine (1.2 equiv), and the mixture was stirred at 80°C for 17–23 h. The mixture was poured into water and then extracted with EtOAc. The organic layer was washed with brine and dried over Na_2SO_4, and the residue was purified with flash column chromatography (SiO_2, 0−100% EtOAc in hexane) to give the title compounds.

4-(6-bromo-1H-indol-1-yl)pyrimidin-2-amine (77).
The reaction was carried out according to general procedure F starting from 6-bromo-1*H*-indole (**71**) (200 mg, 1.02 mmol), cesium carbonate (997 mg, 3.06 mmol), and 4-chloropyrimidin-2-

amine (**73**) (159 mg, 1.22 mmol) in DMF (5 mL) at 80 °C for 19 h to afford the title compound (286 mg, 97% yield). ^{1}H NMR (400 MHz, DMSO-d_6) δ 8.97 (d, J = 1.6 Hz, 1H), 8.28 (d, J = 5.6 Hz, 1H), 8.08 (d, J = 3.6 Hz, 1H), 7.58 (d, J = 8.4 Hz, 1H), 7.35 (dd, J = 8.4, 2.0 Hz, 1H), 6.98 (s, 2H), 6.94 (d, J = 5.6 Hz, 1H), 6.79 (d, J = 3.6 Hz, 1H). ^{13}C NMR (101 MHz, DMSO-d_6) δ 163.31, 159.87, 158.60, 135.37, 129.45, 126.61, 124.91, 122.30, 118.80, 116.39, 106.78, 97.72. HRMS (ESI): m/z calculated for $C_{12}H_{10}BrN_4$ [M + H]$^+$: 289.0089. Found: 289.0077.

4-(6-bromo-1H-indazol-1-yl)pyrimidin-2-amine (*78*).

The reaction was carried out according to general procedure F starting from 6-bromo-1*H*-indazole (**72**) (200 mg, 1.02 mmol), cesium carbonate (992 mg, 3.05 mmol), and 4-chloropyrimidin-2-amine (**73**) (158 mg, 1.22 mmol) in DMF (5 mL) at 80 °C for 18 h to afford the title compound (131.4 mg, 45% yield). ^{1}H NMR (400 MHz, DMSO-d_6) δ 9.14 (dt, J = 1.6, 0.8 Hz, 1H), 8.49 (d, J = 0.8 Hz, 1H), 8.30 (d, J = 5.6 Hz, 1H), 7.85 (dd, J = 8.4, 0.8 Hz, 1H), 7.51 (dd, J = 8.4, 1.6 Hz, 1H), 7.09 (d, J = 5.6 Hz, 3H). ^{13}C NMR (214 MHz, DMSO-d_6) δ 163.13, 159.92, 159.59, 138.85, 138.76, 126.52, 125.03, 123.05, 122.26, 118.35, 97.20. HRMS (ESI): m/z calculated for $C_{11}H_9BrN_5$ [M + H]$^+$: 290.0041. Found: 290.0033.

4-(6-bromo-1H-indazol-1-yl)-5-methoxypyrimidin-2-amine (*79*).

The reaction was carried out according to general procedure F starting from 6-bromo-1*H*-indazole (**72**) (100 mg, 508 μmol), cesium carbonate (496 mg, 1.52 mmol), and 4-chloro-5-methoxypyrimidin-2-amine (**74**) (97.2 mg, 609 μmol) in DMF (3 mL) at 80 °C for 17 h to afford the title compound (95.3 mg, 59% yield). ^{1}H NMR (400 MHz, DMSO-d_6) δ 8.44 (d, J = 1.2 Hz, 1H), 8.37 (s, 1H), 8.34 (dt, J = 2.0, 0.8 Hz, 1H), 7.84 (dd, J = 8.4, 0.8 Hz, 1H), 7.46 (dd, J = 8.4, 1.6 Hz, 1H), 6.71 (s, 2H), 3.75 (s, 3H). ^{13}C NMR (126 MHz, DMSO-d_6) δ 158.68, 150.52, 148.46, 139.81, 137.48, 136.91, 125.79, 123.69, 122.76, 121.23, 116.26, 59.30. HRMS (ESI): m/z calculated for $C_{12}H_{11}BrN_5O$ [M + H]$^+$: 320.0147. Found: 320.0140.

4-(6-bromo-1H-indazol-1-yl)-5-methylpyrimidin-2-amine (*80*).

The reaction was carried out according to general procedure F starting from 6-bromo-1*H*-indazole (**72**) (200 mg, 1.02 mmol), cesium carbonate (992 mg, 3.05 mmol), and 4-chloro-5-methylpyrimidin-2-amine (**75**) (175 mg, 1.22 mmol) in DMF (5 mL) at 80 °C for 22 h to afford the title compound (182.7 mg, 59% yield). ^{1}H NMR (400 MHz, DMSO-d_6) δ 8.71 (dt, J = 1.6, 0.8 Hz, 1H), 8.45 (d, J = 0.8 Hz, 1H), 8.26 (d, J = 0.8 Hz, 1H), 7.84 (m, 1H), 7.48 (dd, J = 8.4, 1.6 Hz, 1H), 6.83 (s, 2H), 2.33 (s, 3H). ^{13}C NMR (126 MHz, DMSO-d_6) δ 162.69, 161.85, 156.80, 139.80, 137.08, 126.09, 123.84, 122.74, 121.47, 117.62, 108.33, 16.52. HRMS (ESI): m/z calculated for $C_{12}H_{11}BrN_5$ [M + H]$^+$: 304.0198. Found: 304.0191.

4-(6-bromo-1H-indazol-1-yl)-6-methylpyrimidin-2-amine (*81*).

The reaction was carried out according to general procedure F starting from 6-bromo-1*H*-indazole (**72**) (200 mg, 1.02 mmol), cesium carbonate (992 mg, 3.05 mmol), and 4-chloro-6-methylpyrimidin-2-amine (**76**) (175 mg, 1.22 mmol) in DMF (5 mL) at 80 °C for 23 h to afford the title compound (162 mg, 53% yield). ^{1}H NMR (400 MHz, DMSO-d_6) δ 9.13 (t, J = 0.8 Hz, 1H), 8.47 (d, J = 0.8 Hz, 1H), 7.85 (d, J = 8.8 Hz, 1H), 7.50 (dd, J = 8.4, 2.0 Hz, 1H), 7.01 (s, 1H), 6.98 (s, 2H), 2.31 (s, 3H). ^{13}C NMR (126 MHz, DMSO-d_6) δ 169.28, 162.97, 159.89, 138.92, 138.45, 126.37, 124.92, 122.99, 122.12, 118.34, 96.10, 23.95. HRMS (ESI): m/z calculated for $C_{12}H_{11}BrN_5$ [M + H]$^+$: 304.0198. Found: 304.0191.

*4-(6-(3-(dimethylamino)prop-1-yn-1-yl)-1H-indol-1-yl)pyrimidin-2-amine (**22**).*
The reaction was carried out according to general procedure A starting from 4-(6-bromo-1*H*-indol-1-yl)pyrimidin-2-amine (**77**) (30 mg, 0.10 mmol), *N*,*N*-dimethylprop-2-yn-1-amine (26 mg, 0.31 mmol), TEA (21 mg, 0.21 mmol), Pd(PPh$_3$)$_4$ (12 mg, 10 μmol), and CuI (2.0 mg, 10 μmol) in DMF (1 mL) at 85 °C overnight to afford the title compound (11 mg, 27% yield) as a TFA salt. ^{1}H NMR (400 MHz, CD$_3$OD) δ 9.04 (dt, *J* = 1.2, 0.8 Hz, 1H), 8.22 (d, *J* = 7.2 Hz, 1H), 8.08 (d, *J* = 4.0 Hz, 1H), 7.66 (dd, *J* = 8.0, 0.8 Hz, 1H), 7.48 (dd, *J* = 8.0, 1.6 Hz, 1H), 7.25 (d, *J* = 7.2 Hz, 1H), 6.94 (dd, *J* = 4.0, 0.8 Hz, 1H), 4.35 (s, 2H), 3.06 (s, 6H). ^{13}C NMR (101 MHz, CD$_3$OD) δ 162.91, 158.09, 148.41, 136.40, 134.25, 129.07, 128.49, 122.66, 122.40, 118.46, 112.09, 100.20, 92.03, 77.73, 48.69, 42.85 (2C). HPLC purity: 100%. HRMS (ESI): *m/z* calculated C$_{17}$H$_{18}$N$_5$ for [M + H]$^+$: 292.1562. Found: 292.1556.

*4-(1-(2-aminopyrimidin-4-yl)-1H-indol-6-yl)-2-methylbut-3-yn-2-ol (**23**).*
The reaction was carried out according to general procedure B starting from 4-(6-bromo-1*H*-indol-1-yl)pyrimidin-2-amine (**77**) (30 mg, 0.10 mmol), 2-methylbut-3-yn-2-ol (35 mg, 0.42 mmol), DIPA (21 mg, 0.21 mmol), PdCl$_2$(PPh$_3$)$_2$ (7.3 mg, 10 μmol), and CuI (2.0 mg, 10 μmol) in 1-propanol (1 mL) at 85 °C overnight to afford the title compound (17 mg, 56% yield). ^{1}H NMR (400 MHz, CD$_3$OD) δ 8.89 (dt, *J* = 1.2, 0.8 Hz, 1H), 8.20 (d, *J* = 7.2 Hz, 1H), 8.01 (d, *J* = 4.0 Hz, 1H), 7.59 (dd, *J* = 8.0, 0.8 Hz, 1H), 7.36 (dd, *J* = 8.0, 1.2 Hz, 1H), 7.26 (d, *J* = 7.6 Hz, 1H), 6.91 (dd, *J* = 3.6, 0.8 Hz, 1H), 1.61 (s, 6H). ^{13}C NMR (101 MHz, CD$_3$OD) δ 162.83, 157.69, 147.58, 136.48, 133.02, 128.98, 127.62, 122.31, 121.51, 121.01, 112.28, 100.16, 94.97, 83.41, 66.11, 31.80 (2C). HPLC purity: >98%. HRMS (ESI): *m/z* calculated for C$_{17}$H$_{17}$N$_4$O [M + H]$^+$: 293.1402. Found: 293.1395.

*4-(6-(3-(dimethylamino)prop-1-yn-1-yl)-1H-indazol-1-yl)pyrimidin-2-amine (**24**).*
The reaction was carried out according to general procedure A starting from 4-(6-bromo-1*H*-indazol-1-yl)pyrimidin-2-amine (**78**) (25 mg, 86 μmol), *N*,*N*-dimethylprop-2-yn-1-amine (21 mg, 0.26 mmol), TEA (17 mg, 0.17 mmol), Pd(PPh$_3$)$_4$ (10 mg, 8.6 μmol), and CuI (1.6 mg, 8.6 μmol) in DMF (0.9 mL) at 85 °C overnight to afford the title compound (6.5 mg, 19% yield) as a TFA salt. ^{1}H NMR (400 MHz, CD$_3$OD) δ 9.09 (s, 1H), 8.52 (s, 1H), 8.27 (d, *J* = 6.8 Hz, 1H), 7.93 (d, *J* = 8.4 Hz, 1H), 7.60 (dd, *J* = 8.4, 1.6 Hz, 1H), 7.57 (d, *J* = 6.8 Hz, 1H), 4.39 (s, 2H), 3.07 (s, 6H). ^{13}C NMR (101 MHz, CD$_3$OD) δ 163.47, 159.96, 151.59, 142.44, 139.80, 129.22, 128.98, 123.18, 123.11, 121.33, 100.36, 90.95, 79.65, 48.50, 42.97 (2C). HPLC purity: 100%. HRMS (ESI): *m/z* calculated C$_{16}$H$_{17}$N$_6$ for [M + H]$^+$: 293.1515. Found: 293.1512.

*4-(1-(2-aminopyrimidin-4-yl)-1H-indazol-6-yl)-2-methylbut-3-yn-2-ol (**25**).*
The reaction was carried out according to general procedure B starting from 4-(6-bromo-1*H*-indazol-1-yl)pyrimidin-2-amine (**78**) (25 mg, 86 μmol), 2-methylbut-3-yn-2-ol (29 mg, 0.34 mmol), DIPA (17 mg, 0.17 mmol), PdCl$_2$(PPh$_3$)$_2$ (6.0 mg, 8.6 μmol), and CuI (1.6 mg, 8.6 μmol) in 1-propanol (0.9 mL) at 85 °C overnight to afford the title compound (15 mg, 59% yield). ^{1}H NMR (400 MHz, CD$_3$OD) δ 8.96 (m, 1H), 8.28 (d, *J* = 0.8 Hz, 1H), 8.24 (d, *J* = 5.6 Hz, 1H), 7.77 (dd, *J* = 8.4, 0.8 Hz, 1H), 7.35 (dd, *J* = 8.4, 1.2 Hz, 1H), 7.26 (d, *J* = 5.6 Hz, 1H), 1.62 (s, 6H). ^{13}C NMR (214 MHz, DMSO-*d$_6$*) δ 163.18, 159.82, 159.80, 138.63, 137.96, 126.55, 125.44, 122.66, 121.65, 118.34, 97.44, 97.22, 80.93, 63.75, 31.60 (2C). HPLC purity: >98%. HRMS (ESI): *m/z* calculated for C$_{16}$H$_{16}$N$_5$O [M + H]$^+$: 294.1355. Found: 294.1352.

*4-(6-(3-(dimethylamino)prop-1-yn-1-yl)-1H-indazol-1-yl)-5-methoxypyrimidin-2-amine (**26**).*
The reaction was carried out according to general procedure A starting from 4-(6-bromo-1*H*-indazol-1-yl)-5-methoxypyrimidin-2-amine (**79**) (30 mg, 94 μmol), *N*,*N*-dimethylprop-2-yn-1-amine (31 mg, 0.37 mmol), TEA (19 mg, 0.19 mmol), Pd(PPh$_3$)$_4$ (22 mg, 19 μmol), and CuI (3.6 mg, 19 μmol) in DMF (1 mL) at 85 ℃ overnight to afford the title compound (6 mg, 15% yield) as a TFA salt. ^{1}H NMR (400 MHz, CD$_3$OD) δ 8.71 (s, 1H), 8.49 (s, 1H), 8.23 (s, 1H), 7.93 (dd, *J* = 8.4, 0.8 Hz, 1H), 7.56 (dd, *J* = 8.4, 1.2 Hz, 1H), 4.38 (s, 2H), 3.91 (s, 3H), 3.06 (s, 6H). ^{13}C NMR (214 MHz, CD$_3$OD) δ 158.71, 154.40, 145.05, 141.97, 141.89, 140.14, 129.53, 128.64, 124.11, 123.41, 121.26, 92.36, 80.54, 61.22, 49.79, 44.21 (2C). HPLC purity: 100%. HRMS (ESI): *m/z* calculated C$_{17}$H$_{19}$N$_6$O for [M + H]$^+$: 323.1620. Found: 323.1611.

*4-(6-(3-(dimethylamino)prop-1-yn-1-yl)-1H-indazol-1-yl)-5-methylpyrimidin-2-amine (**27**).*
The reaction was carried out according to general procedure A starting from 4-(6-bromo-1*H*-indazol-1-yl)-5-methylpyrimidin-2-amine (**80**) (30 mg, 99 μmol), *N*,*N*-dimethylprop-2-yn-1-amine (33 mg, 0.39 mmol), TEA (20 mg, 0.20 mmol), Pd(PPh$_3$)$_4$ (23 mg, 20 μmol), and CuI (3.8 mg, 20 μmol) in DMF (1 mL) at 85 ℃ overnight to afford the title compound (4.5 mg, 11% yield) as a TFA salt. ^{1}H NMR (400 MHz, CD$_3$OD) δ 8.97 (s, 1H), 8.50 (d, *J* = 1.2 Hz, 1H), 8.18 (s, 1H), 7.93 (dd, *J* = 8.4, 0.8 Hz, 1H), 7.59 (dd, *J* = 8.4, 1.2 Hz, 1H), 4.38 (s, 2H), 3.07 (s, 6H), 2.60 (s, 3H). ^{13}C NMR (214 MHz, CD$_3$OD) δ 161.92, 158.27, 152.95, 141.03, 140.89, 129.00, 127.93, 122.89, 122.52, 121.45, 112.50, 91.11, 79.39, 48.53, 42.96 (2C), 18.48. HPLC purity: 100%. HRMS (ESI): *m/z* calculated C$_{17}$H$_{19}$N$_6$ for [M + H]$^+$: 307.1671. Found: 307.1661.

*4-(6-(3-(dimethylamino)prop-1-yn-1-yl)-1H-indazol-1-yl)-6-methylpyrimidin-2-amine (**28**).*
The reaction was carried out according to general procedure A starting from 4-(6-bromo-1*H*-indazol-1-yl)-6-methylpyrimidin-2-amine (**81**) (30 mg, 99 μmol), *N*,*N*-dimethylprop-2-yn-1-amine (33 mg, 0.39 mmol), TEA (20 mg, 0.20 mmol), Pd(PPh$_3$)$_4$ (23 mg, 20 μmol), and CuI (3.8 mg, 20 μmol) in DMF (1 mL) at 85 ℃ overnight to afford the title compound (13.8 mg, 33% yield) as a TFA salt. ^{1}H NMR (400 MHz, CD$_3$OD) δ 9.10 (q, *J* = 1.2 Hz, 1H), 8.50 (d, *J* = 0.8 Hz, 1H), 7.93 (dd, *J* = 8.0, 0.8 Hz, 1H), 7.59 (dd, *J* = 8.0, 1.2 Hz, 1H), 7.48 (s, 1H), 4.39 (s, 2H), 3.07 (s, 6H), 2.54 (s, 3H). ^{13}C NMR (214 MHz, CD$_3$OD) δ 163.86, 161.30, 158.65, 142.95, 139.93, 129.49, 129.08, 123.33, 123.24, 121.41, 99.58, 90.83, 79.81, 48.47, 42.96 (2C), 19.84. HPLC purity: 100%. HRMS (ESI): *m/z* calculated C$_{17}$H$_{19}$N$_6$ for [M + H]$^+$: 307.1671. Found: 307.1661.

*4-(5-(3-(Diethylamino)prop-1-yn-1-yl)-1H-indol-3-yl)pyrimidin-2-amine (**29**).*
The reaction was carried out according to general procedure A starting from 4-(5-bromo-1*H*-indol-3-yl)pyrimidin-2-amine (**49**) (30 mg, 0.1 mmol), *N*,*N*-diethylprop-2-yn-1-amine (46 mg, 0.42 mmol), TEA (21 mg, 0.21 mmol), Pd(PPh$_3$)$_4$ (12 mg, 10 μmol), and CuI (2.0 mg, 10 μmol) in DMF (1 mL) at 85 ℃ overnight to afford the title compound (4.3 mg, 10% yield) as a TFA salt. ^{1}H NMR (400 MHz, CD$_3$OD) δ 8.86 (dd, *J* = 1.6, 0.8 Hz, 1H), 8.54 (s, 1H), 7.99 (d, *J* = 6.8 Hz, 1H), 7.54 (dd, *J* = 8.4, 0.8 Hz, 1H), 7.46 (dd, *J* = 8.4, 1.6 Hz, 1H), 7.36 (d, *J* = 7.2 Hz, 1H), 4.39 (s, 2H), 3.43 (q, *J* = 7.2 Hz, 4H), 1.43 (t, *J* = 7.2 Hz, 6H). ^{13}C NMR (101 MHz, CD$_3$OD) δ 170.56, 157.40, 143.84, 139.59, 136.48, 128.59, 128.28, 126.65, 116.01, 114.67, 113.87, 106.77, 92.44, 76.02, 49.29, 43.11 (2C), 9.68 (2C). HPLC purity: 100%. HRMS (ESI): *m/z* calculated for C$_{19}$H$_{22}$N$_5$ [M + H]$^+$: 320.1875. Found: 320.1866.

4-(5-(3-(Methylamino)prop-1-yn-1-yl)-1H-indol-3-yl)pyrimidin-2-amine (30).
The reaction was carried out according to general procedure A starting from 4-(5-bromo-1*H*-indol-3-yl)pyrimidin-2-amine (**49**) (30 mg, 0.1 mmol), *N*-methylprop-2-yn-1-amine (29 mg, 0.42 mmol), TEA (21 mg, 0.21 mmol), Pd(PPh$_3$)$_4$ (12 mg, 10 μmol), and CuI (2.0 mg, 10 μmol) in DMF (1 mL) at 85 °C overnight to afford the title compound (8 mg, 20% yield) as a TFA salt. ^{1}H NMR (400 MHz, CD$_3$OD) δ 8.85 (dd, *J* = 1.6, 0.8 Hz, 1H), 8.52 (s, 1H), 7.97 (d, *J* = 6.8 Hz, 1H), 7.52 (dd, *J* = 8.4, 0.8 Hz, 1H), 7.42 (dd, *J* = 8.4, 1.6 Hz, 1H), 7.34 (d, *J* = 7.2 Hz, 1H), 4.18 (s, 2H), 2.86 (s, 3H). ^{13}C NMR (101 MHz, CD$_3$OD) δ 170.66, 157.22, 143.41, 139.46, 136.51, 128.44, 128.27, 126.65, 116.40, 114.60, 113.78, 106.70, 90.92, 77.87, 39.74, 32.69. HPLC purity: 100%. HRMS (ESI): *m/z* calculated C$_{16}$H$_{16}$N$_5$ for [M + H]$^+$: 278.1406. Found: 278.1398

4-(5-(3-(Dimethylamino)but-1-yn-1-yl)-1H-indol-3-yl)pyrimidin-2-amine (31).
The reaction was carried out according to general procedure B starting from 4-(5-bromo-1*H*-indol-3-yl)pyrimidin-2-amine (**49**) (30 mg, 0.1 mmol), *N*,*N*-dimethylbut-3-yn-2-amine 2,2,2-trifluoroacetate (66 mg, 0.31 mmol), DIPA (21 mg, 0.21 mmol), PdCl$_2$(PPh$_3$)$_2$ (15 mg, 21 μmol), and CuI (4.0 mg, 21 μmol) in 1-propanol (1 mL) at 85 °C overnight to afford the title compound (8.8 mg, 21% yield) as a TFA salt. ^{1}H NMR (400 MHz, CD$_3$OD) δ 8.85 (dd, *J* = 1.6, 0.8 Hz, 1H), 8.53 (s, 1H), 7.98 (d, *J* = 6.8 Hz, 1H), 7.54 (dd, *J* = 8.4, 0.8 Hz, 1H), 7.46 (dd, *J* = 8.4, 1.6 Hz, 1H), 7.35 (d, *J* = 6.8 Hz, 1H), 4.69 (q, *J* = 6.8 Hz, 1H), 3.03 (s, 6H), 1.73 (d, *J* = 6.8 Hz, 3H). ^{13}C NMR (214 MHz, CD$_3$CN) δ 169.44, 157.87, 144.35, 138.65, 135.42, 127.96, 127.93, 126.21, 115.84, 114.01, 113.91, 106.25, 91.00, 80.94, 55.25, 41.45, 39.02, 17.32. HPLC purity: 100%. HRMS (ESI): *m/z* calculated for C$_{18}$H$_{20}$N$_5$ [M + H]$^+$: 306.1719. Found: 306.1711.

4-(5-(4-(Dimethylamino)but-1-yn-1-yl)-1H-indol-3-yl)pyrimidin-2-amine (32).
The reaction was carried out according to general procedure A starting from 4-(5-bromo-1*H*-indol-3-yl)pyrimidin-2-amine (**49**) (30 mg, 0.1 mmol), *N*,*N*-dimethylbut-3-yn-1-amine (30 mg, 0.31 mmol), TEA (21 mg, 0.21 mmol), Pd(PPh$_3$)$_4$ (12 mg, 10 μmol), and CuI (2.0 mg, 10 μmol) in DMF (1 mL) at 85 °C overnight to afford the title compound (13 mg, 31% yield) as a TFA salt. ^{1}H NMR (400 MHz, CD$_3$OD) δ 8.76 (dd, *J* = 1.6, 0.8 Hz, 1H), 8.46 (s, 1H), 7.94 (d, *J* = 7.2 Hz, 1H), 7.46 (dd, *J* = 8.4, 0.8 Hz, 1H), 7.36 (dd, *J* = 8.4, 1.6 Hz, 1H), 7.30 (d, *J* = 6.8 Hz, 1H), 3.44 (t, *J* = 6.8 Hz, 2H), 3.02–2.98 (m, 8H). ^{13}C NMR (214 MHz, CD$_3$OD) δ 170.41, 157.54, 143.95, 138.92, 135.99, 128.34, 127.68, 126.62, 117.97, 114.55, 113.49, 106.71, 85.78, 82.56, 57.34, 43.70 (2C), 16.76. HPLC purity: 100%. HRMS (ESI): *m/z* calculated C$_{18}$H$_{20}$N$_5$ for [M + H]$^+$: 306.1719. Found: 306.1712.

N-(3-(3-(2-Aminopyrimidin-4-yl)-1H-indol-5-yl)prop-2-yn-1-yl)-N-methylacetamide (33).
The reaction was carried out according to general procedure B starting from 4-(5-bromo-1*H*-indol-3-yl)pyrimidin-2-amine (**49**) (30 mg, 0.1 mmol), *N*-methyl-*N*-(prop-2-yn-1-yl)acetamide (35 mg, 0.31 mmol), DIPA (21 mg, 0.21 mmol), PdCl$_2$(PPh$_3$)$_2$ (7.3 mg, 21 μmol), and CuI (2.0 mg, 10 μmol) in 1-propanol (1 mL) at 85 °C overnight to afford the title compound (9.0 mg, 27% yield) as an inseparable mixture of isomers. major: ^{1}H NMR (400 MHz, CD$_3$CN) δ 10.40 (s, 1H), 8.68 (s, 1H), 8.28 (d, *J* = 3.2 Hz, 1H), 7.88 (d, *J* = 6.4 Hz, 1H), 7.52 (d, *J* =8.4, 1H), 7.36 (dd, *J* = 8.4, 2.0 Hz, 1H), 7.16 (d, *J* = 6.8 Hz, 1H), 4.41 (s, 2H), 3.14 (s, 3H), 2.08 (s, 3H). minor: ^{1}H NMR (400 MHz, CD$_3$CN) δ 10.40 (s, 1H), 8.68 (s, 1H), 8.29 (d, *J* = 3.2 Hz, 1H), 7.90 (d, *J* = 6.4 Hz, 1H), 7.53 (d, *J* =8.4, 1H), 7.37 (dd, *J* = 8.4, 2.0 Hz, 1H), 7.18 (d, *J* = 6.8 Hz, 1H), 4.35 (s, 2H), 3.00 (s, 3H), 2.17 (s, 3H). ^{13}C NMR (126 MHz, CD$_3$OD) δ 173.40, 173.17, 170.74, 157.13, 143.19, 143.12,

139.07, 138.95, 136.36, 136.28, 128.62, 128.55, 127.85, 127.59, 126.64, 126.61, 118.13, 117.76, 114.58, 114.54, 113.62, 113.50, 106.69, 106.64, 86.64, 85.55, 83.31, 82.65, 41.99, 37.91, 35.98, 33.74, 21.58, 21.38. HPLC purity: 100%. HRMS (ESI): m/z calculated for $C_{18}H_{18}N_5O$ [M + H]$^+$: 320.1511. Found: 320.1503.

N-(3-(3-(2-Aminopyrimidin-4-yl)-1H-indol-5-yl)prop-2-yn-1-yl)acetamide (34).
The reaction was carried out according to general procedure B starting from 4-(5-bromo-1*H*-indol-3-yl)pyrimidin-2-amine (**49**) (50 mg, 0.17 mmol), *N*-(prop-2-yn-1-yl)acetamide (50 mg, 0.52 mmol), DIPA (35 mg, 0.35 mmol), PdCl$_2$(PPh$_3$)$_2$ (12 mg, 17 µmol), and CuI (3.3 mg, 17 µmol) in 1-propanol (1 mL) at 85 ℃ overnight to afford the title compound (7.8 mg, 15% yield). ^{1}H NMR (400 MHz, CD$_3$OD) δ 8.73 (dd, J = 1.6, 0.8 Hz, 1H), 8.43 (s, 1H), 7.91 (d, J = 7.2 Hz, 1H), 7.44 (dd, J = 8.4, 0.8 Hz, 1H), 7.33 (dd, J = 8.4, 1.6 Hz, 1H), 7.26 (d, J = 6.8 Hz, 1H), 4.21 (s, 2H), 2.01 (s, 3H). ^{13}C NMR (214 MHz, CD$_3$OD) δ 173.02, 170.34, 157.59, 144.01, 138.85, 135.81, 128.31, 127.76, 126.64, 118.18, 114.57, 113.41, 106.67, 84.63, 84.37, 30.47, 22.46. HPLC purity: >99%. HRMS (ESI): m/z calculated for $C_{17}H_{16}N_5O$ [M + H]$^+$: 306.1355. Found: 306.1348.

4-(5-(3-(Pyrrolidin-1-yl)prop-1-yn-1-yl)-1H-indol-3-yl)pyrimidin-2-amine (35).
The reaction was carried out according to general procedure A starting from 4-(5-bromo-1*H*-indol-3-yl)pyrimidin-2-amine (**49**) (50 mg, 0.17 mmol), 1-(prop-2-yn-1-yl)pyrrolidine (76 mg, 0.69 mmol), TEA (35 mg, 0.35 mmol), Pd(PPh$_3$)$_4$ (20 mg, 17 µmol), and CuI (3.3 mg, 17 µmol) in DMF (1.5 mL) at 85 ℃ overnight to afford the title compound (10 mg, 14% yield) as a TFA salt. ^{1}H NMR (400 MHz, CD$_3$OD) δ 8.85 (dd, J = 1.6, 0.8 Hz, 1H), 8.50 (s, 1H), 7.96 (d, J = 6.8 Hz, 1H), 7.52 (dd, J = 8.4, 0.8 Hz, 1H), 7.43 (dd, J = 8.4, 1.6 Hz, 1H), 7.32 (d, J = 7.2 Hz, 1H), 4.38 (s, 2H), 3.71 (bs, 2H), 3.40 (bs, 2H), 2.17 (s, 4H). ^{13}C NMR (214 MHz, CD$_3$OD) δ 169.97, 158.14, 145.17, 139.49, 135.80, 128.36, 128.30, 126.65, 115.92, 114.74, 113.75, 106.80, 91.45, 77.33, 54.63 (2C), 45.29, 24.47 (2C). HPLC purity: 100%. HRMS (ESI): m/z calculated $C_{19}H_{20}N_5$ for [M + H]$^+$: 318.1719. Found: 318.1711.

4-(5-(3-Morpholinoprop-1-yn-1-yl)-1H-indol-3-yl)pyrimidin-2-amine (36).
The reaction was carried out according to general procedure A starting from 4-(5-bromo-1*H*-indol-3-yl)pyrimidin-2-amine (**49**) (50 mg, 0.17 mmol), 4-(prop-2-yn-1-yl)morpholine (87 mg, 0.69 mmol), TEA (35 mg, 0.35 mmol), Pd(PPh$_3$)$_4$ (20 mg, 17 µmol), and CuI (3.3 mg, 17 µmol) in DMF (1.5 mL) at 85 ℃ overnight to afford the title compound (4.4 mg, 6% yield) as a TFA salt. ^{1}H NMR (400 MHz, CD$_3$OD) δ 8.88 (dd, J = 1.6, 0.8 Hz, 1H), 8.53 (s, 1H), 7.98 (d, J = 6.8 Hz, 1H), 7.53 (dd, J = 8.4, 0.8 Hz, 1H), 7.45 (dd, J = 8.8, 1.6 Hz, 1H), 7.35 (d, J = 6.8 Hz, 1H), 4.37 (s, 2H), 3.98 (bs, 4H), 3.48 (bs, 4H). ^{13}C NMR (214 MHz, CD$_3$OD) δ 170.29, 157.74, 144.44, 139.45, 136.09, 128.44, 128.23, 126.66, 116.34, 114.70, 113.75, 106.79, 92.01, 77.42, 65.67 (2C), 52.77 (2C), 48.23. HPLC purity: 100%. HRMS (ESI): m/z calculated $C_{19}H_{20}N_5O$ for [M + H]$^+$: 334.1668. Found: 334.1659.

4-(3-(2-Aminopyrimidin-4-yl)-1H-indol-5-yl)-2-(5-methylisoxazol-3-yl)but-3-yn-2-ol (37).
The reaction was carried out according to general procedure A starting from 4-(5-bromo-1*H*-indol-3-yl)pyrimidin-2-amine (**49**) (32 mg, 0.11 mmol), 2-(5-methylisoxazol-3-yl)but-3-yn-2-ol (67 mg, 0.44 mmol), TEA (22 mg, 0.22 mmol), Pd(PPh$_3$)$_4$ (13 mg, 11 µmol), and CuI (2.1 mg, 11 µmol) in DMF (1.5 mL) at 85 ℃ overnight to afford the title compound (11.6 mg, 29% yield). ^{1}H NMR (400 MHz, DMSO-d_6) δ 11.85 (s, 1H), 8.59 (d, J = 1.6 Hz, 1H), 8.24 (d, J = 2.8 Hz, 1H), 8.12 (d,

J = 5.6 Hz, 1H), 7.43 (dd, J = 8.4, 0.8 Hz, 1H), 7.20 (dd, J = 8.4, 1.6 Hz, 1H), 7.01 (d, J = 5.2 Hz, 1H), 6.45 (s, 2H), 6.41 (s, 1H), 6.39 (d, J = 0.8 Hz, 1H), 2.41 (d, J = 1.2 Hz, 3H), 1.83 (s, 3H). ^{13}C NMR (101 MHz, DMSO-d_6) δ 169.27, 168.44, 163.57, 162.29, 157.17, 136.71, 129.39, 125.60, 125.51, 125.03, 113.90, 113.64, 112.26, 105.49, 100.42, 89.99, 84.69, 63.80, 29.97, 11.85. HPLC purity: 100%. HRMS (ESI): m/z calculated $C_{20}H_{18}N_5O_2$ for [M + H]$^+$: 360.1460. Found: 360.1450.

4-(3-(2-Aminopyrimidin-4-yl)-1H-indol-5-yl)-2-(thiazol-2-yl)but-3-yn-2-ol (38).

The reaction was carried out according to general procedure A starting from 4-(5-bromo-1H-indol-3-yl)pyrimidin-2-amine (49) (30 mg, 0.10 mmol), 2-(thiazol-2-yl)but-3-yn-2-ol (64 mg, 0.42 mmol), TEA (21 mg, 0.21 mmol), Pd(PPh$_3$)$_4$ (12 mg, 10 μmol), and CuI (2.0 mg, 10 μmol) in DMF (1.5 mL) at 85 ℃ overnight to afford the title compound (15.2 mg, 41% yield). ^{1}H NMR (400 MHz, DMSO-d_6) δ 11.86 (s, 1H), 8.58 (m, 1H), 8.24 (d, J = 2.8 Hz, 1H), 8.12 (s, 1H), 7.77 (d, J = 3.2 Hz, 1H), 7.68 (d, J = 3.2 Hz, 1H), 7.43 (dd, J = 8.4, 0.8 Hz, 1H), 7.20 (dd, J = 8.4, 1.6 Hz, 1H), 7.00 (d, J = 4.8 Hz, 1H), 6.93 (s, 1H), 6.44 (s, 2H), 1.92 (s, 3H). ^{13}C NMR (101 MHz, DMSO-d_6) δ 176.38, 163.58, 162.27, 157.18, 142.47, 136.74, 129.41, 125.53, 125.51, 125.03, 120.34, 113.93, 113.55, 112.30, 105.51, 90.26, 84.89, 67.95, 31.66. HPLC purity: 100%. HPLC purity: >95%. HRMS (ESI): m/z calculated $C_{19}H_{16}N_5OS$ for [M + H]$^+$: 362.1076. Found: 362.1071.

4-(3-(2-Aminopyrimidin-4-yl)-1H-indol-5-yl)-2-(pyrazin-2-yl)but-3-yn-2-ol (39).

The reaction was carried out according to general procedure A starting from 4-(5-bromo-1H-indol-3-yl)pyrimidin-2-amine (49) (47 mg, 0.16 mmol), 2-(pyrazin-2-yl)but-3-yn-2-ol (96 mg, 0.65 mmol), TEA (33 mg, 0.33 mmol), Pd(PPh$_3$)$_4$ (19 mg, 16 μmol), and CuI (3.1 mg, 16 μmol) in DMF (1.5 mL) at 85 ℃ overnight to afford the title compound (13 mg, 22% yield). ^{1}H NMR (400 MHz, CD$_3$OD) δ 9.11 (d, J = 1.6 Hz, 1H), 8.72 (dd, J = 1.6, 0.8 Hz, 1H), 8.63 (dd, J = 2.8, 1.6 Hz, 1H), 8.58 (d, J = 2.8 Hz, 1H), 8.39 (s, 1H), 7.95 (d, J = 6.8 Hz, 1H), 7.45 (dd, J = 8.4, 0.8 Hz, 1H), 7.36 (dd, J = 8.4, 1.6 Hz, 1H), 7.24 (d, J = 6.8 Hz, 1H), 1.96 (s, 3H). ^{13}C NMR (101 MHz, CD$_3$OD) δ 169.80, 160.76, 158.25, 145.31, 144.77, 144.69, 142.91, 138.96, 135.32, 128.25, 127.40, 126.59, 117.50, 114.71, 113.47, 106.76, 91.02, 87.19, 70.45, 31.37. HPLC purity: >98%. HRMS (ESI): m/z calculated $C_{20}H_{17}N_6O$ for [M + H]$^+$: 357.1464. Found: 357.1455.

4-(5-(3-(Methylthio)prop-1-yn-1-yl)-1H-indol-3-yl)pyrimidin-2-amine (40).

The reaction was carried out according to general procedure B starting from 4-(5-bromo-1H-indol-3-yl)pyrimidin-2-amine (49) (30 mg, 0.10 mmol), methyl(prop-2-yn-1-yl)sulfane (27 mg, 0.31 mmol), DIPA (21 mg, 0.21 mmol), PdCl$_2$(PPh$_3$)$_2$ (15 mg, 21 μmol), and CuI (4.0 mg, 21 μmol) in 1-propanol (1 mL) at 85 ℃ overnight to afford the title compound (5.3 mg, 17% yield). ^{1}H NMR (400 MHz, CD$_3$OD) δ 8.69 (m, 1H), 8.41 (s, 1H), 7.90 (d, J = 6.8 Hz, 1H), 7.43 (dd, J = 8.4, 0.8 Hz, 1H), 7.32 (dd, J = 8.4, 1.6 Hz, 1H), 7.26 (d, J = 6.8 Hz, 1H), 3.53 (s, 2H), 2.29 (s, 3H). ^{13}C NMR (214 MHz, CD$_3$OD) δ 170.61, 157.33, 143.48, 138.79, 136.05, 128.53, 127.43, 126.64, 118.70, 114.56, 113.46, 106.70, 84.83, 84.78, 22.88, 15.32. HPLC purity: >97%. HRMS (ESI): m/z calculated for $C_{16}H_{15}N_4S$ [M + H]$^+$: 295.1017. Found: 295.1014.

4-(5-(Pent-1-yn-1-yl)-1H-indol-3-yl)pyrimidin-2-amine (41).

The reaction was carried out according to general procedure B starting from 4-(5-bromo-1H-indol-3-yl)pyrimidin-2-amine (49) (30 mg, 0.10 mmol), pent-1-yne (21 mg, 0.31 mmol), DIPA (21 mg, 0.21 mmol), PdCl$_2$(PPh$_3$)$_2$ (15 mg, 21 μmol), and CuI (4.0 mg, 21 μmol) in 1-propanol (1 mL) at

85 °C overnight to afford the title compound (15.8 mg, 55% yield). ^{1}H NMR (400 MHz, CD$_3$OD) δ 8.64 (d, J = 1.6 Hz, 1H), 8.39 (s, 1H), 7.89 (d, J = 6.8 Hz, 1H), 7.40 (dd, J = 8.4, 0.8 Hz, 1H), 7.28 (dd, J = 8.4, 1.2 Hz, 1H), 7.25 (d, J = 7.2 Hz, 1H), 2.41 (t, J = 7.2 Hz, 2H), 1.65 (h, J = 7.2 Hz, 2H), 1.08 (t, J = 7.2 Hz, 3H). ^{13}C NMR (214 MHz, CD$_3$OD) δ 170.55, 157.24, 143.22, 138.42, 135.88, 128.48, 127.04, 126.59, 119.70, 114.48, 113.27, 106.63, 89.09, 82.71, 23.51, 22.19, 13.96. HPLC purity: 100%. HRMS (ESI): m/z calculated for C$_{17}$H$_{17}$N$_4$ [M + H]$^+$: 277.1453. Found: 277.1443.

4-(5-(3-Fluorophenyl)-1H-indol-3-yl)pyrimidin-2-amine (42).

The reaction was carried out according to general procedure C starting from 4-(5-bromo-1H-indol-3-yl)pyrimidin-2-amine (49) (20 mg, 69 µmol), (3-fluorophenyl)boronic acid (15 mg, 0.10 mmol), K$_2$CO$_3$ (19 mg, 0.14 mmol), and Pd(PPh$_3$)$_4$ (4.0 mg, 3.5 µmol) in a mixture of 1,4-dioxane (0.7 mL) and water (0.1 mL) at 85 °C overnight to afford the title compound (14.6 mg, 69% yield). ^{1}H NMR (400 MHz, CD$_3$OD) δ 8.80 (t, J = 1.2 Hz, 1H), 8.43 (s, 1H), 7.89 (d, J = 7.2 Hz, 1H), 7.56–7.53 (m, 3H), 7.48–7.46 (m, 1H), 7.45–7.42 (m, 1H), 7.29 (d, J = 6.8 Hz, 1H), 7.08–7.02 (m, 1H). ^{13}C NMR (101 MHz, CD$_3$OD) δ 170.74, 165.86, 163.43, 157.15, 145.94, 142.95, 139.09, 136.13, 131.30, 127.25, 124.43, 122.20, 115.20, 114.98, 114.35, 114.14, 113.76, 106.66. HPLC purity: 100%. HRMS (ESI): m/z calculated for C$_{18}$H$_{14}$N$_4$F [M + H]$^+$: 305.1202. Found: 305.1192.

4-(5-(2-Fluorophenyl)-1H-indol-3-yl)pyrimidin-2-amine (43).

The reaction was carried out according to general procedure C starting from 4-(5-bromo-1H-indol-3-yl)pyrimidin-2-amine (49) (20 mg, 69 µmol), (2-fluorophenyl)boronic acid (19 mg, 0.14 mmol), K$_2$CO$_3$ (19 mg, 0.14 mmol), and Pd(PPh$_3$)$_4$ (8.0 mg, 6.9 µmol) in a mixture of 1,4-dioxane (0.7 mL) and water (0.1 mL) at 85 °C overnight to afford the title compound (14.6 mg, 69% yield). ^{1}H NMR (400 MHz, CD$_3$OD) δ 8.74 (dt, J = 2.0, 0.8 Hz, 1H), 8.47 (s, 1H), 7.92 (d, J = 6.8 Hz, 1H), 7.59–7.54 (m, 2H), 7.46 (dt, J = 8.4, 1.6 Hz, 1H), 7.39–7.34 (m, 1H), 7.32 (d, J = 7.2 Hz, 1H), 7.27 (td, J = 7.2, 1.2 Hz, 1H), 7.19 (ddd, J = 10.8, 8.0, 1.2 Hz, 1H). ^{13}C NMR (101 MHz, CD$_3$OD) δ 170.66, 162.46, 160.02, 157.23, 143.25, 138.78, 135.86, 132.68, 131.93, 129.81, 126.89, 126.35, 125.51, 124.24, 116.91, 114.85, 113.14, 106.70. HPLC purity: 100%. HRMS (ESI): m/z calculated for C$_{18}$H$_{14}$N$_4$F [M + H]$^+$: 305.1202. Found: 305.1193.

4-(3-(2-Aminopyrimidin-4-yl)-1H-indol-5-yl)phenol (44).

The reaction was carried out according to general procedure C starting from 4-(5-bromo-1H-indol-3-yl)pyrimidin-2-amine (49) (40 mg, 0.14 mmol), (4-hydroxyphenyl)boronic acid (29 mg, 0.21 mmol), K$_2$CO$_3$ (38 mg, 0.28 mmol), and Pd(PPh$_3$)$_4$ (16 mg, 14 µmol) in a mixture of 1,4-dioxane (1.4 mL) and water (0.2 mL) at 85 °C overnight to afford the title compound (6.3 mg, 15% yield). ^{1}H NMR (400 MHz, CD$_3$OD) δ 8.54 (dd, J = 1.6, 0.8 Hz, 1H), 8.11 (d, J = 5.6 Hz, 1H), 8.03 (s, 1H), 7.55–7.52 (m, 2H), 7.46 (dd, J = 8.4, 0.8 Hz, 1H), 7.41 (dd, J = 8.4, 1.6 Hz, 1H), 7.08 (d, J = 5.6 Hz, 1H), 6.89–6.86 (m, 2H). ^{13}C NMR (101 MHz, CD$_3$OD) δ 165.64, 164.57, 157.43 (2C), 137.98, 135.88, 135.49, 129.74, 129.42 (2C), 127.24, 123.01, 120.33, 116.49 (2C), 115.59, 112.93, 107.64. HPLC purity: >99%. HRMS (ESI): m/z calculated for C$_{18}$H$_{15}$N$_4$O [M + H]$^+$: 303.1246. Found: 303.1237.

4-(5-(4-(Trifluoromethyl)phenyl)-1H-indol-3-yl)pyrimidin-2-amine (45).

The reaction was carried out according to general procedure C starting from 4-(5-bromo-1H-indol-3-yl)pyrimidin-2-amine (49) (20 mg, 69 µmol), (4-(trifluoromethyl)phenyl)boronic acid (26 mg,

0.14 mmol), K_2CO_3 (19 mg, 0.14 mmol), and $Pd(PPh_3)_4$ (8.0 mg, 6.9 µmol) in a mixture of 1,4-dioxane (0.7 mL) and water (0.1 mL) at 85 °C overnight to afford the title compound (6.2 mg, 25% yield). ^1H NMR (400 MHz, CD$_3$OD) δ 8.93 (m, 1H), 8.50 (s, 1H), 7.95–7.92 (m, 3H), 7.75 (d, J = 8.4 Hz, 2H), 7.65–7.60 (m, 2H), 7.35 (d, J = 7.2 Hz, 1H). ^{13}C NMR (101 MHz, CD$_3$OD) δ 170.73, 157.35, 147.24, 143.39, 139.32, 136.18, 135.77, 129.84 (2C), 129.52, 129.02, 127.38, 126.60, 126.56, 124.47, 122.60, 115.00, 113.92, 106.72. HPLC purity: >99%. HRMS (ESI): m/z calculated for $C_{19}H_{14}N_4F_3$ [M + H]$^+$: 354.1171. Found: 355.1163.

4-(5-(4-(Dimethylamino)phenyl)-1H-indol-3-yl)pyrimidin-2-amine (46).

The reaction was carried out according to general procedure C starting from 4-(5-bromo-1*H*-indol-3-yl)pyrimidin-2-amine (**49**) (30 mg, 0.10 mmol), (4-(dimethylamino)phenyl)boronic acid (34 mg, 0.21 mmol), K_2CO_3 (29 mg, 0.21 mmol), and $Pd(PPh_3)_4$ (12 mg, 10 µmol) in a mixture of 1,4-dioxane (0.8 mL) and water (0.1 mL) at 85 °C overnight to afford the title compound (11.2 mg, 33% yield). ^1H NMR (400 MHz, CD$_3$OD) δ 8.55 (dd, J = 1.6, 0.8 Hz, 1H), 8.10 (d, J = 5.6 Hz, 1H), 8.02 (s, 1H), 7.59–7.55 (m, 2H), 7.47–7.41 (m, 2H), 7.07 (d, J = 5.6 Hz, 1H), 6.89 – 6.85 (m, 2H), 2.94 (s, 6H). ^{13}C NMR (214 MHz, DMSO-d_6) δ 163.54, 162.71, 157.01, 149.24, 135.93, 133.12, 129.67, 128.65, 127.38 (2C), 125.90, 120.71, 118.79, 113.91, 112.86 (2C), 112.04, 105.44, 40.26 (2C). HPLC purity: >98%. HRMS (ESI): m/z calculated for $C_{20}H_{20}N_5$ [M + H]$^+$: 330.1719. Found: 330.1711.

4-(5-(4-(Methylamino)phenyl)-1H-indol-3-yl)pyrimidin-2-amine (47).

The reaction was carried out according to general procedure C starting from 4-(5-bromo-1*H*-indol-3-yl)pyrimidin-2-amine (**49**) (30 mg, 0.10 mmol), *N*-methyl-4-(4,4,5,5-tetramethyl-1,3,2-dioxaborolan-2-yl)aniline hydrochloride (56 mg, 0.21 mmol), K_2CO_3 (29 mg, 0.21 mmol), and $Pd(PPh_3)_4$ (12 mg, 10 µmol) in a mixture of 1,4-dioxane (0.8 mL) and water (0.1 mL) at 85 °C overnight to afford the title compound (5.3 mg, 16% yield). ^1H NMR (400 MHz, CD$_3$OD) δ 8.89 (t, J = 1.6 Hz, 1H), 8.50 (s, 1H), 7.95 (d, J = 7.2 Hz, 1H), 7.92–7.88 (m, 2H), 7.60 (d, J = 1.2 Hz, 2H), 7.48–7.44 (m, 2H), 7.36 (d, J = 6.8 Hz, 1H), 3.09 (s, 3H). ^{13}C NMR (214 MHz, CD$_3$OD) δ 170.86, 157.17, 143.03, 138.96, 136.28, 136.20, 130.05 (2C), 127.38, 124.91, 124.33, 123.69, 121.99, 120.54, 114.92, 113.83, 113.31, 106.76, 35.80. HPLC purity: 100%. HRMS (ESI): m/z calculated for $C_{19}H_{18}N_5$ [M + H]$^+$: 316.1562. Found: 316.1559.

4-(5-(4-((Dimethylamino)methyl)phenyl)-1H-indol-3-yl)pyrimidin-2-amine (48).

The reaction was carried out according to general procedure C starting from 4-(5-bromo-1*H*-indol-3-yl)pyrimidin-2-amine (**49**) (30 mg, 0.10 mmol), (4-((dimethylamino)methyl)phenyl)boronic acid (56 mg, 0.31 mmol), K_2CO_3 (29 mg, 0.21 mmol), and $Pd(PPh_3)_4$ (12 mg, 10 µmol) in a mixture of 1,4-dioxane (0.8 mL) and water (0.1 mL) at 85 °C overnight to afford the title compound (17.8 mg, 50% yield). ^1H NMR (400 MHz, CD$_3$OD) δ 8.88 (t, J = 1.2 Hz, 1H), 8.46 (s, 1H), 7.92–7.86 (m, 3H), 7.62–7.57 (m, 4H), 7.31 (d, J = 7.2 Hz, 1H), 4.37 (s, 2H), 2.90 (s, 6H). ^{13}C NMR (126 MHz, CD$_3$OD) δ 170.66, 157.34, 145.33, 143.33, 139.15, 136.08, 136.06, 132.38 (2C), 129.38 (2C), 129.19, 127.35, 124.39, 122.29, 114.95, 113.87, 106.71, 61.98, 42.86 (2C). HPLC purity: 100%. HRMS (ESI): m/z calculated for $C_{21}H_{22}N_5$ [M + H]$^+$: 344.1875. Found: 344.1867.

Biological Evaluation.

NanoBRET Assays.

Human embryonic kidney (HEK293) cells from ATCC were cultured in Dulbecco's Modified Eagle's medium (DMEM, Gibco) supplemented with 10% (v/v) fetal bovine serum (FBS, Corning). These cells were incubated at 37 °C in 5% CO_2 and passaged every 72 hours with trypsin (Gibco) and never allowed to reach confluency.

Constructs for NanoBRET measurements of PIKfyve (PIKfyve-NLuc), PIP4K2C (PIP4K2C-NLuc), CDK10 + Cyclin L2 (CDK10-NLuc + Cyclin L2), PIP5K1B (PIP5K1B-NLuc), MKNK2 (MKNK2-NLuc), MYLK4 (MYLK4-NLuc), PRXK (PRXK-NLuc), and NEK3 (NEK3-NLuc) included in Tables 1–4, and Figures 4, S3, and S4 were kindly provided by Promega. The NLuc orientation used in each assay is indicated in parentheses after the listed construct. The NanoBRET assays were executed in dose–response format (11-pt curves) as described previously.[16, 45, 46] Assays were carried out as recommended by the manufacturer using 0.13 μM of tracer K8 for PIKfyve, 0.063 μM of tracer K8 for PIP4K2C, 0.5 μM of tracer K10 for CDK10/Cyclin L2, 0.25 μM of tracer K8 for PIP5K1B, 0.5 μM of tracer K10 for MKNK2, 0.13 μM of tracer K10 for MYLK4, , 0.5 μM of tracer K5 for PRXK, and 0.25 μM of tracer K10 for NEK3. Titration curves for PIP4K2C, CDK10 + Cyclin L2, PIP5K1B, MKNK2, MYLK4, PRXK, and NEK3 are included in Figure S3. The PIKfyve NanoBRET curve for **40** is included in Figure S4.

Enzymatic Assays.

SignalChem previously developed an ADP-Glo assay (Promega) to evaluate the enzymatic inhibition of PIKFYVE in dose–response format (10-pt curve).[16] This assay was executed in duplicate allowed for calculation of IC_{50} values.

Eurofins kinase enzymatic radiometric assays were executed at the K_m value for ATP in duplicate using a single concentration (1 μM) to generate PoC values for TTBK1 (accession number: NM_032538.1, 1–479 recombinant construct) and TTBK2 (accession number: BC071556.1, 1–333 recombinant construct). TTBK1/2 was incubated with the substrate (2 mg/mL casein) and tracer (γ-33P ATP) in 8 mM MOPS (pH 7.0), 0.2 mM EDTA, and 10 mM magnesium acetate. The reaction was started by adding the Mg/ATP mix. After incubating at room temperature for 40 min, the reaction was stopped by adding phosphoric acid (0.5%). The reaction mixture was then spotted onto a filter, washed four times with phosphoric acid (4 min in 0.425%) and once with methanol, and dried prior to scintillation counting. Staurosporine was used as a positive control compound for the assay. Further information for these two kinase assays is available on the Eurofins website: https://www.eurofinsdiscoveryservices.com.

Kinetic Solubility.

Analiza, Inc quantified the aqueous kinetic solubility of an aliquot of a 10 mM DMSO stock of each test compound dissolved in phosphate buffered saline solution (PBS) at pH 7.4 as previously described.[16, 47] The reported solubility values have been corrected for background nitrogen present in the DMSO and media.

Microsomal Stability Analysis.

Analiza, Inc analyzed the mouse microsomal stability using an aliquot of a 10 mM DMSO stock solution of each test compound. Stock solutions were diluted with DMSO upon arrival to a concentration of 0.5 mM, and diluted again to with acetonitrile (ACN) to yield final solutions containing 0.1 mM of test compounds in 20/80% DMSO/ACN as described previously.[16, 47] The

stability of the compound was calculated as the percent remaining of the parent compound at T = 30 min relative to the peak area at T= 0 min.

Cell Viability Assay.
A549–ACE2 cells were plated in DMEM high-glucose, 10% fetal bovine serum, 1X non-essential amino acids, and 2 mM L-glutamine on a 384-well plate at a seeding density of 2000 cells/well and allowed to adhere overnight. Cells were treated with 1 or 10 µM of a PIKfyve inhibitor, 0.01% DMSO (negative control), or 10% DMSO (positive control) for 48 hours. CellTiter-Glo reagent (Promega) was added to each well and luminescence was detected using a GloMax plate reader (Promega). Two biological replicates of each treatment in quadruplicate were analyzed. Raw data was used to calculate cell viability according to the following formula: ((raw RLU value - average of positive control wells)/(average of negative control wells - average of positive control wells))*100. GraphPad Prism was used to generate all plots, and the data included in Tables 1–4 and Figure S2.

Selectivity Profiling Using K192 Assay at UNC.
The NanoBRET Target Engagement K192 Kinase Selectivity assay was performed as previously published with modifications detailed below.[44, 48, 49] Kinases are grouped according to K10 tracer concentrations. A top control well (tracer and DMSO control) defined the maximum BRET/0% fractional occupancy, and a sample well (tracer and compound) was prepared for each kinase. Bottom control wells (expressing NanoLuc control vector pNL1.1.CMV[Nluc/CMV]) defined zero BRET/100% fractional occupancy. Reagents were provided by Promega (Promega #NP4060).

***DNA plate preparation*:** NanoBRET Target Engagement K192 vector plates A and B (Promega #NP401) containing DNA were prepared by addition of TE buffer (Promega #V6231, 250 µL) to each well.

***Assay plate preparation*:** For each kinase, 10 µL of transfection ready working DNA from plates A and B was transferred into 96-well assay plates (Corning #3917), with one well corresponding to a top control well and one to a sample well. This was followed by addition of Fugene HD transfection reagent (Promega #E2311), 30 µL of 20 µL/mL stock in each well containing DNA. Assay plates were mixed on an orbital shaker for 15 seconds at 300 rpm and incubated at room temperature for 30 min. HEK293 cells at 2.5 x 10^5 cells/mL in Opti-MEM without phenol red (Gibco #11058-021) containing 1% FBS (Avantor Seradigm #97068-085) were added to the assay plate (60 µL per well) and incubated for 20–24 hours at 37°C and 5% CO_2. Prior to tracer and inhibitor addition, the assay plates were equilibrated at room temperature for 15 min.

***Tracer addition*:** 20X K10 tracer (Promega #N264B) in tracer dilution buffer (Promega #N219B) was prepared from 100X of K10 in DMSO to yield final assay concentrations of 25 nM, 100 nM, 250 nM, and 1 µM for the respective kinases. 20X K10 (5 µL) was added to each well, excluding background wells and the bottom control wells (zero BRET). Assay plates were mixed on an orbital shaker for 15 seconds at 300 rpm.

***Inhibitor addition*:** 10 µL of 10X each test compound (**46** or **40**) in Opti-MEM without phenol red was added to sample wells for a final assay concentration of 1 µM, and 10X DMSO in Opti-MEM without phenol red was added to the top control wells. Assay plates were mixed on an orbital shaker for 15 seconds at 300 rpm and incubated for 2 hours at 37°C and 5% CO_2.

BRET measurement: Assay plates were equilibrated at room temperature for 15 min. A 3X solution of complete substrate plus inhibitor was prepared with NanoGlo substrate (1:166 dilution, Promega #N157D) and extracellular NanoLuc inhibitor (1:500 dilution, Promega #N235C) in Opti-MEM without phenol red. For one 96-well assay plate, this consists of 30 µL of NanoGlo substrate and 10 µL of extracellular NanoLuc inhibitor in 4,960 mL of Opti-MEM without phenol red. 3X complete substrate plus inhibitor (50 µL) was added to each well and the plates mixed on an orbital shaker for 15 seconds at 300 rpm. The plates were read on a GloMax Discover luminometer (Promega) containing a 450 nm BP filter (donor) and a 600 nm LP filter (acceptor) at a 0.3 s integration time. Raw BRET values were calculated as a ratio of acceptor (600 nm) to donor (450 nm) emissions.

Fractional occupancy calculation: The fractional occupancy of each kinase was determined based on the following formula:

$$\% \ Occupancy = \left(1 - \frac{(X-Z)}{(Y-Z)}\right) * 100$$

X = BRET values for sample wells (containing tracer and compound), Y = BRET value for the top controls (containing tracer and DMSO control), and Z = average BRET values for the bottom control wells. This assay was performed as a single replicate.

Molecular Docking

The initial structure of PIKfyve (PDB code: 7K2V, chain P) was prepared using the Schrödinger Protein Preparation Wizard.[50] We used the standard settings in this program: adding and optimizing the positions of hydrogen atoms and adjusting residue ionization and tautomer states using PROPKA at pH 7,[51, 52] removing water molecules located more than 3 Å away from heteroatoms, performing restrained structural minimization using the OPLS4 force field,[53] and converging the heavy atoms to a root mean square deviation (RMSD) of 0.3 Å. The 3D ligand structures were generated using Schrödinger LigPrep tool to sample all possible conformational models during the docking protocol. The Induced Fit Docking[54, 55] protocol was used to produce the initial model for the binding pose of **1** in the PIKfyve active site. To further refine the structural model of the protein–ligand complex, we performed molecular dynamics (MD) simulations using pmemd.cuda in Amber 22.[56-58]

We used a similar MD simulation protocol to that reported in our previous work.[59] Briefly, the initial simulation system was set up with AmberTools (tleap and antechamber)[60, 61] and Amber forcefields (*ff14SB*, *gaff2* and *tip3p*).[62-65] The protein–ligand complex structure was solvated in a rectangular box and the minimum distance between box edges and complex was set to 12 Å. The total system charge was neutralized by adding chlorine ions. After initial energy equilibration, the system temperature was increased to 298 K using NVT ensemble over 100 ps with 10.0 kcal/(mol·Å^2) harmonic restraints added to the heavy atoms of the protein–ligand complex. The restraints were then gradually released over 1 ns in NPT ensembles. An additional 100 ns simulation was performed under a constant temperature (298 K) and constant pressure (1 bar) regulated by *Langevin* thermostat and Monte Carlo barostat, respectively. The simulation timestep was 2.0 fs and the SHAKE algorithm[66] was applied to constrain bonds involving hydrogens. The cutoff of nonbonded interactions was set to 10 Å and long-range electrostatic interactions were calculated with Particle mesh Ewald (PME) methods.[67] The average structure of the 100 ns simulation was computed with cpptraj package[68] and the simulation frame with the lowest RMSD from the averaged structure was selected as the refined model for further docking study.

The refined complex model then was used to generate a docking grid file using the Schrödinger Receptor Grid Generation tool. We used the Glide[69, 70] SP mode to produce and score the ligand binding poses. All protein and ligand preparation, grid generation, and ligand docking were implemented using the Schrödinger Maestro graphical user interface. The complex structure and protein–ligand interactions were visualized using PyMol and Schrödinger Maestro interfaces. Results are included in Figures 2 and S1.

Structural Comparison between TTBK1 and PIKfyve ATP-Binding Sites.
The low amino acid sequence identity between PIKfyve and TTBK1 precluded the use of sequence alignment to identify structurally equivalent residues within the ATP-binding sites of both proteins. To overcome this challenge, we combined three rigid (jFATCAT-rigid, jCE, TM-align) and one flexible (jFATCAT-flexible) pairwise structure alignment method through the Pairwise Structural Alignment Tool in the RCSB PDB website - https://www.rcsb.org/alignment.[71] Pairwise structural alignments were executed with default parameters (jFATCAT-rigid: RMSD Cutoff: 3; AFP Distance Cutoff: 1600; Fragment Length: 8 / jCE: Maximum Gap Size: 30; Gap Opening Penalty: 5; Gap Extension Penalty: 0.5; Fragment Size: 8; RMSD Threshold: 3; Maximum RMSD: 99 / jFATCAT-rigid: RMSD Cutoff: 3; AFP Distance Cutoff: 1600; Fragment Length: 8; Max Number of Twists: 8). Inputs for these analyses were the co-crystal structure of TTBK1 kinase domain (residues 21–317) bound to **2** (PDB ID 7ZHO chain A)[43] and the Cryo-EM structure of the kinase domain of PIKFYVE (residues 1822–2085) in complex with Fig4 and Vac14 (PDB ID 7K2V chain A).[72] Similar analyses were also performed using the AlphaFold2-computed structure model of the kinase domain of PIKfyve (residues 1822–2085; AlphaFold DB: AF-Q9Y2I7-F1, last modified 2022-09-30).[73-75]

Pharmacokinetic (PK) Studies
Preliminary snapshot PK studies were executed at Pharmaron as previously described.[47] Male CD-1 mice (6–8 weeks, 20–30 grams) were dosed with a test compound via intraperitoneal (IP) or oral (PO) administration. A single dose of the compound (10 mg/kg) was administered to two mice as a 1 mg/mL solution in NMP/solutol/PEG-400/normal saline (v/v/v/v, 10:5:30:55). Mice had free access to food and water throughout the study. Blood (0.03 mL) was collected from the dorsal metatarsal vein at 0.5, 1, 3, and 5 h time points. Blood from each sample was transferred into a plastic microcentrifuge tube containing EDTA-K_2 and then centrifuged at 4000 g for 5 min at 4 °C to separate and collect plasma. Samples were preserved at −75 °C prior to analysis. Compound concentration in the plasma samples was determined using a Prominence LC-30AD, AB Sciex Triple Quan 5500 LC-MS/MS instrument fitted with a YMC-Triart C18 column (3 μm, 2.1 x 33 mm), eluting with a mobile phase of 5–95% acetonitrile in water with 0.1% formic acid. PK parameters were calculated from the mean plasma concentration versus time and a non-compartmental model that relied on WinNonlin 8.3 (Phoenix).

Associated Content
The Supporting Information is available free of charge at http://pubs.acs.org.
Molecular Formula Strings file (CSV), additional docking poses, cellular viability data and plots for **46** and **40**, NanoBRET curves, K192/K240 percent occupancy data, purity chromatograms, and NMR spectra are included (PDF).

Supporting Information

Author Information

*E-mail: alison.axtman@unc.edu.

Corresponding Author

Author Contributions

All authors have given approval to the final version of the manuscript.

Notes

The authors declare no competing financial interest.

Acknowledgment

Abbreviations

ACN, acetonitrile; ACE2, angiotensin-converting enzyme 2; AcOH, acetic acid; BSA, bovine serum albumin; DCM, dichloromethane; DIPA, *N, N*-diisopropylamine; DMA, *N, N*-dimethylacetamide; DMAP, 4-dimethylaminopyridine; DMF, *N, N*-dimethylformamide; DMSO, dimethyl sulfoxide; EDC, 1-ethyl-3-(3-dimethylaminopropyl)carbodiimide; EtOAc, ethyl acetate; HPLC, high-performance liquid chromatography; IC$_{50}$, half maximal inhibitory concentration; K$_m$, Michaelis constant; LC–MS, liquid chromatography–mass spectrometry; MLM, mouse liver microsome; NanoBRET, bioluminescence resonance energy transfer using NanoLuciferase; NaOMe, sodium methoxide; NLuc, NanoLuciferase; NMR, nuclear magnetic resonance; TEA, triethylamine; TFA, trifluoroacetic acid; SAR, structure–activity relationships; v/v, volume for volume.

References

(1) Gayle, S.; Landrette, S.; Beeharry, N.; Conrad, C.; Hernandez, M.; Beckett, P.; Ferguson, S. M.; Mandelkern, T.; Zheng, M.; Xu, T.; Rothberg, J.; Lichenstein, H. Identification of apilimod as

a first-in-class PIKfyve kinase inhibitor for treatment of B-cell non-Hodgkin lymphoma. *Blood* **2017**, *129*, 1768–1778. DOI: 10.1182/blood-2016-09-736892.

(2) Liu, S.; Cao, C.; Wang, Y.; Hu, L.; Liu, Q. Novel therapies for ANCA-associated vasculitis: Apilimod ameliorated endothelial cells injury through TLR4/NF-κB pathway and NLRP3 inflammasome. *Curr Pharm Des* **2024**, *30*, 2325–2344. DOI: 10.2174/0113816128312530240607051608.

(3) Hou, Y.; He, H.; Ma, M.; Zhou, R. Apilimod activates the NLRP3 inflammasome through lysosome-mediated mitochondrial damage. *Front Immunol* **2023**, *14*, 1128700. DOI: 10.3389/fimmu.2023.1128700.

(4) Xu, J.; Li, J.; Hu, Y.; Dai, K.; Gan, Y.; Zhao, J.; Huang, M.; Zhang, X. IL-23, but not IL-12, plays a critical role in inflammation-mediated bone disorders. *Theranostics* **2020**, *10*, 3925–3938. DOI: 10.7150/thno.41378.

(5) Cai, X.; Xu, Y.; Kim, Y. M.; Loureiro, J.; Huang, Q. PIKfyve, a class III lipid kinase, is required for TLR-induced type I IFN production via modulation of ATF3. *J Immunol* **2014**, *192*, 3383–3389. DOI: 10.4049/jimmunol.1302411.

(6) Cai, X.; Xu, Y.; Cheung, A. K.; Tomlinson, R. C.; Alcázar-Román, A.; Murphy, L.; Billich, A.; Zhang, B.; Feng, Y.; Klumpp, M.; Rondeau, J.-M.; Fazal, A. N.; Wilson, C. J.; Myer, V.; Joberty, G.; Bouwmeester, T.; Labow, M. A.; Finan, P. M.; Porter, J. A.; Ploegh, H. L.; Baird, D.; De Camilli, P.; Tallarico, J. A.; Huang, Q. PIKfyve, a class III PI kinase, is the target of the small molecular IL-12/IL-23 inhibitor apilimod and a player in Toll-like receptor signaling. *Chem Biol* **2013**, *20*, 912–921. DOI: 10.1016/j.chembiol.2013.05.010.

(7) Krausz, S.; Boumans, M. J.; Gerlag, D. M.; Lufkin, J.; van Kuijk, A. W.; Bakker, A.; de Boer, M.; Lodde, B. M.; Reedquist, K. A.; Jacobson, E. W.; O'Meara, M.; Tak, P. P. Brief report: a phase IIa, randomized, double-blind, placebo-controlled trial of apilimod mesylate, an interleukin-12/interleukin-23 inhibitor, in patients with rheumatoid arthritis. *Arthritis Rheum* **2012**, *64*, 1750–1755. DOI: 10.1002/art.34339.

(8) Sands, B. E.; Jacobson, E. W.; Sylwestrowicz, T.; Younes, Z.; Dryden, G.; Fedorak, R.; Greenbloom, S. Randomized, double-blind, placebo-controlled trial of the oral interleukin-12/23 inhibitor apilimod mesylate for treatment of active Crohn's disease. *Inflamm Bowel Dis* **2010**, *16*, 1209–1218. DOI: 10.1002/ibd.21159.

(9) Billich, A. Drug evaluation: apilimod, an oral IL-12/IL-23 inhibitor for the treatment of autoimmune diseases and common variable immunodeficiency. *IDrugs* **2007**, *10*, 53–59.

(10) Wada, Y.; Lu, R.; Zhou, D.; Chu, J.; Przewloka, T.; Zhang, S.; Li, L.; Wu, Y.; Qin, J.; Balasubramanyam, V.; Barsoum, J.; Ono, M. Selective abrogation of Th1 response by STA-5326, a potent IL-12/IL-23 inhibitor. *Blood* **2007**, *109*, 1156–1164. DOI: 10.1182/blood-2006-04-019398.

(11) Babu, S.; Nicholson, K. A.; Rothstein, J. D.; Swenson, A.; Sampognaro, P. J.; Pant, P.; Macklin, E. A.; Spruill, S.; Paganoni, S.; Gendron, T. F.; Prudencio, M.; Petrucelli, L.; Nix, D.; Landrette, S.; Nkrumah, E.; Fandrick, K.; Edwards, J.; Young, P. R. Apilimod dimesylate in C9orf72 amyotrophic lateral sclerosis: a randomized phase 2a clinical trial. *Brain* **2024**, *147*, 2998–3008. DOI: 10.1093/brain/awae109.

(12) Bakkar, N.; Starr, A.; Rabichow, B. E.; Lorenzini, I.; McEachin, Z. T.; Kraft, R.; Chaung, M.; Macklin-Isquierdo, S.; Wingfield, T.; Carhart, B.; Zahler, N.; Chang, W.-H.; Bassell, G. J.; Betourne, A.; Boulis, N.; Alworth, S. V.; Ichida, J. K.; August, P. R.; Zarnescu, D. C.; Sattler, R.; Bowser, R. The M1311V variant of ATP7A is associated with impaired trafficking and copper

homeostasis in models of motor neuron disease. *Neurobiol Dis* **2021**, *149*, 105228. DOI: 10.1016/j.nbd.2020.105228.

(13) Hung, S.-T.; Linares, G. R.; Chang, W.-H.; Eoh, Y.; Krishnan, G.; Mendonca, S.; Hong, S.; Shi, Y.; Santana, M.; Kueth, C.; Macklin-Isquierdo, S.; Perry, S.; Duhaime, S.; Maios, C.; Chang, J.; Perez, J.; Couto, A.; Lai, J.; Li, Y.; Alworth, S. V.; Hendricks, E.; Wang, Y.; Zlokovic, B. V.; Dickman, D. K.; Parker, J. A.; Zarnescu, D. C.; Gao, F.-B.; Ichida, J. K. PIKFYVE inhibition mitigates disease in models of diverse forms of ALS. *Cell* **2023**, *186*, 786–802.e728. DOI: 10.1016/j.cell.2023.01.005.

(14) Baker, J.; Ombredane, H.; Daly, L.; Knowles, I.; Rapeport, G.; Ito, K. Pan-antiviral effects of a PIKfyve inhibitor on respiratory virus infection in human nasal epithelium and mice. *Antimicrob Agents Chemother* **2024**, *68*, e0105023. DOI: 10.1128/aac.01050-23.

(15) Logue, J.; Chakraborty, A. R.; Johnson, R.; Goyal, G.; Rodas, M.; Taylor, L. J.; Baracco, L.; McGrath, M. E.; Haupt, R.; Furlong, B. A.; Soong, M.; Prabhala, P.; Horvath, V.; Carlson, K. E.; Weston, S.; Ingber, D. E.; DePamphilis, M. L.; Frieman, M. B. PIKfyve-specific inhibitors restrict replication of multiple coronaviruses in vitro but not in a murine model of COVID-19. *Commun Biol* **2022**, *5*, 808. DOI: 10.1038/s42003-022-03766-2.

(16) Drewry, D. H.; Potjewyd, F. M.; Bayati, A.; Smith, J. L.; Dickmander, R. J.; Howell, S.; Taft-Benz, S.; Min, S. M.; Hossain, M. A.; Heise, M.; McPherson, P. S.; Moorman, N. J.; Axtman, A. D. Identification and utilization of a chemical probe to interrogate the roles of PIKfyve in the lifecycle of β-coronaviruses. *J Med Chem* **2022**, *65*, 12860–12882. DOI: 10.1021/acs.jmedchem.2c00697.

(17) Kettunen, P.; Lesnikova, A.; Räsänen, N.; Ojha, R.; Palmunen, L.; Laakso, M.; Lehtonen, Š.; Kuusisto, J.; Pietiläinen, O.; Saber, S. H.; Joensuu, M.; Vapalahti, O. P.; Koistinaho, J.; Rolova, T.; Balistreri, G. SARS-CoV-2 infection of human neurons is TMPRSS2 independent, requires endosomal cell entry, and can be blocked by inhibitors of host phosphoinositol-5 kinase. *J Virol* **2023**, *97*, e0014423. DOI: 10.1128/jvi.00144-23.

(18) Kumar, P.; Mathayan, M.; Smieszek, S. P.; Przychodzen, B. P.; Koprivica, V.; Birznieks, G.; Polymeropoulos, M. H.; Prabhakar, B. S. Identification of potential COVID-19 treatment compounds which inhibit SARS Cov2 prototypic, Delta and Omicron variant infection. *Virology* **2022**, *572*, 64–71. DOI: 10.1016/j.virol.2022.05.004.

(19) Plescia, C. B.; Lindstrom, A. R.; Quintero, M. V.; Keiser, P.; Anantpadma, M.; Davey, R.; Stahelin, R. V.; Davisson, V. J. Evaluation of phenol-substituted diphyllin derivatives as selective antagonists for ebola virus entry. *ACS Infect Dis* **2022**, *8*, 942–957. DOI: 10.1021/acsinfecdis.1c00474.

(20) Finch, C. L.; Dyall, J.; Xu, S.; Nelson, E. A.; Postnikova, E.; Liang, J. Y.; Zhou, H.; DeWald, L. E.; Thomas, C. J.; Wang, A.; Xu, X.; Hughes, E.; Morris, P. J.; Mirsalis, J. C.; Nguyen, L. H.; Arolfo, M. P.; Koci, B.; Holbrook, M. R.; Hensley, L. E.; Jahrling, P. B.; Schmaljohn, C.; Johansen, L. M.; Olinger, G. G.; Schiffer, J. T.; White, J. M. Formulation, stability, pharmacokinetic, and modeling studies for tests of synergistic combinations of orally available approved drugs against ebola virus in vivo. *Microorganisms* **2021**, *9*, 566. DOI: 10.3390/microorganisms9030566.

(21) Rihn, S. J.; Merits, A.; Bakshi, S.; Turnbull, M. L.; Wickenhagen, A.; Alexander, A. J. T.; Baillie, C.; Brennan, B.; Brown, F.; Brunker, K.; Bryden, S. R.; Burness, K. A.; Carmichael, S.; Cole, S. J.; Cowton, V. M.; Davies, P.; Davis, C.; De Lorenzo, G.; Donald, C. L.; Dorward, M.; Dunlop, J. I.; Elliott, M.; Fares, M.; da Silva Filipe, A.; Freitas, J. R.; Furnon, W.; Gestuveo, R. J.; Geyer, A.; Giesel, D.; Goldfarb, D. M.; Goodman, N.; Gunson, R.; Hastie, C. J.; Herder, V.;

Hughes, J.; Johnson, C.; Johnson, N.; Kohl, A.; Kerr, K.; Leech, H.; Lello, L. S.; Li, K.; Lieber, G.; Liu, X.; Lingala, R.; Loney, C.; Mair, D.; McElwee, M. J.; McFarlane, S.; Nichols, J.; Nomikou, K.; Orr, A.; Orton, R. J.; Palmarini, M.; Parr, Y. A.; Pinto, R. M.; Raggett, S.; Reid, E.; Robertson, D. L.; Royle, J.; Cameron-Ruiz, N.; Shepherd, J. G.; Smollett, K.; Stewart, D. G.; Stewart, M.; Sugrue, E.; Szemiel, A. M.; Taggart, A.; Thomson, E. C.; Tong, L.; Torrie, L. S.; Toth, R.; Varjak, M.; Wang, S.; Wilkinson, S. G.; Wyatt, P. G.; Zusinaite, E.; Alessi, D. R.; Patel, A. H.; Zaid, A.; Wilson, S. J.; Mahalingam, S. A plasmid DNA-launched SARS-CoV-2 reverse genetics system and coronavirus toolkit for COVID-19 research. *PLoS Biol* **2021**, *19*, e3001091. DOI: 10.1371/journal.pbio.3001091.

(22) Zhao, Z.; Qin, P.; Huang, Y. W. Lysosomal ion channels involved in cellular entry and uncoating of enveloped viruses: Implications for therapeutic strategies against SARS-CoV-2. *Cell Calcium* **2021**, *94*, 102360. DOI: 10.1016/j.ceca.2021.102360.

(23) Baranov, M. V.; Bianchi, F.; van den Bogaart, G. The PIKfyve inhibitor apilimod: A double-edged sword against COVID-19. *Cells* **2021**, *10*, 30. DOI: 10.3390/cells10010030.

(24) Kang, Y. L.; Chou, Y. Y.; Rothlauf, P. W.; Liu, Z.; Soh, T. K.; Cureton, D.; Case, J. B.; Chen, R. E.; Diamond, M. S.; Whelan, S. P. J.; Kirchhausen, T. Inhibition of PIKfyve kinase prevents infection by Zaire ebolavirus and SARS-CoV-2. *Proc Natl Acad Sci U S A* **2020**, *117*, 20803–20813. DOI: 10.1073/pnas.2007837117.

(25) Hulseberg, C. E.; Fénéant, L.; Szymańska-de Wijs, K. M.; Kessler, N. P.; Nelson, E. A.; Shoemaker, C. J.; Schmaljohn, C. S.; Polyak, S. J.; White, J. M. Arbidol and other low-molecular-weight drugs that inhibit lassa and ebola viruses. *J Virol* **2019**, *93*, e02185–02218. DOI: 10.1128/jvi.02185-18.

(26) Nelson, E. A.; Dyall, J.; Hoenen, T.; Barnes, A. B.; Zhou, H.; Liang, J. Y.; Michelotti, J.; Dewey, W. H.; DeWald, L. E.; Bennett, R. S.; Morris, P. J.; Guha, R.; Klumpp-Thomas, C.; McKnight, C.; Chen, Y.-C.; Xu, X.; Wang, A.; Hughes, E.; Martin, S.; Thomas, C.; Jahrling, P. B.; Hensley, L. E.; Olinger Jr, G. G.; White, J. M. The phosphatidylinositol-3-phosphate 5-kinase inhibitor apilimod blocks filoviral entry and infection. *PLoS Negl Trop Dis* **2017**, *11*, e0005540. DOI: 10.1371/journal.pntd.0005540.

(27) Cinato, M.; Guitou, L.; Saidi, A.; Timotin, A.; Sperazza, E.; Duparc, T.; Zolov, S. N.; Giridharan, S. S. P.; Weisman, L. S.; Martinez, L. O.; Roncalli, J.; Kunduzova, O.; Tronchere, J.; Boal, F. Apilimod alters TGFβ signaling pathway and prevents cardiac fibrotic remodeling. *Theranostics* **2021**, *11*, 6491–6506. DOI: 10.7150/thno.55821.

(28) Oh, K. K.; Adnan, M.; Cho, D. H. New insight into drugs to alleviate atopic march via network pharmacology-based analysis. *Curr Issues Mol Biol* **2022**, *44*, 2257–2274. DOI: 10.3390/cimb44050153.

(29) Wada, Y.; Cardinale, I.; Khatcherian, A.; Chu, J.; Kantor, A. B.; Gottlieb, A. B.; Tatsuta, N.; Jacobson, E.; Barsoum, J.; Krueger, J. G. Apilimod inhibits the production of IL-12 and IL-23 and reduces dendritic cell infiltration in psoriasis. *PloS One* **2012**, *7*, e35069. DOI: 10.1371/journal.pone.0035069.

(30) Ikonomov, O. C.; Sbrissa, D.; Shisheva, A. Small molecule PIKfyve inhibitors as cancer therapeutics: Translational promises and limitations. *Toxicol Appl Pharmacol* **2019**, *383*, 114771. DOI: 10.1016/j.taap.2019.114771.

(31) Hou, J. Z.; Xi, Z. Q.; Niu, J.; Li, W.; Wang, X.; Liang, C.; Sun, H.; Fang, D.; Xie, S. Q. Inhibition of PIKfyve using YM201636 suppresses the growth of liver cancer via the induction of autophagy. *Oncol Rep* **2019**, *41*, 1971–1979. DOI: 10.3892/or.2018.6928.

(32) Gu, M.; Wang, Z.; Feng, F.; Yang, Y.; Sun, X.; Yang, D. Inhibition of PIKfyve ameliorates the proliferation and migration of vascular smooth muscle cells and vascular intima hyperplasia by reducing mTORC1 activity. *J Cardiovasc Pharmacol* **2022**, *79*, 739–748. DOI: 10.1097/FJC.0000000000001243.

(33) Stewart, A. K.; Li, Z.; Issakova, O.; Sepetov, N.; Trudel, S. PIK-001 a novel small molecule inhibitor of Pikfyve for treatment of multiple myeloma (MM). *Blood* **2021**, *138*, 1602. DOI: 10.1182/blood-2021-151208.

(34) Sano, O.; Kazetani, K.; Funata, M.; Fukuda, Y.; Matsui, J.; Iwata, H. Vacuolin-1 inhibits autophagy by impairing lysosomal maturation via PIKfyve inhibition. *FEBS Lett* **2016**, *590*, 1576–1585. DOI: 10.1002/1873-3468.12195.

(35) Ye, Z.; Wang, D.; Lu, Y.; He, Y.; Yu, J.; Wei, W.; Chen, C.; Wang, R.; Zhang, L.; Zhang, L.; Le, M. T. N.; Cho, W. C.; Yang, M.; Zhang, H.; Yue, J. Vacuolin-1 inhibits endosomal trafficking and metastasis via CapZβ. *Oncogene* **2021**, *40*, 1775–1791. DOI: 10.1038/s41388-021-01662-3.

(36) Feng, L.; Chen, K.; Huang, W.; Jiang, Y.; Sun, X.; Zhou, Y.; Li, L.; Li, Y.; Deng, X.; Xu, B. Pharmacological targeting PIKfyve and tubulin as an effective treatment strategy for double-hit lymphoma. *Cell Death Discov* **2022**, *8*, 39. DOI: 10.1038/s41420-022-00833-9.

(37) Lu, Z.; Lai, Q.; Li, Z. F.; Zhong, M. Y.; Jiang, Y. L.; Feng, L. Y.; Zha, J.; Yao, J. W.; Li, Y.; Deng, X. M.; Xu, B. Novel PIKfyve/tubulin dual-target inhibitor as a promising therapeutic strategy for B-cell acute lymphoblastic leukemia. *Curr Med Sci* **2024**, *44*, 298–308. DOI: 10.1007/s11596-024-2847-5.

(38) Li, H.; Jin, X.; Zhang, S.; Li, B.; Zeng, L.; He, Y.; Zhang, C. APY0201 represses tumor growth through inhibiting autophagy in gastric cancer cells. *J Oncol* **2022**, *2022*, 7104592. DOI: 10.1155/2022/7104592.

(39) Qiao, Y.; Choi, J. E.; Tien, J. C.; Simko, S. A.; Rajendiran, T.; Vo, J. N.; Delekta, A. D.; Wang, L.; Xiao, L.; Hodge, N. B.; Desai, P.; Mendoza, S.; Juckette, K.; Xu, A.; Soni, T.; Su, F.; Wang, R.; Cao, X.; Yu, J.; Kryczek, I.; Wang, X.-M.; Wang, X.; Siddiqui, J.; Wang, Z.; Bernard, A.; Fernandez-Salas, E.; Navone, N. M.; Ellison, S. J.; Ding, K.; Eskelinen, E.-L.; Heath, E. I.; Klionsky, D. J.; Zou, W.; Chinnaiyan, A. M. Autophagy inhibition by targeting PIKfyve potentiates response to immune checkpoint blockade in prostate cancer. *Nat Cancer* **2021**, *2*, 978–993. DOI: 10.1038/s43018-021-00237-1.

(40) Van Daele, S. H.; Masrori, P.; Van Damme, P.; Van Den Bosch, L. The sense of antisense therapies in ALS. *Trends Mol Med* **2024**, *30*, 252–262. DOI: 10.1016/j.molmed.2023.12.003.

(41) Drewry, D. H.; Annor-Gyamfi, J. K.; Wells, C. I.; Pickett, J. E.; Dederer, V.; Preuss, F.; Mathea, S.; Axtman, A. D. Identification of pyrimidine-based lead compounds for understudied kinases implicated in driving neurodegeneration. *J Med Chem* **2022**, *65*, 1313–1328. DOI: 10.1021/acs.jmedchem.1c00440.

(42) Rydberg, P.; Gloriam, D. E.; Zaretzki, J.; Breneman, C.; Olsen, L. SMARTCyp: A 2D method for prediction of cytochrome p450-mediated drug metabolism. *ACS Med Chem Lett* **2010**, *1*, 96–100. DOI: 10.1021/ml100016x.

(43) Bashore, F. M.; Marquez, A. B.; Chaikuad, A.; Howell, S.; Dunn, A. S.; Beltran, A. A.; Smith, J. L.; Drewry, D. H.; Beltran, A. S.; Axtman, A. D. Modulation of tau tubulin kinases (TTBK1 and TTBK2) impacts ciliogenesis. *Sci Rep* **2023**, *13*, 6118. DOI: 10.1038/s41598-023-32854-4.

(44) Robers, M. B.; Wilkinson, J. M.; Vasta, J. D.; Berger, L. M.; Berger, B. T.; Knapp, S. Single tracer-based protocol for broad-spectrum kinase profiling in live cells with NanoBRET. *STAR Protoc* **2021**, *2*, 100822. DOI: 10.1016/j.xpro.2021.100822.

(45) Drewry, D. H.; Potjewyd, F. M.; Smith, J. L.; Howell, S.; Axtman, A. D. Identification of a chemical probe for lipid kinase phosphatidylinositol-5-phosphate 4-kinase gamma (PI5P4Kγ). *Curr Res Chem Biol* **2023**, *3*, 100036. DOI: 10.1016/j.crchbi.2022.100036.

(46) Wells, C. I.; Drewry, D. H.; Pickett, J. E.; Tjaden, A.; Krämer, A.; Müller, S.; Gyenis, L.; Menyhart, D.; Litchfield, D. W.; Knapp, S.; Axtman, A. D. Development of a potent and selective chemical probe for the pleiotropic kinase CK2. *Cell Chem Biol* **2021**, *28*, 546–558.e510. DOI: 10.1016/j.chembiol.2020.12.013.

(47) Yang, X.; Ong, H. W.; Dickmander, R. J.; Smith, J. L.; Brown, J. W.; Tao, W.; Chang, E.; Moorman, N. J.; Axtman, A. D.; Willson, T. M. Optimization of 3-cyano-7-cyclopropylamino-pyrazolo[1,5-a]pyrimidines toward the development of an in vivo chemical probe for CSNK2A. *ACS Omega* **2023**, *8*, 39546–39561. DOI: 10.1021/acsomega.3c05377.

(48) Ong, H. W.; Yang, X.; Smith, J. L.; Dickmander, R. J.; Brown, J. W.; Havener, T. M.; Taft-Benz, S.; Howell, S.; Sanders, M. K.; Capener, J. L.; Couñago, R. M.; Chang, E.; Krämer, A.; Moorman, N. J.; Heise, M.; Axtman, A. D.; Drewry, D. H.; Willson, T. M. More than an amide bioisostere: Discovery of 1,2,4-triazole-containing pyrazolo[1,5-a]pyrimidine host CSNK2 inhibitors for combatting β-coronavirus replication. *J Med Chem* **2024**, *67*, 12261–12313. DOI: 10.1021/acs.jmedchem.4c00962.

(49) Vasta, J. D.; Corona, C. R.; Wilkinson, J.; Zimprich, C. A.; Hartnett, J. R.; Ingold, M. R.; Zimmerman, K.; Machleidt, T.; Kirkland, T. A.; Huwiler, K. G.; Ohana, R. F.; Slater, M.; Otto, P.; Cong, M.; Wells, C. I.; Berger, B.-T., Hanke, T.; Glas, C.; Ding, K.; Drewry, D. H.; Huber, K. V. M.; Willson, T. M.; Knapp, S.; Müller, S.; Meisenheimer, P. L.; Fan, F.; Wood, K. V.; Robers, M. B. Quantitative, wide-spectrum kinase profiling in live cells for assessing the effect of cellular ATP on target engagement. *Cell Chem Biol* **2018**, *25*, 206–214. DOI: 10.1016/j.chembiol.2017.10.010.

(50) Sastry, G. M.; Adzhigirey, M.; Day, T.; Annabhimoju, R.; Sherman, W. Protein and ligand preparation: parameters, protocols, and influence on virtual screening enrichments. *J Comput Aided Mol Des* **2013**, *27*, 221–234. DOI: 10.1007/s10822-013-9644-8.

(51) Søndergaard, C. R.; Olsson, M. H.; Rostkowski, M.; Jensen, J. H. Improved treatment of ligands and coupling effects in empirical calculation and rationalization of pKa values. *J Chem Theory Comput* **2011**, *7*, 2284–2295. DOI: 10.1021/ct200133y.

(52) Olsson, M. H.; Søndergaard, C. R.; Rostkowski, M.; Jensen, J. H. PROPKA3: Consistent treatment of internal and surface residues in empirical pKa predictions. *J Chem Theory Comput* **2011**, *7*, 525–537. DOI: 10.1021/ct100578z.

(53) Lu, C.; Wu, C.; Ghoreishi, D.; Chen, W.; Wang, L.; Damm, W.; Ross, G. A.; Dahlgren, M. K.; Russell, E.; Von Bargen, C. D.; Abel, R.; Friesner, R. A.; Harder, E. D. OPLS4: Improving force field accuracy on challenging regimes of chemical space. *J Chem Theory Comput* **2021**, *17*, 4291–4300. DOI: 10.1021/acs.jctc.1c00302.

(54) Sherman, W.; Beard, H. S.; Farid, R. Use of an induced fit receptor structure in virtual screening. *Chem Biol Drug Des* **2006**, *67*, 83–84. DOI: 10.1111/j.1747-0285.2005.00327.x.

(55) Sherman, W.; Day, T.; Jacobson, M. P.; Friesner, R. A.; Farid, R. Novel procedure for modeling ligand/receptor induced fit effects. *J Med Chem* **2006**, *49*, 534–553. DOI: 10.1021/jm050540c.

(56) Götz, A. W.; Williamson, M. J.; Xu, D.; Poole, D.; Le Grand, S.; Walker, R. C. Routine microsecond molecular dynamics simulations with AMBER on GPUs. 1. Generalized born. *J Chem Theory Comput* **2012**, *8*, 1542–1555. DOI: 10.1021/ct200909j.

(57) Salomon-Ferrer, R.; Götz, A. W.; Poole, D.; Le Grand, S.; Walker, R. C. Routine microsecond molecular dynamics simulations with AMBER on GPUs. 2. Explicit solvent Particle mesh Ewald. *J Chem Theory Comput* **2013**, *9*, 3878–3888. DOI: 10.1021/ct400314y.

(58) Le Grand, S.; Götz, A. W.; Walker, R. C. SPFP: Speed without compromise—A mixed precision model for GPU accelerated molecular dynamics simulations. *Comp Phys Commun* **2013**, *184*, 374–380. DOI: 10.1016/j.cpc.2012.09.022.

(59) Reddy Sammeta, V.; Anderson, B. M.; Norris, J. D.; Torrice, C. D.; Joiner, C.; Liu, S.; Li, H.; Popov, K. I.; Fanning, S. W.; McDonnell, D. P.; Willson, T. M. Structural determinants of the binding and activation of estrogen receptor α by phenolic thieno[2,3-d]pyrimidines. *Helv Chim Acta* **2023**, *106*, e202300097. DOI: 10.1002/hlca.202300097.

(60) Tsai, H.-C.; Lee, T.-S.; Ganguly, A.; Giese, T. J.; Ebert, M. C.; Labute, P.; Merz, K. M., Jr.; York, D. M. AMBER free energy tools: A new framework for the design of optimized alchemical transformation pathways. *J Chem Theory Comput* **2023**, *19*, 640–658. DOI: 10.1021/acs.jctc.2c00725.

(61) Wang, J.; Wang, W.; Kollman, P. A.; Case, D. A. Automatic atom type and bond type perception in molecular mechanical calculations. *J Mol Graph Model* **2006**, *25*, 247–260. DOI: 10.1016/j.jmgm.2005.12.005.

(62) He, X.; Man, V. H.; Yang, W.; Lee, T. S.; Wang, J. A fast and high-quality charge model for the next generation general AMBER force field. *J Chem Phys* **2020**, *153*, 114502. DOI: 10.1063/5.0019056.

(63) Maier, J. A.; Martinez, C.; Kasavajhala, K.; Wickstrom, L.; Hauser, K. E.; Simmerling, C. ff14SB: Improving the accuracy of protein side chain and backbone parameters from ff99SB. *J Chem Theory Comput* **2015**, *11*, 3696–3713. DOI: 10.1021/acs.jctc.5b00255.

(64) Wang, J.; Wolf, R. M.; Caldwell, J. W.; Kollman, P. A.; Case, D. A. Development and testing of a general amber force field. *J Comput Chem* **2004**, *25*, 1157–1174. DOI: 10.1002/jcc.20035.

(65) Jorgensen, W. L.; Chandrasekhar, J.; Madura, J. D.; Impey, R. W.; Klein, M. L. Comparison of simple potential functions for simulating liquid water. *J Chem Phys* **1983**, *79*, 926–935. DOI: 10.1063/1.445869.

(66) Ryckaert, J.-P.; Ciccotti, G.; Berendsen, H. J. C. Numerical integration of the cartesian equations of motion of a system with constraints: molecular dynamics of n-alkanes. *J Comput Phys* **1977**, *23*, 327–341. DOI: 10.1016/0021-9991(77)90098-5.

(67) Darden, T.; York, D.; Pedersen, L. Particle mesh Ewald: An N·log(N) method for Ewald sums in large systems. *J Chem Phys* **1993**, *98*, 10089–10092. DOI: 10.1063/1.464397.

(68) Roe, D. R.; Cheatham, T. E., III. PTRAJ and CPPTRAJ: Software for processing and analysis of molecular dynamics trajectory data. *J Chem Theory Comput* **2013**, *9*, 3084–3095. DOI: 10.1021/ct400341p.

(69) Friesner, R. A.; Banks, J. L.; Murphy, R. B.; Halgren, T. A.; Klicic, J. J.; Mainz, D. T.; Repasky, M. P.; Knoll, E. H.; Shelley, M.; Perry, J. K.; Shaw, D. E.; Francis, P.; Shenkin, P. S. Glide: A new approach for rapid, accurate docking and scoring. 1. Method and assessment of docking accuracy. *J Med Chem* **2004**, *47*, 1739–1749. DOI: 10.1021/jm0306430.

(70) Halgren, T. A.; Murphy, R. B.; Friesner, R. A.; Beard, H. S.; Frye, L. L.; Pollard, W. T.; Banks, J. L. Glide: A new approach for rapid, accurate docking and scoring. 2. Enrichment factors in database screening. *J Med Chem* **2004**, *47*, 1750–1759. DOI: 10.1021/jm030644s.

(71) Bittrich, S.; Segura, J.; Duarte, J. M.; Burley, S. K.; Rose, Y. RCSB protein Data Bank: exploring protein 3D similarities via comprehensive structural alignments. *Bioinformatics* **2024**, *40*, btae370. DOI: 10.1093/bioinformatics/btae370.

(72) Lees, J. A.; Li, P.; Kumar, N.; Weisman, L. S.; Reinisch, K. M. Insights into lysosomal PI(3,5)P(2) homeostasis from a structural-biochemical analysis of the PIKfyve lipid kinase complex. *Molecular cell* **2020**, *80*, 736–743.e734. DOI: 10.1016/j.molcel.2020.10.003.

(73) Jumper, J.; Evans, R.; Pritzel, A.; Green, T.; Figurnov, M.; Ronneberger, O.; Tunyasuvunakool, K.; Bates, R.; Žídek, A.; Potapenko, A.; Bridgland, A.; Meyer, C.; Kohl, S. A. A.; Ballard, A. J.; Cowie, A.; Romera-Paredes, B.; Nikolov, S.; Jain, R.; Adler, J.; Back, T.; Petersen, S.; Reiman, D.; Clancy, E.; Zielinski, M.; Steinegger, M.; Pacholska, M.; Berghammer, T.; Bodenstein, S.; Silver, D.; Vinyals, O.; Senior, A. W.; Kavukcuoglu, K.; Kohli, P.; Hassabis, D. Highly accurate protein structure prediction with AlphaFold. *Nature* **2021**, *596*, 583–589. DOI: 10.1038/s41586-021-03819-2.

(74) Varadi, M.; Bertoni, D.; Magana, P.; Paramval, U.; Pidruchna, I.; Radhakrishnan, M.; Tsenkov, M.; Nair, S.; Mirdita, M.; Yeo, J.; Kovalevskiy, O.; Tunyasuvunakool, K.; Laydon, A.; Žídek, A.; Tomlinson, H.; Hariharan, D.; Abrahamson, J.; Green, T.; Jumper, J.; Birney, E.; Steinegger, M.; Hassabis, D.; Velankar, S. AlphaFold Protein Structure Database in 2024: providing structure coverage for over 214 million protein sequences. *Nucleic Acids Res* **2024**, *52*, D368–D375. DOI: 10.1093/nar/gkad1011.

(75) Varadi, M.; Anyango, S.; Deshpande, M.; Nair, S.; Natassia, C.; Yordanova, G.; Yuan, D.; Stroe, O.; Wood, G.; Laydon, A.; Žídek, A.; Green, T.; Tunyasuvunakool, K.; Petersen, S.; Jumper, J.; Clancy, E.; Green, R.; Vora, A.; Lutfi, M.; Figurnov, M.; Cowie, A.; Hobbs, N.; Kohli, P.; Kleywegt, G.; Birney, E.; Hassabis, D.; Sameer, V. AlphaFold Protein Structure Database: massively expanding the structural coverage of protein-sequence space with high-accuracy models. *Nucleic Acids Res* **2022**, *50*, D439–D444. DOI: 10.1093/nar/gkab1061.
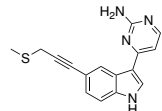
(76) Eid, S.; Turk, S.; Volkamer, A.; Rippmann, F.; Fulle, S. KinMap: a web-based tool for interactive navigation through human kinome data. *BMC Bioinformatics* **2017**, *18*, 16. DOI: 10.1186/s12859-016-1433-7.

For Table of Contents Only
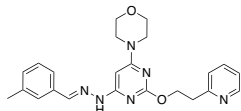
Approved drug
Apilimod

➤ PIKfyve enzyme IC_{50} = 3.4 nM
➤ PIKfyve NB IC_{50} = 0.31 nM
➤ No off-targets in cell-free selectivity assays
➤ Human $T_{1/2}$ (h) = 3–6.5

2nd Generation PIKfyve chemical probe **40**

➤ PIKfyve enzyme IC_{50} = 0.60 nM
➤ PIKfyve NB IC_{50} = 0.35 nM
➤ No off-targets in cellular selectivity assays
➤ Mouse $T_{1/2}$ (h) >5